Breath gating of cardiac PET using 13N-NH3: An optimization for dynamic analysis

Martin Lyngby Lassen

Kongens Lyngby 2012
IMM-M.Sc.-2012-4

Technical University of Denmark
Informatics and Mathematical Modelling
Building 321, DK-2800 Kongens Lyngby, Denmark
Phone +45 45253351, Fax +45 45882673
reception@imm.dtu.dk
www.imm.dtu.dk

IMM-M.Sc.: ISSN 0909-3192

Summary

In this project a correction of the breath-induced movement of the heart for dynamic PET-scans is investigated. The scans in this project was carried out using ^{13}N-NH_3 on two different PET/CT scanners: a Siemens Biograph 64 and a Siemens mCT PET/CT scanner, respectively. The dynamic analyses are used in the clinic to obtain information on the perfusion in the heart. From the findings in the perfusion it is possible to estimate whether the patient has a disease or not, and to distinguish different diseases. The dynamic analysis is traditionally carried out using a non-gated set-up in which it is impossible to correct for the breath induced movements of the heart. It is estimated that a correction for these motions will improve the dynamic analysis, as the gating might change both the estimated flow values inside a defect, and even change the size and outline of the defect.

In this project the breath-motion was estimated using an affine transformation on the obtained images, from which the translation, the rotation, scaling and torsion of the heart is found and corrected for. The method was tried on 6 patients who are known to suffer from different heart defects which alters the perfusion in the heart.

The results from the breath-motion corrected data were compared to a non breath-gated gold standard to validate the effect of the gating protocol. The estimated flows were changed for all the patients, when analysed using the breath-gated set-up. The changes in the flow were explainable by analyzing the correcting parameters. The results were furthermore analysed by statistical analyses of the measured perfusion values and a blind test of the measured flows.

Resumé

I dette projekt er der søgt at optimere på dynamiske PET undersøgelser af hjertet ved at korrigere for vejrtrækningsbevægelser. Skanningerne i dette projekt er udført ved brug af ^{13}N-NH_3 på to skannere, henholdsvis en Siemens Biograph 64 og en Siemens mCT PET/CT-skanner. Dynamiske analyser bliver i den kliniske praksis udført for at kvantificere hjertets perfusion, hvorved man kan udtale sig om eventuelle sygdomme i hjertet. Disse analyser er traditionelt blevet udført i en ikke-gated opsætning, hvorved det ikke er muligt at korrigere for vejrtræknings bevægelser. Det er estimeret at en korrektion for disse bevægelser vil forbedre den dynamiske analyse, da man formoder at defekt områder vil ændre størrelse og gennemstrømningsværdier.

I dette projekt blev vejrtrækningensbevægelsen estimeret ved brug af en affin transformation af data, hvorved man korrigerer for både bevægelse, rotation, skalering og vridning af hjertet. Selve metoden er blevet testet på 6 patienter som er kendt for at have forskellige hjertesygdomme som ændrer gennemstrømingen af hjertemuskulaturen.

De bevægelseskorrigerede resultater blev holdt op mod en ikke bevægelses korrigeret guld-standard, for at analysere hvorvidt at bevægelseskorrektionen forbedrede analysen. For alle patienterne blev der fundet ændrede gennemstrømningsværdier som kunne beskrives ud for bevægelseskorrektionen. Resultaterne blev ydermere analyseret vha. statistiske analyser af de målte perfusionsværdier samt en blindtest af de målte resultater.

Preface

This report is the result of a compulsory M.Sc. project for obtaining the Master of Science degree in Medicine and Technology (Biomedical engineering). This education is a collaboration between Ørsted - DTU, the Technical University of Denmark and the Panum Institute, the Medical Faculty of the University of Copenhagen, KU SUND Rigshospitalet.

The project took place from the 1st of September 2011 to the 15th of February 2012, and is a 30 ECTS-point project in the education. The project is performed in collaboration between Department of Informatics and Mathematical Modelling, IMM DTU, and the PET and cyclotron unit, department of Clinical Physiology and Nuclear Medicine, Copenhagen University Hospital (Rigshospitalet). The following supervisors have been attached to the project:

- Rasmus Larsen, Professor, M.Sc.(Eng), Ph.D. DTU Informatics, DTU. He was attached as main supervisor on this project.
- Knut Conradsen, Professor, DTU Informatics, DTU. He was attached as internal supervisor.
- Flemming Andersen, Computer Scientist, Ph.D, Department of Clinical Physiology and Nuclear Medicine, PET and cyclotron unit, Rigshosptialet, Copenhagen University Hospital. He was attached as external supervisor on the project.
- Philip Hasbak, Chief Physician, MD, Department of Clinical Physiology and Nuclear Medicine, PET and cyclotron unit, Rigshosptialet, Copenhagen University Hospital. He was attached as external supervisor on the project.

Acknowledgements

I want to thank my supervisors Rasmus Larsen, Knut Conradsen, Flemming Andersen and Philip Hasbak for supporting me from the very beginning of the project. They have all been a steady source for ideas and suggestions throughout the project. Furthermore I want to thank the physicists and medical laboratory scientists at Rigshospitalet who have helped me obtaining the best data possible.

I want to thank my family and friends for their support and encouraging comments throughout the project.

Martin Lyngby Lassen

Abbreviations

AC	Attenuation Correction
AHA	American Heart Association
ANOVA	ANalysis Of VAriance
CC	Cross Correlation
cFOV	centre Field Of View
CT	Computed Tomography
DICOM	Digital Image and COmmunications in Medicine
DF	Deformation Field
DOE	Design Of Experiments
DoF	Degrees of Freedom
ECG	Electrocardiography
EM	Expectation Maximization
FBP	Filtered Back Projection
FDA	Food and Drug Administration
FOV	Field Of View
FWHM	Full Width at Half Maximum
IDH	Ischemic Heart Disease
IF	Input Function
LAD	Left Anterior Descending
LCX	Left Circumflex
LM	Listmode
LOR	Line Of Response
MANOVA	Multivariate ANalysis Of VAriance
MI	Myocardial Infarction
MRI	Magnetic Resonance Imaging
OSEM	Ordered Subset Expectation Maximization
OSEM-TOF	Ordered Subset Expectation Maximization - With use of Time-Of-Flight
PET	Positron Emission Tomography
PSF	Point Spread Function
PVE	Partial Volume Effect
R	Reference (Image)
RCA	Right Coronary Artery
SNR	Signal To Noise Ratio
SPECT	Single-Photon Emission Computed Tomography
SS	Sum of Squares
SSD	Sum of Squared Difference
T	Template (Image)
TAC	Time-Activity-Curve
TT	Takotsubo cardiomyopathy
Voxel	Volume pixel

Units:	Bq	Becquerel (one decay per second)
	c	speed of light (299 792 458 $\frac{m}{s}$
	eV	electron Volt (1.60217646 $\cdot 10^{-19}$ J)
	g	grams
	Hz	Hertz
	J	Joules
	M	Mega
	MeV	Mega electron Volt
	min	minute
	ml	millilitre
	mm	millimetre
	s	seconds

Contents

Chapter 1

Introduction

Patients with known cardiac diseases are scanned on a routinely basis at the PET (Positron Emission Tomography) centre at Rigshospitalet, Copenhagen University Hospital. The patients are scanned using a radioactive labelled tracer (Ammonia), which is used to obtain knowledge of the blood flow in the myocardial tissue surrounding the left ventricle of the heart. The flow values are crucial to know when analyzing patients who are expected to suffer from different diseases. Areas having abnormal flow values (below 0.6 ml/g/min or above 1.2 ml/g/min in rest)[1] in parts of the left ventricle are known to suffer from either an Myocardial Infarction(MI), Takotsubo cardiomyoptahy(TT) or Ischemic heart disease(IHD). The size of the non-normal flow area determine which treatment the patient are offered. For patients with myocardial infarction the infarction size is determining whether the patient is going to undergo surgery or not. If the infarction area is smaller than a Danish 5-kroner coin, the patient is treated with medicine as the infarction-size is too small to gain benefit from by-pass surgery.

The dynamic PET scans consists of multiple frames of short time durations which are around 60 seconds or more. From these images it is possible to extract information on the kinetic changes in the heart. Due to the frame durations the cardiac studies have two dislocating factors, which are known to introduce errors to the estimated flow values. The two factors are the hearts own movement during the cardiac cycle, and a dislocation of the heart introduced by the breathing. These movements cannot be detected directly on the PET images as the patient have multiple heart beats and breath cycles during each frame. Using a non-gated study will give an average image of the heart with both motions introduced to the image. These effects will introduce both blurring effects and produce some non-true activity estimates in both the lumen of the ventricle and the cardiac wall.

A correction for the breath-cycle is thought to be crucial as the motion has been measured to be in the range from 1 to 11 mm during the breath-cycle. [2] A motion of 11 mm is known to introduce some errors in the estimated activity levels in the heart, and thereby introducing an erroneous flow estimate in the cardiac wall. Such great translations will furthermore give a blurring of an eventual MI. Here the infected area will have a low uptake of the tracer, while the healthy tissue surrounding the infarction will have a normal uptake. During the motion the infarct will be translated into the areas of the healthy tissue, and vice versa. This may result in an infarct will be analysed as a area with a reduced uptake, and it will not be classified as an infarction. By correcting for the breath induced motion it is estimated that one will have a better chance of estimating infarctions.

Chapter 2

Project description

There exists multiple theories on how to correct for the breath induced movement of the heart. The different theories are trying to correct for the movement on either the reconstructed images, or in the Listmode (LM) data which is used to reconstruct the images.

Listmode correcting is a method that is often used to correct for breath induced motions in the torso of the patient. Using this method one is correcting the measured decays on an individual basis, so that the heart is positioned the same in all the images. By doing this one are obliged to generate a new normalization file, which is used to correct for non-uniform detection of the decays in the detectors. This is required as one is shifting the measured annihilations, so that the heart is estimated in the same region. This gives that the annihilations are measured in different crystals, than they are translated into. The change of crystals require a new normalization file, as there might exist different levels of detections in the respective crystals. This method is thought to give the best results, as all the images are reconstructed using the same position of the heart throughout the scan. However this approach is thought to be too time-demanding to implement during the time-span of a master thesis.
Therefore the breath-gating is performed on the reconstructed images, using a breath-gated reconstruction method in this project. In the literature the breath-gating has been performed on static images, as the static images contains data from several minutes. By using several minutes of data one is able to obtain a good approximation of the breath-induced movements. It is assumed that the breath cycles stays homogeneous throughout the scan, when generating the static images. It is possible to find the hearts transformation from the different part of the breath-cycle by analyzing the static images. These deformation fields are thought to be applicable on the short-frame duration images, as the breath-cycle is estimated to be homogeneous throughout the entire scan.

The approach used in this thesis is shown in the list shown below.

1. Analyse the optimum frame lengths of the reconstructed images.
2. Co-registering of non-dynamic data
3. Apply the co-registering matrices on the short frame length data
4. Convert the corrected short frame length data into a dynamic scan
5. Compare the flow analysis from the movement corrected images to the conventional method

A description on the different steps is given on the next pages.

1. It is required to obtain knowledge on the optimum frame length due to two aspects.

The first aspect involves the dynamic analysis of the heart. The flows in the different parts of the heart are estimated using kinetic models. These models are using the activity measured in the lumen of the left ventricle and the activity in the myocardial tissue to estimate the flow. By having too long frame durations in the initial phase one is loosing the dynamic information. This is due to the activity estimated in the lumen will be reduced as the peak of the bolus will pass through the heart within few seconds (5-10 seconds). A long frame duration will furthermore lead to a great uptake of the tracer in the tissues, which eventually will lead to a non-correct flow estimate in the heart. This problematic is discussed in greater detail in section 3.3.

The second aspect is the breath-gating of the data. The breath-gating is dividing the breath cycle into a number of bins. The binning of the breath cycles are performed by summing the measured coincidence events from the same part of the breath cycles for each frame. The measured coincidence events are used to generate a sinogram which are used to produce an image for each bin. These images are used for estimating the activity within the heart, which are used for the flow estimates. This set-up requires a high number of measurements for each bin in order to get good images. From this perspective one is required to have a long frame duration. Choosing a too short frame duration might give non-correct hot-spots which are introduced by the poor sinograms. This will reduce the diagnostic value of the flow analysis.

From the two aspects it can be seen that the frame durations have counter-indicating aspects when choosing the optimum frame-duration. The determination of the frame-duration is discussed in section 5.1.

2. The breath cycle is measured using a pressure belt fastened around the upper-abdominal region or the lower thoracal region, depending on the breath-pattern. By registering the breath cycles one is able to correct for the translation within the breath cycles. This is possible as one is able to divide the breath cycle into different subsections (bins), each representing a part of the breath cycle.
The translatory effects of the breath cycle is thought to be estimated by using the entire scan duration. By doing this one obtains a good Signal-To-Noise-Ratio(SNR) in the images, from which one is able to obtain good estimates on the motion. It is estimated that one should generate a reference image to which all the bins are registered. The reference image is thought to be estimated as an average image of each of the bins, after they have been co-registered to the first bin. By generating a reference image one is reducing the risk of having an non-true registration of the respective bins.

3. The deformation fields found for the bins using the entire frame duration are thought applicable to the dynamic frames. This is thought possible as the breath cycles are estimated to be homogeneous throughout the scan. This has led to the following assumption on the dynamic analysis.

The heart is thought to have the same translatory effects during the breath cycle, if the breath pattern is kept constant.

4. Once the correction has been done on the short duration images the next step is to convert the data from each frame into a dynamic series. The dynamic series are required to be converted into the DICOM format, as the clinical software only reads this format.

5. A validation on the movement correction is needed. The validation is thought to happen by analyzing the new movement corrected data against the conventional method, which is thought as the gold standard.

Chapter 3

Theory

3.1 Tracer physics

The PET images are generated by detecting radioactive decays from a radioactive labelled tracer injected into an object (human being or phantom). The tracer used in this project is ^{13}N, which is incorporated into an ammonia molecule (NH_3). Other than ammonia, ^{82}Rb and ^{15}O-H_2O are commonly used in dynamic cardiac PET studies. ^{13}N-NH_3 was chosen as the tracer in this study because ^{82}Rb was banned from studies from July 2011. This was due to some bad experiences at other sites, where patients were having non-pure tracers, giving the patients too high dosages.[3] Furthermore was ^{15}O-H_2O discarded due to the short half-life of the tracer (2 minutes and 3 seconds), which gave it was difficult to inject the tracer into the patient at the site of the scanner.

All PET tracers emits positrons from the unstable nucleus, which gives the possibility to obtain the images. A positron is emitted from an unstable atom, where there is a neutron surcharge. To correct for this surcharge one of the protons are converged into a neutron, a positron (β^+ particle), an anti-neutrino along with some kinetic energy which is released during the decay. It can be written in the following equation.

$$p^+ \rightarrow \beta^+ + n + \nu + E_{kin} \tag{3.1}$$

The released kinetic energy is divided between the positron and the anti-neutrino.[4] This gives that the energy delivered to the positron varies within an energy span, which gives that the positron has different path-lengths within the body. The path-length is the distance which the positron travels before it annihilates with an electron. The annihilation happens because the positron is the antimatter of the electron. Once the positron and the electron annihilates the rest-energy of the electron and the positron is turned into two photons, each carrying 511keV of energy. The two photons travels in anti-parallel directions, which makes it possible to obtain the PET-images. The image quality depends on the emission energy of the positron, as the higher the emission energy, the further mean free path-length. A large mean free path-length will result in a poor Point Spread Function (PSF), which eventually will give noisy images when reconstructed.

The emission energy for ^{13}N is lower than for the two other tracers which is a benefit for this study. The maximum emission energies of the three tracers are 1.19MeV for ^{13}N, compared to 1.7MeV for ^{15}O and 3.15MeV for ^{82}Rb[5], hence a longer path length for ^{15}O and ^{82}Rb than ^{13}N.

The mean free path-length, e.g. the path the positron will travel before it annihilates with an electron can be calculated by using the formulas below:

$$\lambda(E) = (\Sigma_i n_{ati} \cdot \sigma(Z_i, E))^{-1} \tag{3.2}$$

where n_{ati} is the number of atoms per volume of the i^{th} element of the surrounding material. E is the energy delivered to the positron, and Z is the number of electrons. σ can be calculated by the formula:

$$\sigma(Z, E) = \frac{Z\pi r_e^2}{\gamma + 1}\left[\frac{\gamma^2 + 4\gamma + 1}{\gamma^2 - 1}\ln\left(\gamma + \sqrt{\gamma^2 - 1}\right) - \frac{\gamma + 3}{\sqrt{\gamma^2 - 1}}\right] \tag{3.3}$$

where E is the kinetic energy of the positron, γ is $\frac{E}{mc^2}$ and r_e is the classical electron radius[6].

Besides the low emission energy ammonia have some good characteristics within the human body. Ammonia is having a lipid solubility, which allows the tracer to travel across the lipids of the cell-membrane. Besides the freely-diffusible characteristics the tracer is also taken into the cell where it is converted into ^{13}N-glutamine. Gluatamine is an amino-acid which is trapped inside the cell [5]. The knowledge of these characteristics enables one to calculate the flow in the heart using kinetic models (see section 3.3).

3.2 Acquisition of PET data

PET data is, as described in the previous section, recordings of decays of unstable atoms. The emitted photons are sent out in anti-parallel directions, which are recorded in a set of PET crystals positioned in the anti-parallel direction of the photons. In the PET crystals the photons are converted into an electric energy in a photo-multiplier tube(PMT). The photon is converted into electric energy from the photoelectric effect inside a photocathode. The photocathode sends out an electron. The electron is accelerated into a dynode, from which a series of electrons are emitted. After interacting with several dynodes are the voltage measured, and it is determined if the initial photon have had enough energy to be within the accepted energy window. If accepted, is the signal stored and compared to the interaction effects in all the crystals which can be connected by a line. The interactions are stored as a coincidence event if one of the opposite crystals measures a photon within the coincidence time window. If no secondary detector measures a photon is the measurement discarded as a single event, which is not included in the reconstruction. Due to the electronics in the detector system are the PET scanners all having a problem with dead-time, which is the time from the measurement of an event, until the detector can measure another. This is a known problem, which is corrected for in the final reconstruction.

3.2.1 Generating the sinograms

3.2.1.1 The conventional method

In the conventional method the coincidence events is stored in a LM file, which contains information on which crystals which has had interactions, and the time of the interaction. These informations are used to generate the sinograms, which are used to reconstruct the images. The time which the coincidence events occurred are used to generate the sinograms for the dynamic data, as there is generated one sinogram for each frame.

From the knowledge about the two crystals that has measured the coincidence events one is able draw a line, called the Line Of Response (LOR). The LOR is used to generate the sinograms, as the sinograms are 2D-intensity plots, showing an angle and a distance from the centre of the FOV (cFOV). The sinogram will have fully visible half-sines, which are introduced by areas having a high activity. The half sine is introduced as the data is recorded using 180 degrees. In figure 3.1 a sinogram is shown.

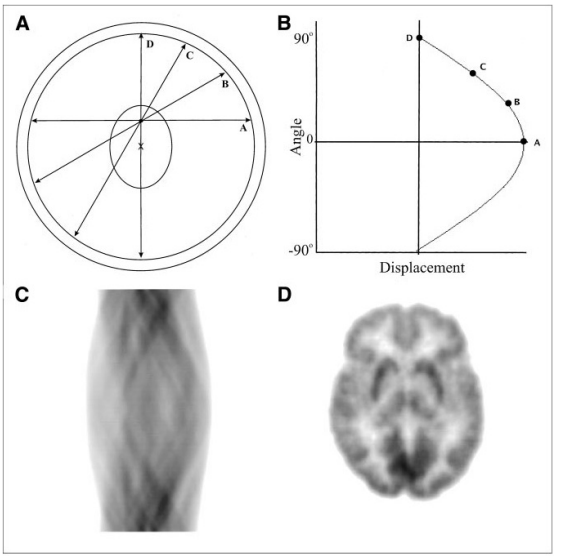

Figure 3.1: Generation of the sinograms. Taken from [7]

In sub-figure A is shown how the coincidence events are measured in the scanned object. The coincidence events are translated into a distance and an angle in sub-figure B. The multiple counts during the scanning gives a sinogram, shown in sub-figure C. When reconstructing the images using a chosen reconstruction algorithm, one is obtaining a PET-image, here showing a tumor in the anterior part of the brain. [7], [8]

3.2.1.2 The time of flight method

When recording the PET-data in the newer generation of scanners the time-delay from the first to the second interaction are stored within the Listmode file. The time-difference gives the possibility to reconstruct the PET images using a Time Of Flight (TOF) approach. The TOF approach is thought to have several benefits when compared to the conventional reconstruction algorithms, as this reconstruction method is thought to reduce the noise in the images. The greatest improvements of the reconstruction method is thought to be seen in patients having a high body-mass, as they are having a high attenuation in the recordings.

The time-difference is used to estimate where the annihilation has occurred. It is not possible to estimate the exact position of the annihilation, due to the limited time-resolution in the crystals. The estimate on position of the annihilation can be calculated by the equation shown below.

$$\Delta t = \frac{2\Delta x}{c} \tag{3.4}$$

where Δt is the time difference between the two measurements and Δx is the shift from the centre of the line. The two Δx are introduced as one of the photons interacts $\frac{\Delta x}{c}$ before it would have if the interaction has occurred in the centre of the line. The other photon is delayed by Δx because it has to travel to the centre of the LOR before it travels its remaining part.

If the crystals could detect the delay with high enough time resolution the sinograms would not be necessary, as all the informations could be calculated directly from the measured decays. [8], [9]

3.3 Kinetic models

The flow-analysis is done in clinical software available at the hospital. There are several products on the market, where Rigshospitalet is using Dynamic PET which is a part of the Syngo Circulation software by Siemens Healthcare. Common for all the programs is that the flows are estimated by using kinetic models. There exists several kinetic models explaining the flows within the heart, depending on the complexity needed and the tracer used.

There exists two models which can be used for estimating the blood flow, when using ^{13}N-NH_3 as tracer. There is a simple one-tissue compartment model which was developed by DeGrado et al ([10], [11]), and a two-tissue compartment model that was developed by Hutchins et al. [12]. The two models are having different approaches to the estimate of the blood flow. The model by DeGrado is preferred when analyzing the first 2 to 4 minutes of the dynamic study [11], while the model by Hutchins are preferred when using 10-15 minutes long studies. In this study the scanning protocol are estimated to be longer than 4 minutes, hence there will be no further discussion on the DeGrado model.

The three-compartment model for ^{13}N-NH_3 was estimated by Hutchins et al from a total of seven volunteers. The model was based on the found activities in the myocardial cells, which was correlated to the model. The model are based on four assumptions on how the tracer is taken into the myocardial cells. The four assumptions are listed below.

- *^{13}N-ammonia behaves like a freely diffusible tracer at the capillary-myocardial tissue interface.*
- *^{13}N-ammonia is converted to ^{13}N-glutamine by glutamine synthase and is, essentially, trapped within the myocardial tissue.*
- *The extracellular and intracellular ^{13}N-ammonia concentration values rapidly equilibrate.*
- *The available glutamine synthase level remains, essentially, unchanged throughout the study, so that the probability of converting an ammonia molecule in the tissue to glutamine remains constant.*

[12]

From the assumptions he was able to set up a two-tissue compartment model, which explained before mentioned assumptions. The two tissues were divided into an arterial phase, an extra vascular phase and an entrapment of the ammonia within the cells. The tracer was estimated to move freely within the two first compartments, as ammonia is assumed to be freely diffusible. The last phase is the entrapment within the myocardial cells, where the ammonia is used in the production of glutamine, which is an amino acid. A schematic drawing of the compartment model is shown below.

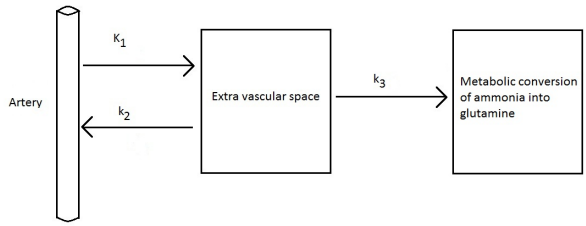

Figure 3.2: Three compartment model. Modified from [12]

It is possible to set up a series of variables which describes the flux of the tracer from the assumptions described above. The influx and efflux of the extra vascular components in the myocardial tissues can be described by two variables called K_1 and k_2 respectively. K_1 is used to estimate the diffusion rate from the blood into the myocardial cells, and k_2 is used to estimate the reverse action. This is visualized in figure 3.2. The rate in which the ammonia is taken into the cells, where it is incorporated into ^{13}N-Glutamine, can be described by the variable k_3, as seen in the above figure.

It was possible to estimate the different flux-rates, and hereby the flow in the heart by using the above assumptions. This was possible by setting up two differential equations describing the flux-rates from the blood into the extra vascular space and the conversion of ammonia into glutamine. The differential equations, and the estimation of the flow is shown below.

$$\frac{dC_E(t)}{dt} = K_1 C_A(t) - k_2 C_E(t) - k_3 C_E(t) \tag{3.5}$$

where C_E is the extra vascular concentration, which can move freely, and C_A is the activity in the artery.

The second differential equation is based on the entrapment of the glutamine in the myocardial cells, and is explained by:

$$\frac{dC_M(t)}{dt} = k_3 C_E(t) \tag{3.6}$$

where C_M is the entrapped glutamine.
The activity measured in the image is a summation of the two differential equations, hence $A_M(t) = C_E(t) + C_M(t)$. The differential equations can be solved to have the relationship:

$$A_M(t) = C_A(t) * \frac{K_1}{k_2 + k_3}\left[k_2 e^{-(k2+k3)t} + k_3\right] \tag{3.7}$$

where * is the convolution term. [5], [12]

The model has been tested by Muzik et al [13] in an animal study, where the dogs were infused with microspheres simultaneously with the tracer. In the animal study the tracer activity was measured continuously during the scan. After the end of the scan the animals were autopsied, where the microspheres were counted in the hearts capillaries. By comparing the activity estimates with the number of microspheres accumulated in the heart, it was possible to validate the model sat up by Hutchins.

3.4 Data

The datasets used in this project are 4D-PET datasets obtained at the PET department at Rigshospitalet. The 4D-datasets are generated from a Listmode file, from which a series of consecutive dynamic frames are reconstructed. Each frame consists of a 3D-data set, covering the torso of the patient. The images are obtained by either a Siemens Biograph 64 TruePoint PET-CT scanner or a Siemens mCT PET-CT scanner.

The patients analysed in this project are either having a follow-up scan to check whether their treatment has helped or not, or patients who are analysed for either having TT or IHD. A description on the two diseases can be found in the next section (section 3.5).

The 4D-datasets are all obtained with the torso of the patient placed in the cFOV. The patients are all scanned for a total of 15 minutes using the ^{13}N-NH_3 tracer. The patients are having a belt measuring the pressure around the rib-cage put on. The breath cycle is estimated by measuring the pressure applied to the belt.

The patients are instructed to have the arms above the head to reduce the attenuation from the body. The patients are having a tomogram scan prior to the injection of the tracer. This is done to ensure that the heart is placed in the centre Field of View (cFOV), from which the best images are obtained. A tomogram scan is a 2D scan, which has similarities to a conventional X-ray scan. Furthermore the patients have a low-dose CT-scan performed which is used correct for the attenuation (attenuation correction). This CT-scan can be used for diagnostic purposes in some cases.

The scans are all reconstructed using an iterative method (Ordered Subset Expectation Maximization (OSEM)). The exact number of iterations and subsets used for the reconstructions are investigated in this report (see section 5.3). A further introduction on the OSEM reconstruction algorithm can be found in section 3.7.1. The 3D datasets are reconstructed to have a voxel size of 1.0364 mm by 1.0364 mm by 2 mm. This leads to two different matrix-sizes, which depends on which scanner the patient was scanned at. If the patient was scanned in the mCT scanner, the matrix size is 400 by 400 by 111 voxels, where the matrix size is 168 by 168 by 111 voxels in the Biograph 64 scanner.

3.5 The left ventricle of the heart

The heart can be divided into two parts, the left and the right. In the right side the venous blood is returning from the body, where there is a low pressure. From the right ventricle the venous blood is pumped into the pulmonary system, where it is re-oxygenated. From the pulmonary system the blood is led back into the left side, from which it is pumped to rest of the body again. The circulation to the body requires a high pressure, which means that the left side of the heart is having a greater proportion of the myocardial cells, than the right. The left ventricle are having a thick muscular part toward the apex, and a thin membranous part toward the atria. This secures that the left ventricle is pumping out all the blood at each contraction. To do this is the thick muscular part requiring a stable perfusion of blood throughout the entire ventricle. An impairment of the flow can cause the heart to have a reduced ejection of the blood, which leads to severe diseases and death if the impairment is too large. Such impairment of the flow can be caused by various diseases.

The patients analysed in this project can be divided into two groups. The first group is a control group, which consists of patients whom are having a follow-up scan in order to check if the respective treatment has helped. The other group is patients whom are about to be diagnosed with either Takotsubo cardiomyopathy (TT) or Ischaemic heart disease (IHD). A brief introduction to the two diseases is given below.

Takotsubo cardiomyopathy

Takotsubo cardiomyopathy is a disease which has a sudden onset, which has the same appearance as a myocardial infarction (MI). The onset is primarily in post menopausal women, undergoing emotional stress such as dead of a loved one. Opposite MI, where the onset is triggered by a rupture of an atherosclerotic plaque, this disease is not having any clogging of the coronary arteries. In TT patients it is possible to measure an increased level of adrenaline/epinephrine, which causes the heart to have a higher contraction rate. This can be measured in the blood-pressure(BP) and the pulse of the patient, as both will be above the normal.(BP normal range =90/110, pulse=60).

The sudden onset of TT often leads to an assumption on the patients is suffering from MI, which is tried diagnosed with a Electrocardiography (ECG) analysis. Both TT and MI have the same change in the ECG-analysis, which is due to the same alternation in the contraction of the heart. From this it is not possible to distinct the two diseases, which leads to either a PET-scan or MRI-scan in order to determine if the whether the patient has TT or MI.

It is possible to analyse if the tissue is viable from a MRI-scan, but it is not possible to determine the exact size of the TT-area if the patient is diagnosed with this disease. Analyzing the patient in a PET-scan it is possible to estimate the flow in the heart by using a dynamic series. From the flow values it is possible to distinct between the two diseases, as the TT area is known to have a normal flow, while the infarct area is having a flow of 0 ml/g/min. The tissues surrounding the TT area is known to be hyper-perfused with flow values above 1.2 ml/g/min. [1] For MI patients it is furthermore possible to analyse whether the tissue near the infarct area is dead, or viable from the flow analysis. If the tissue is estimated to be viable, it might benefit the patient to undergo a bypass surgery. [14]

Ischaemic heart disease

"Ischemic heart disease is the most common cause of heart disease and the major cause of death in the developed countries."[15] IHD have two possible types of onsets, the progressive and the acute form. Both onsets have the same initial phase, where the coronary arteries are being clogged by atherosclerosis or being obstructed by a small thrombi.

In the progressive IHD the atherosclerosis is increasing in size in a moderate tempi, where the myocardial cells are able to generate alternative supply routes to the affected area (anastomoses). Here the atherosclerosis is often produced by a plaque formed by a firm dense cap, which often covered by epithelium.
In the acute form the plaque is produced by foam cells and a lipid-laden core. These plaques are prone to rupture, which triggers the clogging of the artery. The clogging will be experienced in the left ventricle most often, due to the metabolic demands being greatest here. [15]

The patients suffering from IHD have chest pains or discomforts due to the impaired flow through the heart. The pain is centred to the chest, and is described as a constriction, pressure or heaviness. The pain often have radiating effect to the left arm, the left jaw, which is described as angina pectoris. The pain is triggered by a raised level of adenosine, which is a compensatory effect to a raised demand of perfusion in the heart. This is often occurring during physical labour. Another, and more serious variant of IHD, is the unstable angina. These patients has symptoms even a rest, which is lasting for more than 20 minutes. About 10% of the patients suffering from this will progress directly to acute myocardial infarction (AMI), and 5% will die subsequently. [15]

3.6 Segmentations of the heart

The left ventricle is segmented into either 17 or 20 segments in the commercial software available. The number of segments depends on the manufacturer of the software. Some software manufacturers are basing their analysis solely on the American Heart Association (AHA) recommendations. In other software tools it is possible to choose between the AHA notation and the SPECT (Single Photon Emission Computed Tomography) annotation (20 segments).

It is possible to extract a lot of information from the 17 segments. Normally the 17 segments is visualized as a polar plot, from which it is possible to extract information on the different parts of the heart. The outer rings resembles the basal part of the heart. Moving inwards resembles a descend through the long-axis of the heart. The centre of the polar plot are containing the flow estimates for the apical region. The polar plot is shown below.

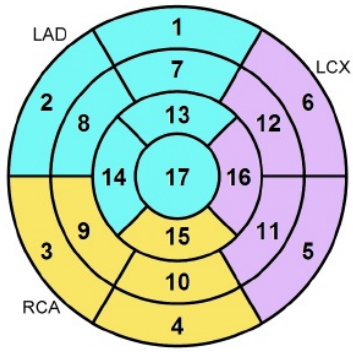

Figure 3.3: 17 segment model. Taken from [11]

The 17 segments is furthermore divided into 3 domains, which are shown with different color notations in the above figure. The 3 domains are determined by the coronary arteries supplying the different parts of the heart. The 3 artery sectors are called the Left Anterior Descending (LAD), the Left Circumflex (LCX) and the Right Coronary Artery (RCA), respectively. [11]

This notation is used by the cardiologists to determine the position of the non-normal flow area, and how great a part of the heart that is affected by the altered flow. In some cases the patient have necrotic areas downstream the site of an embolism. This will show up as an area having a reduced flow on the polar plots. From these plots the cardiologists are able to analyse which treatment that suits the patients the best.

In this project all the analysis are carried out in Dynamic PET by Siemens, as explained in section 3.3. This software tool does not currently use the 17 or the 20 segment models. In this program the heart is segmented into three segments, one for each coronary artery (LAD, LCX and RCA). The program is, however, used in this project as this is the only tool which has been approved for clinical analysis by the Food and Drug Administration (FDA) in the USA.

3.7 Breath gating

There exists several ways to monitor the patients breathing pattern while they are scanned. Each method has both benefits and drawbacks which should be taken into consideration when the method is chosen. Two of the commonly used methods are listed below:

- **Pressure belts.**
  This method uses a belt which is placed around the ribcage or abdominal region on the patient, depending on the breathing pattern of the patient. The belt has a built-in pressure sensor which is connected to a computer. The computer performs the analysis, and stores the measured pressures. The computer sends out a trigger signal once the respiratory peak has been measured. The trigger signal is sent to the PET-CT scanner, where the signal is stored in the LM file.
  The benefits of using this belt is mainly in the precise acquisition of the breath cycles.
  The belt has one drawback, it has to be tightened around the patients ribs to be sure that the belt triggers at the respiratory peak. The tightened belt might impair the normal breath cycle for the patient, which might be uncomfortable during the scan.

- **External video monitoring.**
  This method uses external markers placed on the patients body to monitor the breath cycle. A video-camera records the entire scanning session, which are stored on a computer. The translations are measured by analyzing the motion of the external markers, which has been placed on the chest. Such a set-up has been documented by Dawood et al. [16]
  Among the benefits from this system is that the entire scan is recorded on the PC, which makes it possible to analyse eventually non-normal breath cycles.

  Among the drawbacks of this method is that two or more systems has to be up and running at the same time. This can cause multiple problems when scanning the patients, also the breath gating has to be attached after the end of the scan.

In this project the breath-gating will be performed using a pressure belt - ANZAI AZ-733-V Respiratory gating system by Anzai Medical Co, Tokyo, Japan. This is thought to give the most exact results as the belt is storing the breath cycles directly in the LM file.

3.7.1 Reconstruction of breath gated images

The LM file contains information on all the events that has occurred during the scan, including the gated set-ups. one is able to tune different parameters when reconstructing the images. Four parameters has been analysed in this project. Each of the four parameters are explained in greater detail on the next pages.

3.7.1.1 The reconstruction algorithm

The reconstruction algorithm is an important factor when reconstructing the images, as different algorithms focus on different aspects of the image quality. In this project an iterative algorithm called Ordered Subset Expectation Maximization (OSEM) is used. The OSEM algorithm divides the dataset into a series of subsets, which are used in the reconstruction. Each subset is analysed by an expectation maximum (EM) algorithm, on which the activity is calculated. The resulting reconstruction for each subset is used as the initiation value for the following subset. The first subset needs a guess on the correct image; the guess can be a cylindrical form which represents the body. The number of iterations gives how many times the algorithm runs through all the subsets.[17]. The OSEM algorithm can be described in pseudo-code shown below.

1. m=0, x^m initialised, positive
2. Repeat until convergence of x^m
   (a) $x^1=x^m$, m=m+1
   (b) For subsets i=1:n
   i. *project.*
   Calculate expected values for cumulated counts y as

$$\mu_t^i = \Sigma_{j=1}^J a_{tj} x_j^i \tag{3.8}$$

   ii. *backproject.* Calculate

$$x_j^{i+1} = x_j^i \Sigma_{t\eta S_i} \frac{y_t a_{tj}}{\mu_t^i} / \Sigma_{t\eta S_i} a_{tj} \tag{3.9}$$

[17]

In the pseudo-code above, m represents the iteration number, S the number of subsets and μ is the expected values measured by each detector. x is the image represented in vector form, a is the projection matrix and t is the time.

The OSEM reconstruction method is an iterative method, which means that the quality of the image depends on the number of iterations and subsets. When iterating too few times the image is homogeneous, and when iterating too many times one gets a noisy image. The iteration algorithm for the OSEM reconstruction method is not linear, it is thus not possible to calculate when the image quality is optimal.

The image quality is, however, tried optimized in this thesis. The optimization is based on analyzing a series of reconstructions, from which the best set-up is chosen. This analysis is done in section 5.3.

3.7.1.2 Number of bins

The number of bins used in the reconstruction of the images are of great importance. A bin is a partition of the breath cycle, which can be introduced in two ways. The two possibilities are the amplitude based gating, and the time based gating. The differences of the two gatings are shown in figure 3.4.

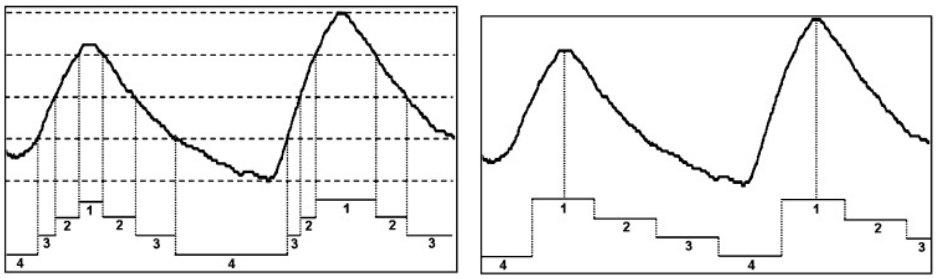

(a) Amplitude based gating (b) Time based gating

Figure 3.4: Amplitude and time based gatings differ in the definitions on the gates, illustrated in figure 3.4a and 3.4b. Taken from [18]

Both set-ups have benefits and drawbacks which takes place in the physiology of the patient and the mathematics in the reconstruction of the images.

The amplitude-based gating is the best gating protocol to use in a hypothetical set-up, but it has drawbacks when used for analysis of patients. This set-up defines the bins on the basis of the amplitude of the breath-cycle, as visualized in figure 3.4a. The breath cycle in this example is divided into four bins, each determined by some arbitrary levels of the breath-cycle.
This is thought to be a great approach, as the translation of the heart depends on the depth of the breath. The diaphragm is not having a great impact on the hearts translation, when breathing superficially. The diaphragm are pushing and pulling the heart in the respective parts of the breath-cycle during profound breath-cycles.
By using the amplitude based gating one is able to detect the position of the heart during hyperventilation, as this breathing pattern is known to be superficial. The entire breath cycle will be within one or two intervals when using the amplitude based gating.

Using the time based gating one is loosing the information on the hearts position when the patient is breathing superficially. The reason for this is that the time based gating divides the breath cycle into a number of bins with the same time-resolution, as seen in figure 3.4b. This set-up has a trigger-level which the breath-cycle must reach to be stored. The scanner is not receiving a trigger to be stored in the LM file if the breath cycle does not reach the trigger level. If this error occurs the computer are estimating one breath cycle to last for two physiological breath cycles. These errors will introduce both blurring and non-true estimates as each bin will contain data from the double time-span.

This indicates that the amplitude-based gating is the best set-up in the perspective of the biological parameters. This is, however, not the case as this gating is suffering in terms of the mathematics in the reconstructions. As shown in figure 3.4a the bins have different time-intervals. The varying time-intervals will introduce poor reconstructions for some bins, which will introduce varying noise levels in the images. These errors cannot be corrected for, when analyzing the data in a dynamic set-up. Due to this the time-based-gating is preferred in the dynamic set-up.

The different set-ups has been analysed by Dawood et al[2], who recommends that one uses the amplitude based gating. Dawood is basing his recommendations on the static images using data from several minutes of scan, which gives a good SNR in all bins due to the many breath cycles.

3.7.1.3 Duration of the scan

The patients were all scanned for a total of 15 minutes. These 15 minutes are reconstructed in different frame-lengths to obtain a dynamic analysis. The gold standard at the hospital are 15 times 60 seconds frames. These frame durations are thought to introduce errors in the gated set-up. The frame durations for the gated set-up will discussed in greater detail in section 5.1.

3.7.1.4 Post-processing of the data

The post-processing of the data is known to have a great influence on the image. Filtrations using a large filtration kernel is known to smooth the images to make the images appear visually appealing. This is, however, known to give underestimated flow values for the healthy tissues. The underestimated flow values are introduced by the reduction in high the activity areas, which are smoothed to the surrounding tissues [19].
This gives a more visually appealing image, which the doctors use for the clinical analysis of the patient.

3.7.2 Bin selection

When reconstructing the gated PET-images it is possible to choose the number of bins the breath cycle is divided into. The number of bins used for the analysis has to be chosen carefully, due to both benefits and drawbacks on the reconstructed images. Below is shown some of the most predominant factors which can either improve the images or introduce more noise.

- ***Partial Volume Effect***

  The Partial Volume Effect (PVE) is a widely known problem when analyzing scans containing data from more than one breath-cycle. This is due to the respiratory movement of the torso, which distorts the heart from the reference image. Any distortion of the images will result in the PVE, as each voxel may contain data from different tissue-types. In this case the PVE will mainly be seen in the outer boundaries of the heart, as these will contain data from the surrounding tissues. Some of the PVE will furthermore be introduced by the finite number of crystals used when measuring the coincidence events. A way to reduce the PVE is to have as many bins as possible as a high number of bins will reduce the continuous motion of the heart within the respective bins. It is, however, not possible to correct for the hearts own movement as the computers cannot reconstruct the data using a dual gated set-up. This restriction is introduced to the computers as a dual gated set-up will give too many bins, each having a poor counting statistics. It is therefore thought impossible to have a good correction for the PVE due to the hearts own motion during the scan.

- ***Estimation on the respiratory movement***

  The estimation on the respiratory movement is thought to be more precise when having multiple bins. This is mainly because the heart is having a continuously translation, where each bin is estimating the average activity within the given part of the breath cycle. A high number of bins will give a better temporal resolution for each image, which will introduce a lower blur in the images. This will furthermore improve the PVE, as explained above. An example of the movement estimated using different number of bins is shown on the next page.

- ***Reduced Signal to Noise Ratio***

  Among the drawback on having multiple bins is the signal to noise ratio (SNR), as the SNR decrease dramatically when the number of bins are increased. This is due to the time length of each bin being shorter and thus containing fewer measured true coincidences. A reduction in the temporal resolution when generating the sinograms will introduce more

noisy images. The number of bins has to be chosen carefully, as the benefits and drawbacks are both having great effect here.

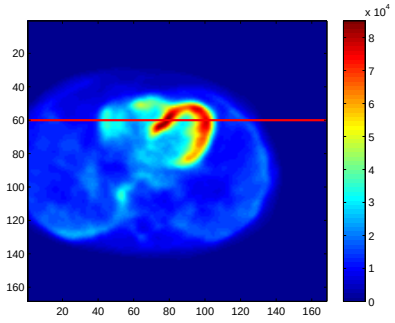

(a) Tomogram of the heart

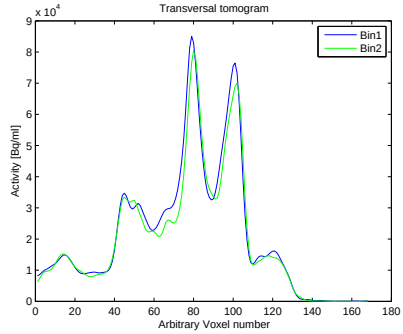

(b) The activities/positions for the given tomogram - 2 Bins

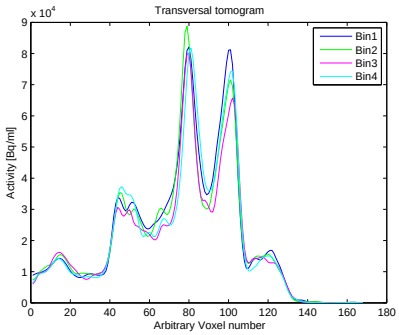

(c) The activities/positions for the given tomogram - 4 Bins

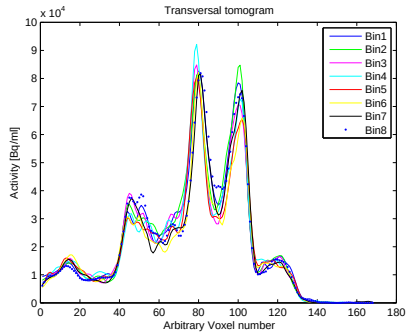

(d) The activities/positions for the given tomogram - 8 Bins

Figure 3.5: Bins in the image reconstruction

On figure 3.5a is a transversal slice of the heart shown. A red line is drawn through the heart, as seen on figure 3.5. Along the red line is the activities from reconstructions using 2, 4 and 8 bins extracted. These activities are shown in the figures 3.5b, 3.5c and 3.5d. In these images the translatory effects are shown in one direction. When analyzing the images above, it can be seen that the peaks are occurring at different voxels numbers. This shows that the heart translates in the sinister-dexter direction during the breath cycle. When analyzing the estimated translations it is seen that an increase in the number of bins increases the estimated translatory motions, which confirms the hypothesis.

3.8 Co-registering of images

The images reconstructed from each bin has to be co-registered in order to correct for the breath-induced movement of the heart. The co-registering of two images are done by choosing a Reference image (R), and a Template (or Target) image (T). The Template image is registered to the reference image in 3 steps, which are explained below:

1. The coordinates in T has to be transformed into R. This can be done by several transformation algorithms. In this project the translation is done by a linear transformation. Among the linear transformations are the rigid transformation and the affine transformation.
2. Measure the dissimilarity of the the registered images. The dissimilarity gives information on how well registered T is to R. There exists several dissimilarity measures. Among the measures often used are the Sum of Squared difference (SSD) and cross-correlation(CC).
3. An optimizing algorithm, which minimizes the dissimilarity. This is required to obtain the best registration possible. There exists several optimizing algorithms. The optimization algorithm used in this project is the simplex method. The simplex method will be explained in greater detail in the optimization subsection.

Each of the three above steps will be explained in greater detail on the next pages.

3.8.1 Transformation algorithms

There exists several Transformation algorithms, as mentioned above. The algorithms mentioned are all widely used in the field of Medical Image Analysis. The rigid transformation is the simplest of the two algorithms. The similarity transformation and the affine transformation are both expanded versions of the simple rigid transformation.

The simple ***rigid transformation*** can be used to register two images which are highly identical. For 3D-images this registration is based on 6 parameters; 3 parameters are assigned to move (translate) the template image into the same coordinate system as the reference image. The other 3 parameters are used to rotate the template image, so that the two image-sets are aligned. The transformation is often written in matrix notation in order to do the transformation correct, as the order of rotation is not insignificant. The matrix notation of a rigid transformation is shown below:

$$y(x; R, t) = Rx + t \tag{3.10}$$

where y(x,R,t) is the transformed voxels from the template image into the reference coordinate system. R is the rotation matrix, and t is the translation of the images.

The equation above is a simple notation of the rigid transformation, which is often used to understand the transformation. However this notation is not used often when implemented into software algorithms as this approach requires two tasks, both a multiplication of a matrix and an addition afterwards. It is possible to reduce the operations to a single multiplication term if the datasets are in a homogeneous coordinate system. This can be done by introducing an additional dimension, which is used to do the transformation of the data. By using this additional dimension the voxels are representing a line in a 4-D space. By transforming the data in the 4D space one is able to align the two images, to have similar coordinate systems. Using this notation the translation is taking place in the 4th dimension, which can be written as

$$t(d_x, d_y, d_z) = \begin{bmatrix} 1 & 0 & 0 & d_x \\ 0 & 1 & 0 & d_y \\ 0 & 0 & 1 & d_z \\ 0 & 0 & 0 & 1 \end{bmatrix} \tag{3.11}$$

when having only a translation in a 3D dataset.

The rotation of the image is done by using the sub 3 by 3 matrix in the upper left corner. A rotation in the z-direction is done by using the following Deformation Field (DF):

$$t(d_x, d_y, d_z) = \begin{bmatrix} \cos\theta & -\sin\theta & 0 & 0 \\ \sin\theta & \cos\theta & 0 & 0 \\ 0 & 0 & 1 & 0 \\ 0 & 0 & 0 & 1 \end{bmatrix} \tag{3.12}$$

where as a rotation around the x-axis can be written as:

$$t(d_x, d_y, d_z) = \begin{bmatrix} 1 & 0 & 0 & 0 \\ 0 & \cos\theta & -\sin\theta & 0 \\ 0 & \sin\theta & \cos\theta & 0 \\ 0 & 0 & 0 & 1 \end{bmatrix} \tag{3.13}$$

and a rotation around the y-axis can be written by the following DF-matrix

$$t(d_x, d_y, d_z) = \begin{bmatrix} \cos\theta & 0 & \sin\theta & 0 \\ 0 & 1 & 0 & 0 \\ -\sin\theta & 0 & \cos\theta & 0 \\ 0 & 0 & 0 & 1 \end{bmatrix} \tag{3.14}$$

By multiplying these 4 matrices one is able to obtain the rigid transformation of two images.

However many body parts are deformed during the scanning procedures, which makes this alignment too crude. Examples of deformable body parts are the lung tissue during respiration, the hearts beating and translation due to the breathing, and bowel movements. These movements are often corrected by the expanded affine transformation.

The affine transformation is still a linear transformation of the template image (T) onto the reference image (R). However this model is able to estimate both scaling differences and skewness (torsion) of the template image. This requires 6 additional parameters, 3 for scaling and 3 to determine the skewness of the images. The notation of the affine transformation can be written using a matrix-notation as 9 of the 12 parameters are transforming T into R notation (scaling, rotation and torsion parameters), and 3 parameters are used for the translation of the images. This gives the following equation

$$y(x; A, t) = Ax + t \tag{3.15}$$

This notation is not used when applying the transformation to the images, as this would require a multiplication and an addition. The DF can be written in the same way as in equation 3.11. The matrix is still having the translation described by the elements (1,4),(2,4) and (3,4). The rotations are described by the same factors as described in equations 3.12 through 3.14. The scaling is applied in the identity of the 3 first columns, and the torsion for the xy-plane can be written as:

$$t(d_x, d_y, d_z) = \begin{bmatrix} s_x & 0 & sh_x & 0 \\ 0 & s_y & sh_y & 0 \\ 0 & 0 & s_z & 0 \\ 0 & 0 & 0 & 1 \end{bmatrix} \tag{3.16}$$

where s_x, s_y and s_z are the scalings in the three directions. sh_x and sh_y are the shearings in the two axes. An equivalent matrix can be sat up for shearing in the x-z plane and in the y-z plane. [20]

This model has previously been used to align 4D breath gated PET images, [21]. In that study it was found that the affine model gives a better estimation on the thickness of the left ventricle than the rigid transformation.

3.8.2 Dissimilarity measurements

There exists several methods to measure the dissimilarity between the Template image and the Reference image, as explained in section 3.8. The dissimilarity measurements mentioned in 3.8 will be explained in greater detail here. Common for all dissimilarity measurements is that they are based on the intensity in the images.

Sum of squared difference

"The sum of squared difference (SSD) is a often used measurement to determine the dissimilarity of two images. The SSD can be expressed by the following equation:

$$D_{SSD}(\omega) = \frac{1}{2}\Sigma_{i\in\Omega}(T(y(x_i,\omega)) - R(x_i))^2 \tag{3.17}$$

, where $y(x_i,\omega)$ is the geometrical transformation of the template image to the reference image. ω are the parameters of the geometrical transformation" [22]. When using the SSD one is assuming that the noise in the images are of Gaussian origin. This assumption is valid for many cases, but there are cases where the noise is of non-Gaussian origin. If the noise cannot be assumed to be Gaussian one is able to use the Cross Correlation dissimilarity measurement instead. In the case of PET-images, the data does not have a Gaussian noise distribution as the data has been found to be Poisson distributed. "This issue can be corrected by a variance stabilizing transformation like the $\sqrt{\cdot}$ or the $\log\cdot$ prior to applying the SSD" [22]. This is due to the common factor of the mean and the variance, λ.

Cross correlation

The cross correlation coefficient is used when the data does not have a Gaussian distribution, which can occur if the scanners are not calibrated. The dissimilarity can be calculated using the following equation:

$$D_{CC}(\omega) = \frac{\Sigma_{i\in\Omega}(T(y(x_i,\omega)) - \bar{T})(R(x_i) - \bar{R})}{\sqrt{\Sigma_{i\eta\Omega}(T(y(x_i,\omega)) - \bar{T})^2\Sigma_{i\in\Omega}(R(x_i)) - \bar{R})^2}} \tag{3.18}$$

, where

$$\bar{T} = \frac{1}{|\Omega|}\Sigma_{i\in\Omega}T(y(x_i;\omega)) \qquad \text{and} \qquad \bar{R} = \frac{1}{|\Omega|}\Sigma_{i\in\Omega}R(x_i)$$

In stead of using this more complicated equation for calculating the dissimilarity of the two images, the data are often normalized to have zero mean and having unit variance. By doing this, it is possible to use the simple SSD approach described above.

3.8.3 Optimizing algorithms

In this project the image transformation is carried out in a software tool called MINC which is available at Rigshospitalet. (BIC- McConnell Brain Imaging Center, Montreal Neurolocial Institute). MINC uses the Simplex optimization algorithm to optimize the image registrations. This optimizing algorithm was found by George Dantzig in 1947, and is widely used in solving of linear optimization processes. The Simplex optimization is a method using boundaries, which are set up by the user. The boundaries, or constraints, are defined by a series of linear equations, which are sat up in a matrix notation. By doing this one is able to find the optimum settings by solving the equations by using Gaussian elimination. This is a linear operation, from which it is possible to find the optimum registration. For the 3D datasets analysed in this report, one is able to optimize in the x-y-z direction, which gives three paths to optimize in. The path that is chosen to be the best is optimized the first until the constraints are met here. When this happens the computer are finding the second best path to optimize in and are doing this until the constraints are fulfilled here and so forth. The MINC software is defining the optimization to be fulfilled when the tolerance level is reduced to 0.005. The software is calculating the tolerance level by using equation 3.19, below.

$$tol > \frac{max(f_{simplex}) - min(f_{simplex})}{(max(f_{simplex}) + min(f_{simplex})} \tag{3.19}$$

, where $f_{simplex}$ is the value of the objective function evaluated at each vertex on the simplex. The objective function is the above mentioned matrix constraints sat up in the mathematical model.[23], [24]

3.9 Statistical analysis

In this thesis the clinical analysis are tried optimized by varying in 3 different factors, the factors being the reconstruction algorithm, the post-filtering of the images and the breath-gated set-up against the non-gated set-up. All the factors are having two possible states, which are a 2mm and a 4 mm filtering, respectively. Furthermore is the data either breath gated, or not. The last factor is the reconstruction of the images. Either are the data reconstructed using the OSEM-reconstruction, or the OSEM-TOF reconstruction algorithm. one is able to set up a 2^k factorial design as each of the factors are having two possible states. In this project are the effect of three parameters analysed, hence a 2^3 factorial design. The factorial designs are having either a plus or a minus, determining which state one is testing for. In this case are a minus representing a 2mm filtration, Non-gated and OSEM reconstructed data, respectively, and vice versa. In this project one is able to set-up the following factorial design.

Filtering	Gating	Reconstruction	Symbol
-	-	-	(1)
+	-	-	a
-	+	-	b
+	+	-	ab
-	-	+	c
+	-	+	ac
-	+	+	bc
+	+	+	abc

Table 3.1: Factorial design of the experiment carried out.

From this design one is able to calculate the effects of the different parameters, by calculating the contrast coefficients. The contrast coefficients for a 2^3 factorial design can be calculated from the scheme on the next page.

	Contrast coefficients						
Symbol	A	B	AB	C	AC	BC	ABC
(1)	-	-	+	-	+	+	-
a	+	-	-	-	-	+	+
b	-	+	-	-	+	-	+
ab	+	+	+	-	-	-	-
c	-	-	+	+	-	-	+
ac	+	-	-	+	+	-	-
bc	-	+	-	+	-	+	-
abc	+	+	+	+	+	+	+

Table 3.2: Contrast coefficients for the 2^3 factorial design

From the above contrast coefficient it can be calculated what the contrast for the respective coefficients are. The individual contrasts are calculated by the equation

$$\text{Contrast} = \Sigma c_i y_i = (\pm(1) \pm a \pm b \pm ab \pm c \pm ac \pm bc \pm abc) \tag{3.20}$$

where one is choosing the contrast coefficients listed in the table above. From the contrasts one is able to estimate the effects of the individual parameters and the sum of squares (SS). The effect of the individual parameters can be calculated by.

$$\text{Effect} = \frac{Contrast}{4n}, \text{n=replicates} \tag{3.21}$$

The equation for the sum of squares are listed below.

$$SS_{Contrast} = \frac{(Contrast)^2}{8n}, \text{n=replicates} \tag{3.22}$$

From the calculations of the Sum of Squares (SS) one is able to fill up an ANOVA table, from which it can be estimated which parameters that are found to be significant. The ANOVA analysis will be explained in the next section.[25]

3.9.1 ANOVA analysis

When testing the outcome of a series of test, using several different variables are the Analysis of Variance (ANOVA) often used. From the analysis of variance it is possible to test if the different factors change the outcome significantly, or if the outcome cannot be differentiated. This can be tested by using the model equation for the ANOVA analysis;

$$Y_{ij} = \mu + \tau_i + \varepsilon_{ij}, \qquad \text{for} \quad i = 1...k; j = 1..n \tag{3.23}$$

In the above equation μ is the overall mean, τ_i the ith treatment effect and ε the random error which occurs in the experiment. This equation can be used to test for the hypothesis if the populations differ. This is done by setting up the null-hypothesis, H_0, which is that all the means are equal. If so, all the τ can be replaced by zeros. This hypothesis is tested against the alternative hypothesis, H_1, which states that at least one of the τ's are non-zero. This gives that the ANOVA analysis is equivalent to the t-test, which can be carried out on tests when having two groups. In the ANOVA analysis one is using an F-test instead of the t-test. The F-test can be calculated by using the equation below

$$F = \frac{\Sigma_{i=1}^{k}(\bar{Y}_i - \bar{Y})^2/(k-1)}{\Sigma_{i=1}^{k}\Sigma_{j=1}^{n_i}(\bar{Y}_{ij} - \bar{Y}_i)^2/(N-k)} = \frac{SS(Tr)/(k-1)}{SSE/(N-k)} \tag{3.24}$$

where $\bar{Y}$ is the grand mean of all the measurements, Y_i is the individual measurements and $N = k \cdot n$. The above calculated F-distribution are having k-1 and N-k degrees of freedom (DoF). The ANOVA analysis can be calculated by using an ANOVA table, which is shown below.

Source of variation	DoF	SS	Mean Square	F
Treatments	k-1	SS(Tr)	MS(Tr)=SS(Tr)/(k-1)	$\frac{MS(Tr)}{MSE}$
Error	N-k	SSE	MSE=SSE/(N-k)	
Total	N-1	SST		

Table 3.3: Factorial design of the experiment carried out.

where $SST = \Sigma_{i=1}^{k}\Sigma_{j=1}^{n_i} y_{ij}^2 - \frac{(\Sigma_{i=1}^{k}\Sigma_{j=1}^{n_i} y_{ij})^2}{N}$,
$SS(Tr) = \Sigma_{i=1}^{k} \frac{(\Sigma_{i=1}^{k}\Sigma_{j=1}^{n_i} y_i)^2}{n_i} - \frac{(\Sigma_{i=1}^{k}\Sigma_{j=1}^{n_i} y_{ij})^2}{N}$ and $SSE = SST - SS(Tr)$
[26],[25]

3.9.2 MANOVA analysis

The ANOVA analysis described in the previous section is analyzing whether or not observations of different factor levels are sampled from the same distribution by analyzing the means for the respective samples for one cardiac region at a time. To obtain these informations one is using a Multiple Analysis of Variance (MANOVA). The MANOVA is a multivariate extension of the ANOVA analysis. The MANOVA is done on vectors of means for the the different groups. [27]

When doing a MANOVA we have a series of stochastically independent variables, which are assumed to be described by

$$\mathbf{Y}_{ij} \in N_p(\mu_i, \Sigma), \quad i = 1, .., k; \quad j = 1, ..., n_i \tag{3.25}$$

where $\mathbf{Y}$ is a matrix containing the observations.

As for the ANOVA the test is sat up on the null-hypothesis that the means of the vectors are equal;

$$H_0 = \mu_1 = \cdots = \mu_k \tag{3.26}$$

against the alternative hypothesis, H_1 that at least one mean is not equal to the others;

$$H_1 = \exists i, j(\mu_i \neq \mu_j) \tag{3.27}$$

As for the ANOVA analysis one is able to set up the sum of squares deviation matrices, which are used to calculate the equivalent to the F-test. The sum of squares are calculated by:

$$\mathbf{Total} = \Sigma_{i=1}^{k}\Sigma_{j=1}^{n_i}(\mathbf{Y}_{ij} - \bar{\mathbf{Y}})(\mathbf{Y}_{ij} - \bar{\mathbf{Y}})' \tag{3.28}$$

$$\mathbf{Within} = \Sigma_{i=1}^{k}\Sigma_{j=1}^{n_i}(\mathbf{Y}_{ij} - \bar{\mathbf{Y}}_i)(\mathbf{Y}_{ij} - \bar{\mathbf{Y}}_i)' \tag{3.29}$$

$$\mathbf{Between} = \Sigma_{i=1}^{k} n(\mathbf{Y}_i - \bar{\mathbf{Y}})(\mathbf{Y}_i - \bar{\mathbf{Y}})' \tag{3.30}$$

where

$$\bar{\mathbf{Y}}_i = \frac{1}{n_i}\Sigma_{j=1}^{n_i}\mathbf{Y}_{ij} \tag{3.31}$$

and

$$\bar{\mathbf{Y}} = \frac{1}{n}\Sigma_{i=1}^{k}\Sigma_{j=1}^{n_i}Y_{ij} \qquad \text{where } n = \Sigma_i n_i \tag{3.32}$$

The Total matrix is calculated by $T = B + W$. It is possible to set up a MANOVA table, as it was done for the ANOVA. For the MANOVA it is sat up to be.

Source of variation	DoF	SS-matrix
Variation between groups	k-1	**B**
Variation within groups	n-k	**W**
Total	n-1	**T**

Table 3.4: Factorial design of the experiment carried out.

In the above table it can be seen that the MANOVA is similar to the ANOVA table in many ways, it is however seen that there exist no F-test for the MANOVA analysis. This is due to the variance-covariance matrix, which is generated in the MANOVA analysis. The SS matrix are instead having a Wishart distribution when analysed under the assumption of normality. The Wishart distribution is a generalization of the χ^2 distribution, which are used for ANOVA analysis. There exists no trivial tests analyzing the Wishart distribution as this distribution is analyzing the multidimensional datasets. There are, however, four estimates which are using different assumptions on estimating the F-test. These are listed below, with a short description of each.

Wilk's lambda (Wilk's Λ), is a widely used F-test approximation which is calculated by the following equation:

$$\Lambda = \frac{\det B}{\det B + W} \tag{3.33}$$

Wilk's lambda is the most common used test when there exists more than two groups, which are formed by the independent variables. We can, however, only use this method when k>2. If k=2 is the rank of the matrix one, hence we are not able to calculate the determinant from the variance-covariance matrix. [28]

When having k=2, as we have in this project, are the three remaining estimates all equal to the Hotelling T^2. The remaining estimates are.

Pillai's trace is considered as the most powerful and robust of the four statistics. Pillai's trace are, as Wilk's lambda, using the eigenvalues of the variance-covariance matrix. The trace is calculated as.

$$\text{Pillai's trace} = \text{trace}(W(W+B)^{-1}) \tag{3.34}$$

The third statistic is the Hotelling-Lawley's trace, which are using the sum of all the eigenvalues in the variance-covariance matrix, which can be written as

$$\text{Hotelling-Lawley's trace} = \text{trace}(B^{-1}W) \tag{3.35}$$

This test is the most common used test, when there exists two groups formed from the independent variables.

The fourth is the Roy's largest root, which are using the largest root in the variance-covariance matrix.

Roy's largest root is often discarded as this gives the upper bound of F, which gives the lower bound of the probability of F. [27], [29]

Chapter 4

Materials and methods

4.1 Breath gating of the patients

The breath cycles in this project are monitored by a pressure belt produced by Anzai medical (Az-733v). This product measures the breath cycles by analyzing the force applied to a sensory head which are monitored inside the belt. The measured pressure is sent to a computer in which the breath cycles are logged. The measured breath cycle compared to the previous breath cycles while they are stored in the computer. From these are the outline of the present breath cycle estimated. The breath cycle is accepted to be a normal breath cycle if the estimate and the actual peak are occurring within a short time interval, which results in a trigger signal is sent to the scanner. The trigger signal is here stored in the listmode file. One is able to choose between three different trigger scenarios which are at; the respiratory peak at inhalation, at expiratory peak, or at both. The respiratory peak is used as the trigger in the chosen set-up. The belt is placed differently on the individual subjects; some patients are breathing mainly with a great motion in the upper abdomen, while others are having the major breath motion around the ribcage. The before mentioned breath cycle measurements are sent to the computer once the belt has been placed correctly. The measured breath cycles are shown on the computer in the software used for the belt. The input (breath measurements) has to be determined within a range of -10 and 125 arbitrary units. One can tune the input by setting the baseline

of the input, and the amplification of the breath-cycle. The amplification is variable from patient to patient, as this is determined by the tightness of the belt. If the belt is too tight, it might give errors in form of erroneous estimated breath-cycles introduced by the tidal volume dead space. However one is having problems with too few breath-cycles if the belt is too loose tightened around the patient. Furthermore one is required to make sure that the respiratory peaks are well above 50 on the arbitrary scale. A lack of this in the set-up will result in a loss of the trigger signals, as the computer only sends out trigger signals when the respiratory peak is above 50.

4.2 Reconstructed data

As mentioned in section 3.7.1 the images are reconstructed using a series of settings. The images used in this project are reconstructed to have:

Attenuation correction

Attenuation correction is needed as many of the photons will be scattered and even taken up in the tissue. The respective alternations of the path of the photon are called the Compton effect and the photoelectric absorption. The Compton effect will alter the path of the photon, when the photon interacts with an electron in the tissue. When undergoing the Compton scattering the photon is having an inelastic collision with an electron, where the photon will deliver some of the energy to the electron. The amount of energy delivered from the photon can be calculated by using the formula.

$$E' = \frac{E}{1 + (\frac{E}{m_0 c^2})(1 - cos(\theta))} \tag{4.1}$$

where E is the initial energy of the photon, m is the mass of the photon, c is the speed of the photon and θ is the angle in which the photon hits the electron. [30] The collision changes the direction of the photon, which will give a false Line of Response (LOR). Furthermore the energy delivered to the scanner crystals will be reduced, which can be used to determine if the photon has changed path during the travel in the body. Due to this is photons within the interval 450keV and 610keV accepted as being "true" photons, while photons having energy outside this interval are discarded as "false" photons.

Besides the Compton effect is the photoelectric effect, which occurs in the dense materials of the body, i.e. the bones. The bones are having many dense atoms such as phosphorous and calcium, which are having many electrons. It is likely that the photon will interact with an electron from the inner shells due to the

high number of electrons in these atoms. The photon might deliver all its energy to the electron, which causes the electron to escape from the atom. This effect gives out radiation in form of Brehmsstrahlung, which is outside the scope of this report. As the photon has delivered all its energy to the electron, the photon is trapped inside the tissue, which gives attenuation.

These two effects can be corrected for by using a low-dose CT scan. This is possible as one is familiar with the energy emitted from the X-ray source. By measuring the energy taken up by the detector, it is possible to calculate the attenuation through the body. This attenuation will also occur on the photons emitted from the decay of the tracer within the body. From the knowledge of the attenuation it is possible to calculate the activity that is present in the body through different reconstruction algorithms.

Furthermore the low-dose CT-image can be used to make a multi-modality analysis of the human body. It can be used to determine the position of hot-spots which might be present if the patient has a tumour. It is not possible to locate the exact position of the hot spot on the PET image, due to the poor anatomical representation. By fusing the PET images with the CT images one is having a great anatomical view, while it is possible to detect pathology in the patient.

Post filtering of the data

The images are post filtered with a Gaussian kernel. The size of the optimum kernel is to be decided later on in this report, due to the different characteristics with the filtration. These characteristics were discussed in section 3.7.1, and will thus not be discussed here.

Triggering options

When reconstructing the images using the breath-gating one is able to choose from a series of possibilities depending on which scanner has been used for the analysis.

On the Siemens Biograph 64 one is able to choose different methods of using the gated set-up. The two possibilities are to use either a percentage deviation from the average respiratory rate, or to choose a lower and an upper number of respiratory rates which are accepted in the reconstruction. From this it is possible to exclude breath-cycles which are known to be erroneous due to different physiological changes throughout the scan. A such erroneous measurement can be introduced if the patient falls asleep during the scan, as this will lower the respiratory rate. This will furthermore give an non-consistent arbitrary trigger level for the scanning of the patient, which will lead to a high rejection rate by

the software that analyses the breathing pattern. Another error can be the motion of one of the arms, as the patient is instructed to keep the arms above the head. This can be painful for the patient, as the patient has to lie in the same position for 20 minutes. This might lead to a small motion in the arms, which are detected by the belt measuring the breath cycle, as this is highly sensitive. This will give an erroneous breath measurement, which will give an erroneous reconstruction of the image.

On the mCT scanner one is having a better opportunity to analyse which respiratory rates that have been measured, as these are shown as a bar plot. For the majority of the patients one is able to see a "normal distribution" of the respiratory rates, which are the normal breathing pattern. Furthermore one is often able to see "outliers" in form of too high or too low respiratory rates, which are introduced by the errors described before.

Reconstruction algorithm

The reconstruction algorithm used in this project is an iterative algorithm (OSEM). The number of iterations and subsets are to be found in the result section, as the images are having different properties depending parameter settings of the OSEM algorithm. Furthermore the images are scatter corrected, and reconstructed to have a global scaling factor. The global scaling factor is used to extract the exact activity in the images, as the DICOM header stores the activity by using 16 bits.

4.3 Registering of the images

In section 3.8 it was described that one can use different transformation algorithms in order to re-align the images. It was explained that one could use either a rigid, an affine or a similarity transformation which is based on translation, rotation and isotropic scaling (i.e. 7 parameters). Finally it is also possible to use 9 parameters, where one obtains an-isotropic scaling, which correct for different scaling properties in the image. Klein et al. ([21]) has described that one obtains the best results by using a full affine transformation. Due to the findings in their analysis is the affine transformation used in this project.

When registering the images in MINC, one is able to choose from a series of parameters such as the measurement of dissimilarity (Cross correlation, Mutal information, among others).

It is assumed that the cross correlation is the best measurement of the dissimilarity, as the images registered in this study all are from the PET scanner. This is due to the nature of the PET images, as the images are highly correlated to each other, i.e. the mutual information will not give a good response.

It is thought required to use a square-root transformation of the images in order to obtain the best image-registration using the cross correlation optimization algorithm. This is due to the quasi-Poisson distribution of the PET images. The images are not having a complete Poisson distribution due to the reconstruction of the data. Assuming a Poisson distribution it is known that the mean and the variance are having the same value, λ. From this it is known that the high-activity areas are having a higher influence by the noise. The heart is having a high mean activity, and thereby a high variance, as the heart is taking up the majority of the ammonia. This might lead to mis-registrations of the images, as the high-activity voxels might be registered to each other, which makes the registrations prone to errors. From this knowledge it is estimated that a transformation of the data may reduce the uncertainty introduced by the variance in the data. This estimate is based on the square-root transformation will have a greater effect on the high-activity areas more than the low activity areas. The data is still having a good contrast to background relationship, which is used to annotate the heart during the registrations.

The co-registering of the images gives out a DF, which can be applied to the non-transformed, from which one obtains a better registration of the images. In figure 4.1 the effect of the square-root transformation of the data is shown.

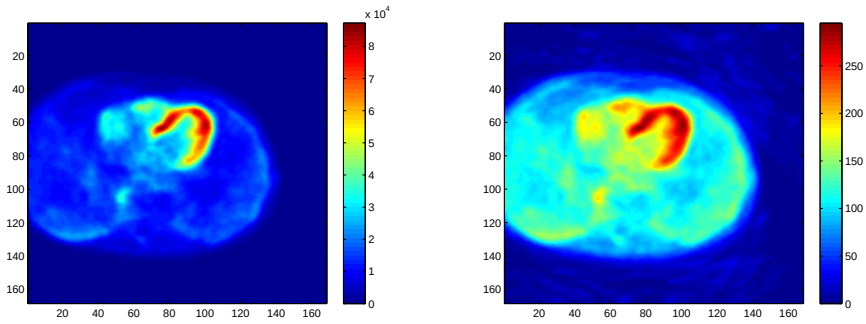

(a) Original data

(b) Square-root transformed data

Figure 4.1: The effect of square-root transforming the data

In figure 4.1 it can be seen that the information in the data is the same. It can, however, be seen that the high-activity areas in the heart is having a more homogeneous appearance, and seems more blurred. By applying this filtration it is known that the noise in the images are reduced, which is thought to give a better image co-registration.

It is required that the images are having similar noise ratios when doing the co-registration of the images, as the noise can affect the registration. When analyzing the dynamic series it can be seen that the noise is varying throughout the scan. This is due to the infusion of the activity. The infusion is given as a continuous infusion lasting 30 seconds, with a 30 seconds wash-out using saline water. Injecting the tracer by a continuous infusion gives a long peak rate, which ensures that the tracer is distributed throughout the heart over a long time. The activity in the blood can be shown as an input-function, which shows the activity level in arterial blood. The input function is changing throughout time as the tracer is taken into the cells (heart, liver tissue, and tissues). Figure 4.2 shows a input function which are derived from the lumen of the left ventricle.

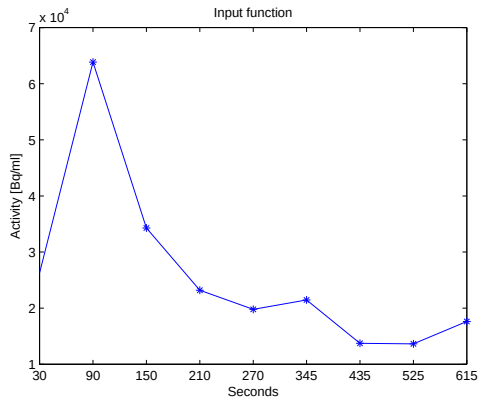

Figure 4.2: Input function for one patient

In figure 4.2 it can be seen that the activity varies with the time. At first the bolus is injected into a vein, from which the bolus is taken to the heart. When the bolus passes through the heart is the blood filled with the tracer, which gives a high peak seen at 90 seconds in the above image. When the bolus has passed through the heart, the activity will be distributed into the aorta arch, from where the activity will be sent to the brain, the arms, the body and the coronary arteries. In this project are we interested in the coronary arteries, as the coronary arteries are responsible for the blood supply to the left ventricle. Some of the tracer molecules will be taken into the myocardial cells, when the tracer is passing through the coronary arteries. This uptake is possible as the tracer is quasi- freely distributed throughout the cells due to the lipid solubility. The tracer not taken up by the myocardial cells will be taken back into the lumen in the heart after passing through the veins. This gives that the tracer not taken into the cells will be diluted, giving a lower activity when the bolus is sent through the heart 2nd and 3rd time. Furthermore some of the tracer molecules will return to the arteries, due to the lipid solubility. These tracer-kinetics leads to a steady activity level seen throughout the scan.

While the activity is taken into the myocardial cells are some of the tracer molecules trapped inside, while others will be freely diffusible between the cells. From this, it is known that the activity will accumulate in the cells after the first passing of the bolus. The accumulation of the tracer within the extravascular space can be shown in a Time-Activity-Curve (TAC). The TAC for a patient studied in this project is shown in figure 4.3.

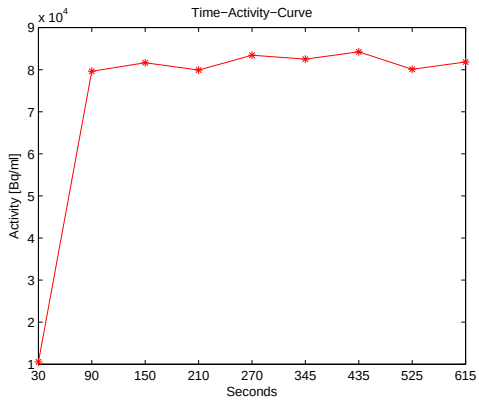

Figure 4.3: Time-Activity-Curve in the heart

In figure 4.3 it can be seen that the activity accumulates in the myocardial cells throughout the scan. By the knowledge of the quasi-Poisson distribution of the PET-data, it is known that the noise is increasing throughout the scan. There is great risks included in co-registering the images frame by frame, as the activity in the images are changing throughout time. This is easily seen when analyzing the data from the first frame against the data from the 7th frame. This is shown in the figures below, where the heart is shown in the transversal plane.

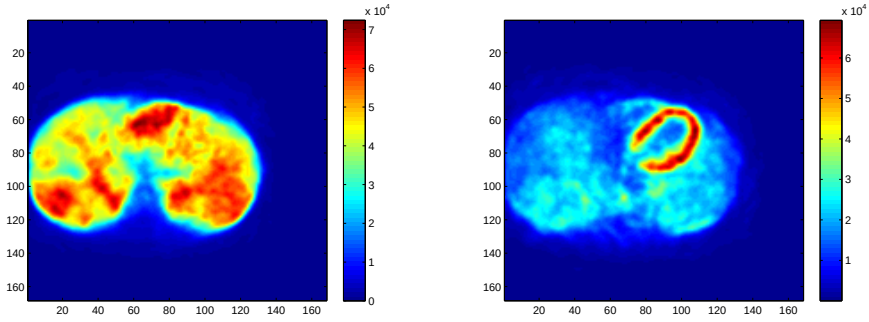

(a) Transversal tomogram of the heart from the first frame

(b) Transversal tomogram of the heart from the seventh frame

Figure 4.4: Dynamic changes of the activity throughout the scan

In figure 4.4 it can be seen that the heart is not visible in the first frame, as the activity is being distributed in the body, as seen in the TAC in figure 4.3. From this knowledge it can be seen that the it is impossible to co-register the first

frame to the 7th frame, as the images are having no similarity. It is estimated that this problem can be corrected using a data for the entire scan instead.

In this project the co-registering of the images are done by using a reference image. The reference image is generated from a static image using the first 11 minutes of the scan. The reference image is produced by co-registering all the bins to the first bin. One is finding the average activity for all the bins when the bins are all aligned in the same coordinate-system. From this one is getting a reference image, to which all the bins are co-registered. By generating a reference image one is reducing the possible errors in the co-registration. An error could occur if the first bin had an erroneous activity within the heart which lead to a mis-coregistering. By using the average of all the bins one is reducing the effect of such errors.

Chapter 5

Results

5.1 Determination of the frame duration

It is of great importance to find the optimum frame-durations for the dynamic series. The frame-durations of the dynamic series has two problems, as discussed briefly in the project description.

Here it was mentioned that the frame duration has to be weighted between the breath-gating of the data and the dynamic information in the data series. From the kinetic models it is known that one has to have a short frame duration in order to obtain the most correct flow values as possible. This is required to obtain a good input function and a precise TAC. A short frame-duration are, however, leading to a poor image-reconstruction when using the breath-gating as the breath-gating is dividing the frame duration into a number of sub-divisions, giving a poor time resolution for each bin.

The gold standard used at the hospital currently is based on a non-gated system, where the dynamic series is based of 15 frames each having a duration of 60 seconds. This has been estimated to give good flow values, when using a non-gated system. This set-up is thought to give poor results when using a breath-gating protocol as the decay of the tracer will reduce SNR in the later frames. The decay of the tracer will result in a lower number of registered coincidence

events per second. A reduced number of measured coincidence events will give a poor sinogram, which will lead to a noisy image. It is estimated that a varying frame-duration will correct for the non-consistent SNR if the later frames are having a longer frame duration than the first frames. It has been estimated that one will obtain a high number of coincidence events within a half of a half-life of the unstable atom. This is equivalent to a 30% decay of the initial activity given to the patient, in this case is this equivalent to an activity of 495MBq within the body.

It is estimated that the activity within the first 5 minutes are sufficient to have a 60 seconds frame duration. From the 5th minute and forth it is estimated that a frame duration of 90 seconds is required to have a good SNR, when generating the binned data.

5.2 Determination of the number of bins

The number of bins have been selected on the basis of the knowledge on the hearts movement. It is expected that the position of the heart is determined the best using multiple bins, as explained in the theory section on the hearts movement. This will reduce the error in the estimated translation of the heart to a minimum, as the position will be monitored more than one time per second, giving a low movement error. Having multiple bins is however considered to introduce errors in the reconstructed images when analyzing dynamic scans because of the short frame duration. Furthermore the breath-gating is only correcting for the breath-induced dislocation of the heart, and not the hearts own motion during the contraction of the heart. This movement is known to move the heart once per second in a rest scan, assuming that the heart-rate is 60 beats per minute. It has been estimated by Dawood et al, [2], that the hearts movement is thought to be estimated the best when dividing the breath cycle into many bins, e.g. 14 bins. Having 14 bins with a respiratory frequency of $1/7$ Hz, will give each bin will have data for half a second. This is under-sampled compared to the heart-rate which will give that the heart is in the diastolic part in one bin (relaxed), and will be in the systolic part (contracted) in the following bin. This gives that the hearts own motion is shown in the reconstructed image, which will give a great deformation of the heart in each bin. By using 4 bins will each bin contain 1.75s of data, which is approximately 2 heart beats per breath cycle. This gives that the translation of the heart is calculated on the mean of the systolic and the diastolic part of the hearts own motion. This is thought to give a more correct estimate of the movement due to the respiratory cycle. From this analysis it is estimated that a total of 4 bins is giving a good approximation of the breath-induced movement of the heart.

5.3 Determination of the reconstruction parameters

One is having multiple parameters to tune when reconstructing the images. One is able to choose from different reconstruction algorithms, such as Filtered Back Projection (FBP), Ordered Subset Expectation Maximization (OSEM) and TrueX. The different reconstruction algorithms are having both gains and drawbacks. The FBP is a simple reconstruction algorithm based on the sinograms which are generated from the listmode file. The gain using this algorithm is the short reconstruction time. The reconstructions are fast, when compared to the iterative reconstructions such as OSEM. The reconstructions are, however, known to have a poor image quality, which origins from streak artifacts and low SNR [31]. In order to reduce these errors it is possible to choose either TrueX or OSEM reconstructions, which does not suffer from streak artifacts. TrueX is a reconstruction algorithm introduced by Siemens, which applies to their scanners using the scanner model to improve the iterations. The reconstruction algorithm is an iterative model, which has similarities to the OSEM. The OSEM model is thought to be superior to the FBP, as this reconstructs the images by iterate the images a number of times defined by the user, see section 3.7.1.

In section 3.7.1 it was described how the different number of iterations and subsets affects the image quality. The optimal setting of iterations and subsets is investigated on the next pages. The optimum number of subsets and iterations are estimated using a static image, reconstructed using data for 15 minutes for a healthy test subject. The optimum settings are chosen using both statistical informations and subjective measurements based on the knowledge of how the perfusion values are estimated. The main analysis of the number of iterations and subsets are based on few iterations, as the reconstruction time is increasing dramatically when the number of iterations are increased. It is estimated that a high number of iterations and subsets are not feasible in the daily clinical praxis due to the long reconstruction time. This is based on the reconstruction computer is used to reconstruct the clinical scans while the patient is scanned. By doing this are the Medical Laboratory Scientists able to analyse if the patient has moved throughout the scan, or if other parameters gives that the patient has to be re-scanned. By having a few iterations and few subsets one is able to reconstruct a frame in order of 10-15 minutes, while a reconstruction of a single frame using 8 iterations and 21 subsets can take up to 30 minutes.

All the images shown in this section are reconstructed using a 2mm FWHM Gaussian filter, using the OSEM reconstruction algorithm. The analysis are done on a tomogram showing the centre of the heart in the transversal plane.

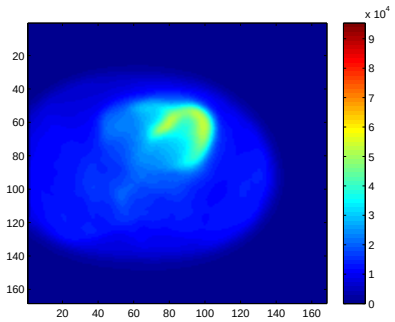

(a) 1 iteration, 4 subsets

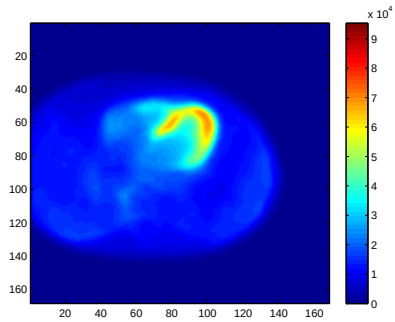

(b) 1 iteration, 8 subsets

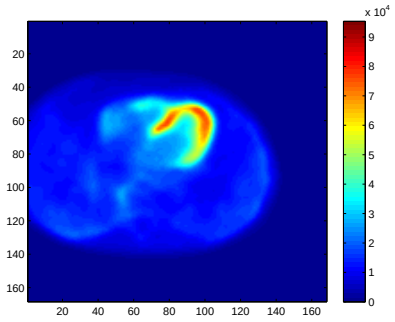

(c) 1 iteration, 14 subsets

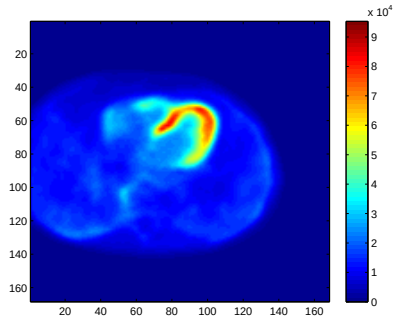

(d) 1 iteration, 21 subsets

Figure 5.1: Reconstructed images using 1 iteration and a varying number of subsets

In the images above it can be seen that the effects of using various numbers subsets are great. It can be seen that the reconstructions using few subsets are more blurry than the images reconstructed by using a large number of subsets. Due to the few number of expectation maximization (EM) calculations was this occurrence expected. By having only 4 EM calculations the image data is not converging towards the correct image, hence the estimated values are based on a crude estimation on the hearts activity. A total of 128 voxel values were extracted in order to analyse the homogeneity of the images. The same voxels were extracted from all the reconstructed images, in order to able to compare the values directly. The results of the analysis of the mean and the variance of the voxels are shown on the next page.

Number of subsets	Mean activity [Bq/ml]	Standard deviation
4	4425	4715
8	5089	5772
14	5111	5942
21	5208	6011

It can be seen that the mean activity is somewhat consistent when using more than 4 subsets. Analyzing the images it can be seen that the heart is having a more distinct curvature when using multiple subsets. Analyzing the reconstruction only having 4 subsets it can be seen that the activity in the lumen is overestimated when compared to the other images. When analyzing figure 5.3b, 5.3c and 5.3d it can be noticed that the thickness of the hearts ventricle is decreasing when the number of subsets are increased. It is estimated that the 21 subsets are giving the best result, when using only 1 iteration. This is based on the flow value is estimated using the activity in the lumen of the left ventricle and in the ventricle wall.

In order to obtain the best image for the analysis is the the same patient analysed using both 2, 3 and 4 iterations using the same number of subsets. These analyses are carried out on the next pages.

Using 2 iterations gave the following image material:

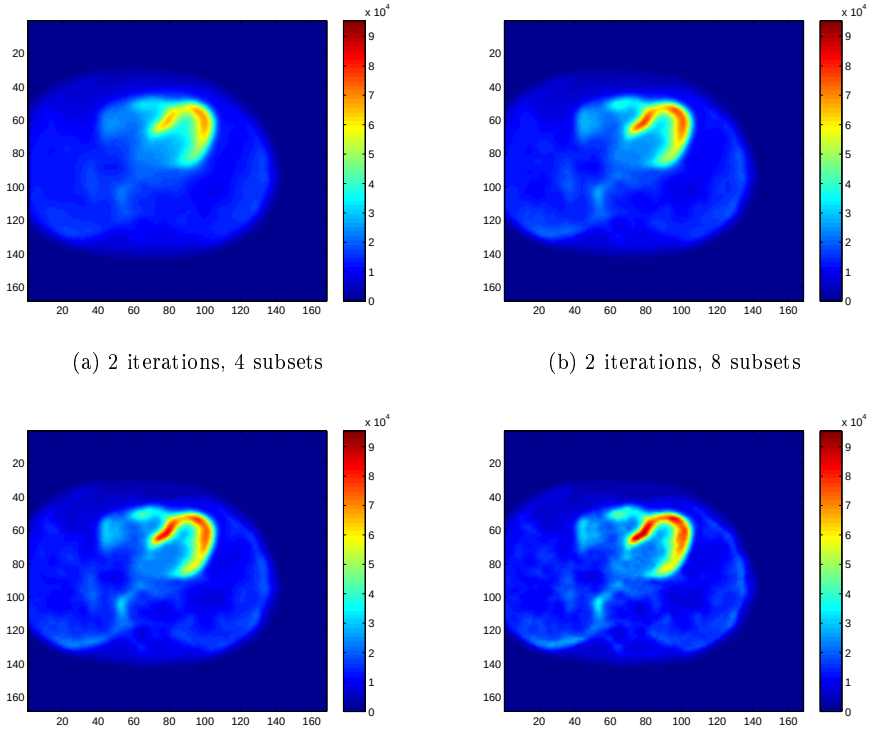

(a) 2 iterations, 4 subsets

(b) 2 iterations, 8 subsets

(c) 2 iterations, 14 subsets

(d) 2 iterations, 21 subsets

Figure 5.2: Reconstructed images using 2 iterations and a varying number of subsets

In the images above it can be seen that the reconstructions are having a similar tendencies as the images reconstructed using 1 iteration. It can, however, be seen that the blurring effects are lower using few subsets, when compared to the images reconstructed using 1 iteration. Analyzing the mean and the standard deviation for the same 128 points, as analysed using 1 iteration, one obtains the following results:

Number of subsets	Mean activity [Bq/ml]	Standard deviation
4	4883	5635
8	5193	5991
14	5147	5984
21	5123	5922

The mean activity and the standard deviation are found to be somewhat similar to the images reconstructed using 1 iteration. However it can be seen that the mean activity and the standard deviation has a tendency to have increased a bit. These changes are results of an increased number of estimations of the activity in the images.

One obtains the images shown below when reconstructing the images using 3 iterations.

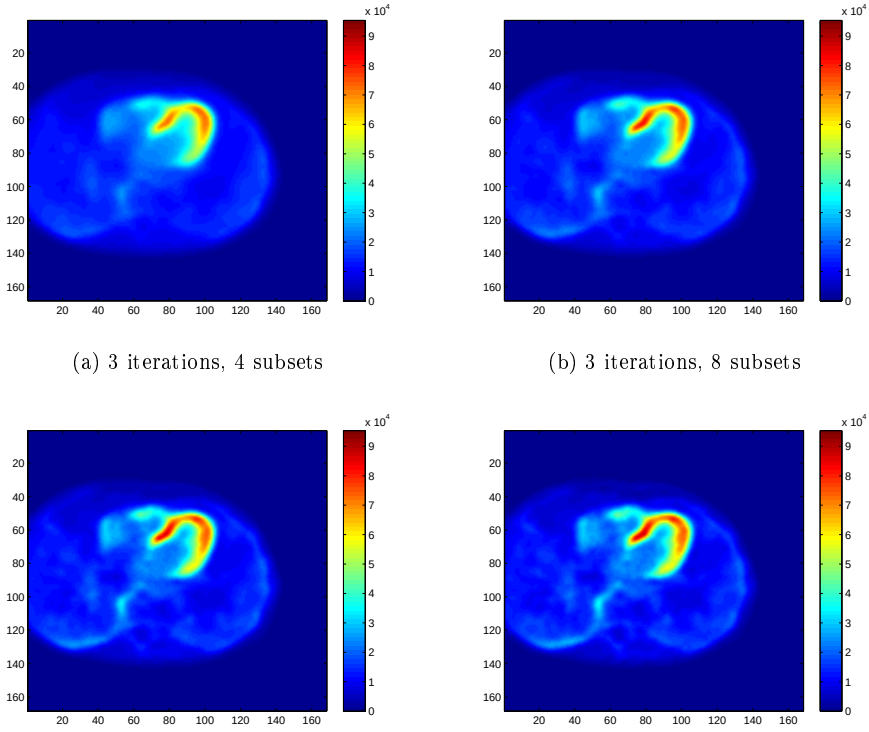

(a) 3 iterations, 4 subsets

(b) 3 iterations, 8 subsets

(c) 3 iterations, 14 subsets

(d) 3 iterations, 21 subsets

Figure 5.3: Reconstructed images using 3 iterations and a varying number of subsets

When analyzing these images it is seen that the image set using 4 subsets is more blurry image than the images having more subsets. This can be seen as the lumen of the ventricle are having a higher estimation of the activity than the lumen in the images having more subsets.

When analyzing the mean activity and the standard deviation of the 128 same voxels as analysed for the other reconstructions one is obtaining the following values:

Number of subsets	Mean activity [Bq/ml]	Standard deviation
4	5315	5916
8	5168	5961
14	5147	5972
21	5106	5903

Analyzing these results it can be seen that both the mean and the standard deviations are found to have a consistent levels. When comparing these results to the results found for images reconstructed using 2 iterations, it is found that the image quality are similar for 8, 14 and 21 subsets. However it can be seen that the activity estimated using 4 subsets are increased.

Below is shown the results using 4 iterations.

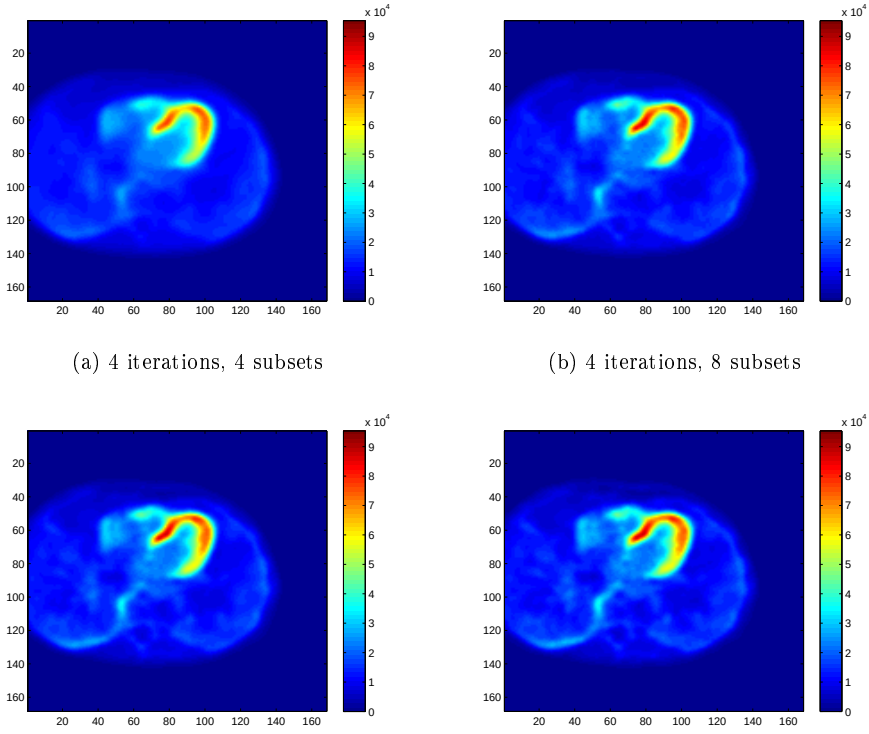

(a) 4 iterations, 4 subsets

(b) 4 iterations, 8 subsets

(c) 4 iterations, 14 subsets

(d) 4 iterations, 21 subsets

Figure 5.4: Reconstructed images using 4 iterations and a varying number of subsets

In the images above it can be seen that reconstructed images are having the same pattern as found for reconstructed images using 1, 2 or 3 iterations. On the next page is shown the mean and the standard deviation for the 128 randomly selected voxels:

Number of subsets	Mean activity [Bq/ml]	Standard deviation
4	5208	5995
8	5164	5987
14	5113	5911
21	5138	5939

Analyzing the mean activity and the standard deviation of the images it can be seen that the images are having similar values for all the reconstructions. However there still is a difference in the images, as it can be seen that the contrast in the images are increasing when the number of subsets are increased.

Using the measured mean activities and standard deviations while comparing them to the contrasts in the images, it can be seen that the images reconstructed using multiple subsets are having a higher differentiation between the heart and the lumen of the left ventricle. From this analysis it is estimated that one obtains the best images for flow determinations when using a high order of subsets, and more than one iteration. From these analyses it is estimated that one obtains the best images using a total of 21 subsets. It is more complicated to chose the number of iterations needed in order to obtain the best contrast. It is estimated that one will obtain the best images using multiple iterations, however it has been found that too many iterations are introducing noise to the images. [19]. They found that one should at least use 6 iterations with 28 subsets, in order to obtain the best images for Cardiac PET scans using ^{13}N-NH_3. As the reconstruction time increases dramatically with the number of subsets and iterations it is found to be impossible to implement these recommendations in the daily clinical praxis. It is therefore estimated that one should use a maximum of 4 iterations and 21 subsets, as these reconstructions takes approximately 20 minutes per frame. An image based on 8 iterations and 21 subsets were reconstructed in order to find the optimum number of iterations. The optimum number of bins were determined by analyzing the percent wise difference between the images reconstructed 2, 3 and 4 iterations when compared to the image reconstructed using 8 iterations. The percent wise differences are shown in figure 5.5:

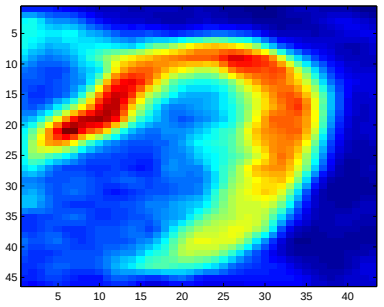

(a) 8 iterations 21 subsets (Gold standard)

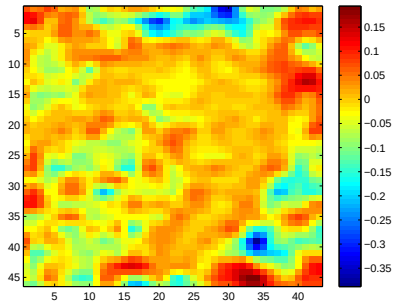

(b) Percent wise difference - 2 iterations

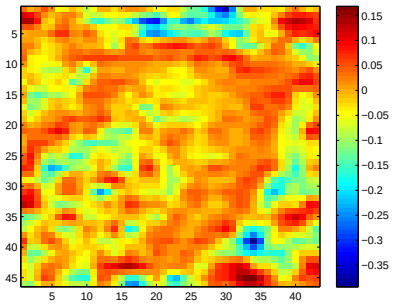

(c) Percent wise difference - 3 iterations

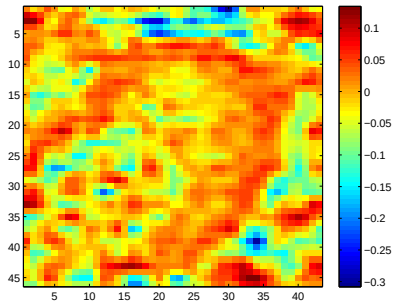

(d) Percent wise difference - 4 iterations

Figure 5.5: Percent wise difference between the 8 iterations and 2, 3 or 4 iterations, with 8 iterations as gold standard

In the images above it can be seen that the percent wise difference is lowest for the data using 4 iterations. This was expected, as these the data has had more estimations to converge towards the gold standard. With these results, and a consultancy with Philip Hasbak, it was determined one will get the best images using 4 iterations and 21 subsets.

By choosing 4 iterations and 21 subsets one is avoiding that the image quality is compromised due to the usage of too few iterations [19]. In the same study it was found that a too high post filtration of the images might give too low Myocardial Blood Flow (MBF) estimations, as filtering with a high FWHM is reducing the activity in the high activity areas. This problem is analysed in section 5.7.

5.4 Image co-registration

As explained in section 4.3, the co-registrations of the images is performed by generating a reference image from the average of all the bins, after registering the remaining bins to bin 1. The reference image is generated upon images reconstructed using data for eleven minutes of the scan. In section 5.2 it was estimated that the optimum number of bins is 4. The effect of the co-registrations will be analysed in this section.

The effect of the breath gating is shown in figure 5.6. The images are showing the mean activity for the first 11 minutes of a patient having a normal blood flow.

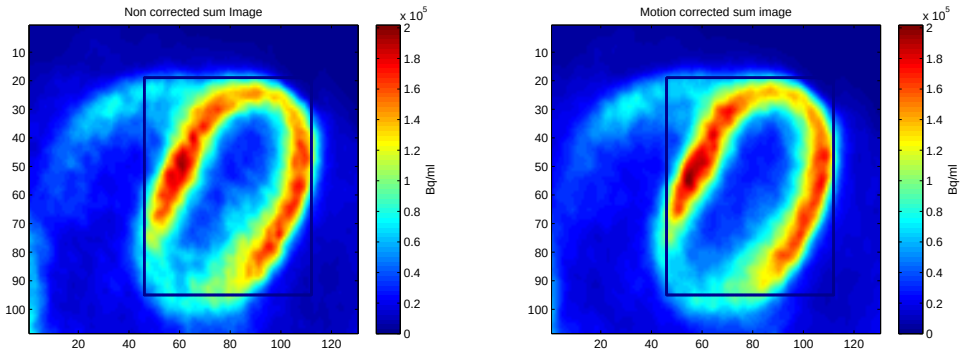

(a) Non-gated data (Gold standard)

(b) Motion corrected data

Figure 5.6: Effect of the breath gating for the dynamic data

The rectangles shown in figure 5.6 shows the outer boundaries of cardiac walls for the motion corrected image. When analyzing the non-gated image in figure 5.6a it can be seen that basal part on the left-hand side has moved towards the centre of the rectangle. Furthermore it can be seen that appearance of the heart has changed when introducing the motion correction. This can be noticed several places on the two images, which will be discussed on the next pages:

It can be noticed that the hot area found on the left basal part (towards the opening in the heart) has changed both appearance and size. On the non-gated image it can be seen that the hot area has small oval appearance, while it has a elongated outline on the motion corrected image. From this it can be seen that the breath-gating changes the appearances of the high-activity areas. The hot area is estimated to be more correct in the motion-corrected image, as the breath

induced motion is corrected in this image. The non corrected image is generated by summarizing the activity levels for all the parts of the breath-cycles, without any correction. This gives a blurring of the images, hence a reduced activity estimate. The reduced activity estimate can be seen by analyzing the colormap of the two images, where the motion corrected images are found to have a higher activity estimate. This will be discussed in greater detail later in this section.

The second difference that one can notice are regarding the blurring of the images. When analyzing the cardiac wall it can be seen that the non gated image are having multiple sections, each containing some hot areas, which are connected by lower activity areas. This can be seen in the area around (x=50;y=110) on the non-corrected image. When analyzing the motion corrected image it can be seen that the cardiac wall is more homogeneous. The increased homogeneity is estimated to be more correct due to the correction for the breath induced movement, as the patient is known to have a healthy heart.

A third difference is the activity estimated at the basal part of the heart in the lumen (at (90;60)), which is the area Simens Syngo uses to extract the input function for the flow estimate. On the non-corrected image it can be seen that this area has a high activity, which is blurred on the entire area, where the motion corrected image has a more correct appearance, as this area is known to have a low activity as this is a part of the low-uptake area in the heart.

A fourth area where a difference can be seen is the outline of the right ventricle, which has a low uptake. The right ventricle can be seen as the arch which is connected to the apical part on the left-hand side of the heart. On the non-corrected image it can be seen that the wall is blurred into the lumen of the right ventricle. The lumen of the right ventricle on the motion corrected image is having a more distinct difference between the lumen and the cardiac wall. The outline of the right ventricle is important when estimating the flow in the heart, as the input function from the right ventricle is used in the PMOD software, which is a research tool used for dynamic analysis.

In figure 5.7 below is shown the activities measured in each bin which, when summarized, generates the activity measured in the respective frame. The activities shown on figure 5.7b, 5.7c, and 5.7d are sampled along the dark line shown on figure 5.7a.

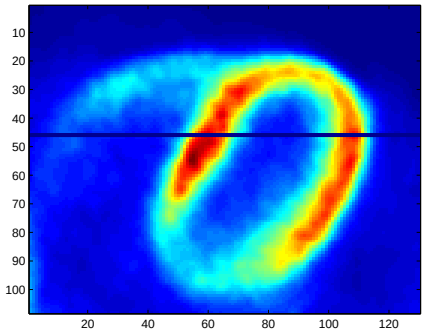

(a) Tomogram of the cardiac appearance. The data is estimated through the dark line

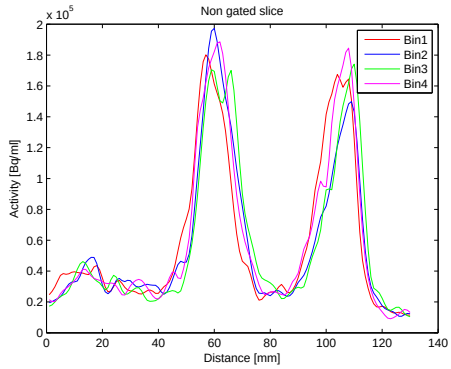

(b) Non corrected data used to generate the image

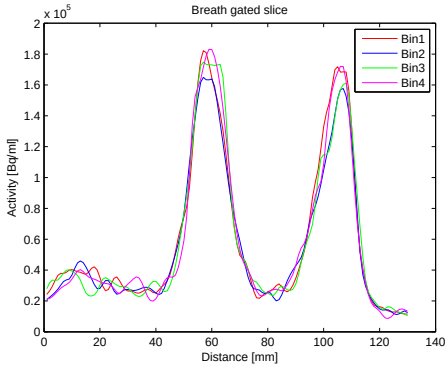

(c) Motion corrected data used to generate the image

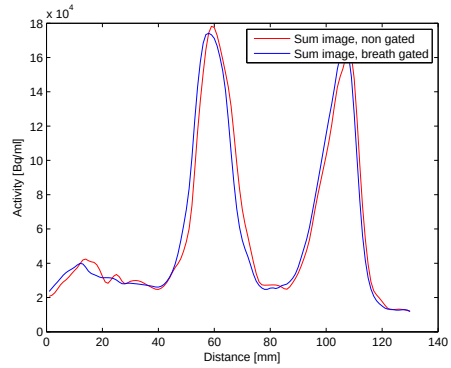

(d) The activity outline from the summarized image

Figure 5.7: Effect of the breath gating for the dynamic data

Figure 5.7b shows the motion of heart during the breath cycle in one dimension. It can be seen that the cardiac wall moves up to 4mm from bin to bin, which gives a great dislocating factor of the heart. In a non-gated set-up the activity of the heart and the lumen in the left ventricle will be estimated used a summation of the four bins. When applying the breath-gating one is able to estimate the average motion of the heart throughout the breath cycle. When correcting for the motion of the heart one is obtaining the activity line shown in figure 5.7c. In

this figure it is visible that the breath gating are correcting the peaks position to a uniform peak. This gives a more homogeneous image, as the cardiac wall is having the same activity levels when inside the cardiac wall. This can be noticed when analyzing the homogeneity of the 4 bins in figure 5.7b and 5.7c, where the cardiac wall is more homogeneous on the breath gated image. When analyzing the activity levels in the two reconstructions one is able to see that the activity levels are differing in both activity and appearance. This is due to the dislocating factors on the heart during the breath cycle. The non-corrected image is therefore containing data from different parts of the heart, as the patient has been estimated to have a high translatory motion throughout the breath cycle. The translation estimated for this analysis is shown in the table below.

Translation [mm]			
Bin number	X-direction	Y-Direction	Z-Direction
1	2.19	-0.39	0.40
2	4.38	0.99	0.69
3	3.69	-0.22	0.97
4	1.60	1.37	-0.34

Table 5.1: Deformation fields applied to the breath gated data

From the translations shown in table 5.1 it can be seen that the motion is found to be large for this patient. This gives that the found activity levels for the non-gated activity levels are estimated to be erroneous. From this it is estimated that the breath gating of the patient has resulted in a better flow estimate, as the motion has been estimated to be of great importance.

5.5 Measured Breath-motion

The patients analysed in this project were scanned in two different scanners. This may give different contrast levels in the images, as the scanners are having different specifications on the crystals. Furthermore the two scanners are having different set-ups on the reconstruction algorithms. The patients analysed in the Siemens Biograph 64 scanner are reconstructed by using 4 iterations and 21 subsets, where the patients scanned in the Siemens mCT scanner is reconstructed using 4 iterations and 24 subsets for the OSEM-reconstruction. The mCT scanner is also having the possibility of reconstructing the images using the OSEM-TOF algorithm. The images reconstructed by using this algorithm is done by 2 iterations and 21 subsets. The lower number of calculations are due to the faster convergence of the data. Furthermore the images are reconstructed using either a 2mm FWHM Gaussian filter, or a 4mm FWHM Gaussian filter. These different set-ups are known to have different effects on the reconstructed images, giving a different estimate on the translations between the different bins. The different translations will be analysed in this section. All the translations given in this section are translations measured as both a 3D-motion, and a craniocaudal motion. The 3D-motion gives information on the general motion in the 3D space, while the craniocaudal motion tells about the effect of the diaphragm. Furthermore the latter is also telling on the possible errors measured in the apical part, as this area is 2mm in diameter [32]. If the translatory effect are greater than 1mm, the apical part is averaged over the activity in the bloodpool, the myocardium and the pericardial-sac. This will give a non-correct estimate of the activity in this part, hence one will obtain a non-true flow estimate for this part.

The estimated translations between each bin are shown in the table below.

Average translation, Rest [mm]				
	2mm Filtration		4mm Filtration	
Translation	OSEM	OSEM-TOF	OSEM	OSEM-TOF
Craniocaudal motion	0.58 ± 0.40	0.65 ± 0.58	0.76 ± 0.95	0.80 ± 0.80
3D motion	1.22 ± 0.63	1.30 ± 0.82	1.47 ± 0.97	1.55 ± 0.82
Average translation, Stress [mm]				
	2mm Filtration		4mm Filtration	
Translation	OSEM	OSEM-TOF	OSEM	OSEM-TOF
Craniocaudal motion	0.68 ± 0.36	0.99 ± 0.32	0.36 ± 0.25	0.94 ± 0.66
3D motion	2.38 ± 1.15	1.89 ± 0.68	1.26 ± 0.40	1.90 ± 0.70

Table 5.2: Average translations between each bin.

In table 5.2 it can be seen that the translations are quite different, depending on the direction in which they are analysed. The standard deviations for the craniocaudal motions are found to be large, which witnesses of a great difference in the motion between the respective bins for the respective patients. It is seen that the craniocaudal translation for the OSEM-TOF reconstruction is estimated to have an average translation on 0.99mm, which indicates that the breath-motion using this reconstruction is great. From this it is estimated that the flows estimated using the non motion corrected data might give some erroneous flow values. The motion for the patients analyzed in this project is found to be low, when compared to the litterature. Martinez-Möller et al. found an translation on 3.1 ± 1.5mm for the apical translation, using an reconstruction AW-OSEM protocol of 4 iterations and 8 subsets. The differences between the translations found in this project, and in the project by Martinez-Möller might be caused by differences in the patient population. They analysed a total of 6 patients (age 61 ± 13 years), who were referred for diagnosis of coronary artery disease.[18] Furthermore they were investigating 6 patients using ^{18}F-Flurodeoxyglucose(FDG), for oncology examination. This might give some different results, as the patients analysed in their study were not all analysed for cardiac purposes. The age of the patients is, however, not thought to introduce any errors (in this study: 58 ± 15 years). This may imply that the patients analysed in this project are having a low respiratory depth, while they are scanned.

The 3D-motions for the patients are found to be rather low, when compared to the article. In the study by Martinez-Möller it was found that the average motion of the heart was 4.9 ± 1.3 mm for the rest studies, and 5.0 ± 2.7mm for the stress studies, when using ammonia as a tracer. This is a high translation, when compared to the motions found in this study. Here the maximum translations were found to be 1.55 ± 0.82mm for the rest study and 2.38 ± 1.15 for the stress study. These low-motion translations might be introduced by the difference of the diseases, as explained in the craniocaudal examination. The differences might also be introduced by the fact, that the patients were not instructed to breathe in a certain pattern. This gives a more natural breath-motion, which may reduce the air in- and exhaled during the breath-cycle. This will lead to a reduced motion of the heart, as the heart is not pushed and pulled by the diaphragm.

5.6 Input functions and Time Activity Curves

The flow values are calculated using the kinetic models described in section 3.3. The kinetic models uses the activity measured in the blood and the myocardial tissue to determine the flow in the left ventricle. This is done by the IF's, as mentioned briefly in section 4.3. It is of great interest to check how the IF's and the TAC's are changing when both the filtration and the reconstruction algorithm changes.
The IF's, and thereby the TAC's, has different outlines depending on the transport phenomena within the patients body. This gives that the peaks are occurring in different frames for the respective patients. In this section the analysis is carried out on the images having the peak activity within the first frame, as the same pattern is found for the patients having the peak in the second frame.

Below is shown the average IF's and TAC's for the patients reconstructed with the different set-ups. In these images it is possible to see how the respective activity estimates vary with the different parameters. From the analysis it is possible to analyse how the different reconstruction algorithms changes the estimated flows. The images below is showing the IF's for the non-gated set-up and the gated set-up, respectively.

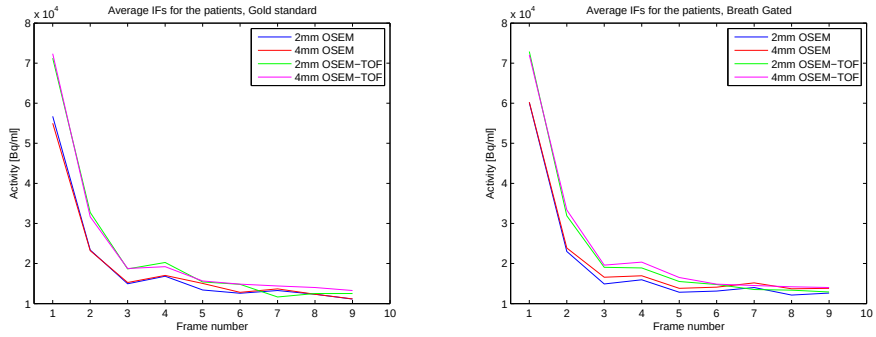

(a) Average IF's, Gold standard

(b) Average IF's, Breath gated

Figure 5.8: Average IF's for the patients having a rest-scan

Two tendencies can be seen in the above figures. The first tendency seen is that the 2mm and the 4mm filtrations are having similar activity estimates for the respective reconstruction algorithms. This was expected as the activities measured for the blood is measured for the blood pools in the images. The box extracting the blood activity is placed at the basal part, near the left atrium. This gives a steady estimate of the activity in the blood, as no tissue components

are having an effect on the estimated activities. The second tendency seen is the OSEM and the OSEM-TOF activity estimates are having different activity estimates within the first 4 frames. The different activity estimates are estimated to be due to the improved activity estimate when using the OSEM-TOF reconstruction.

Below is the TAC's for the same patients analysed, again separated into the non gated set-up and the gated set-up.

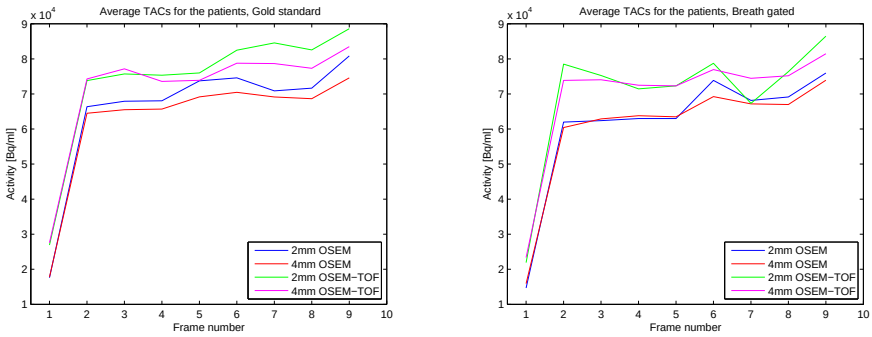

(a) Average TAC's, Gold standard

(b) Average TAC's, Breath gated

Figure 5.9: Average TAC's for the patients having a rest-scan

In the above figure two things are noticeable. The first is the initial activity for the breath gated set-ups are having a reduced activity, when compared to the respective TAC's for the non-gated set-up. This is explained by the stabilized position for the heart in the gated set-up, where the non-gated set-up will move during the breath cycle. This will give that the heart will be in position of the lumen of the left ventricle in a partition of the time for the non-gated set-up, giving a higher activity estimate. Furthermore one is able to see that the OSEM-TOF-activities are estimated to have higher activities for all the frames, which witness on a better estimate of the activity within the heart, due to the reduced attenuation in the body. Again it can be seen that the average TAC is having similar activity estimates for the respective reconstructions in the breath-gated set-up, while the non-gated set-up seems to have a more differing activity estimate throughout the later frames. The measured activities are used in the kinetic models to estimate the perfusion in the heart. By comparing the TAC to the IF it is possible to analyse if an area is suffering from ischemia, due to a reduced TAC activity when compared to the normal myocardial cells.

5.7 Flow values in the left ventricle

The flow values calculated for one of the patients will be analysed in this section. The patient analysed in this section is expected to suffer from the Takotsubo cardiomyopaty, giving this patients is of great interest to analyse. This is due to the knowledge on the hyper-perfusion in the majority of the heart, where the apical parts of the heart is known to have normal perfusion. It is of great interest to analyse if the size and appearance of the Takotsubo area has changed. Furthermore the possibilities are that the flow has altered, when analysed in different set-ups and with different filtrations. The patient is known as patient number 6 throughout the rest of this report, where further analysis are carried out.

The analysis of the remaining patients can be found in Appendix B. The measured flow values for the remaining patients are listed later in this section.

The patient analysed in this section is a 40 year old female, who are scanned in order to establish whether she is suffering from Takotsubo cardiomyopathy or a myocardial infarction. This is not known from the other studies conducted on the patient, as it is not possible to differentiate from the two diseases using the conventional measurements. The patient was reconstructed using both a 2mm and a 4mm filtration and a conventional OSEM reconstruction and the OSEM-TOF reconstruction method. The OSEM reconstruction were performed using 4 iterations, 24 subsets, where the OSEM-TOF reconstruction were conducted using 2 iterations, 21 subsets due to the faster convergence. The analysis will be split into two sections, one for the 2mm filtrations, and one for the 4mm filtrations. The two different set-ups will be compared when the analysis has been fully conducted.

In figure 5.10 are the polar plots for the reconstructions using a 2mm filtration shown.

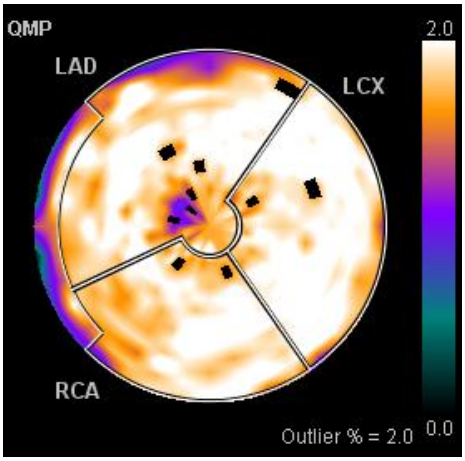

(a) Polar plot of the estimated flow values using the non-gated set-up

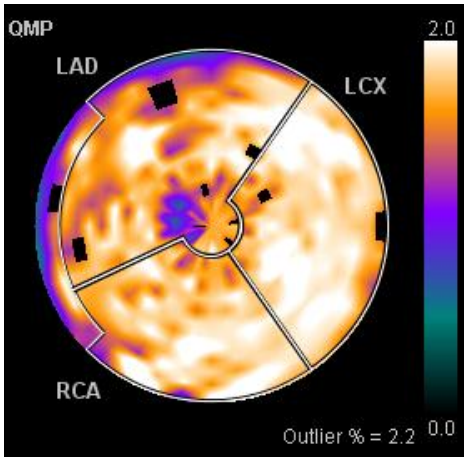

(b) Polar plot of the estimated flow values using motion corrected data

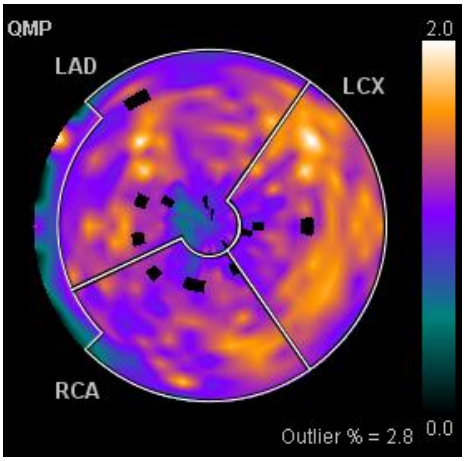

(c) Polar plot of the estimated flow values using the non-gated set-up with the OSEM-TOF reconstruction algorithm

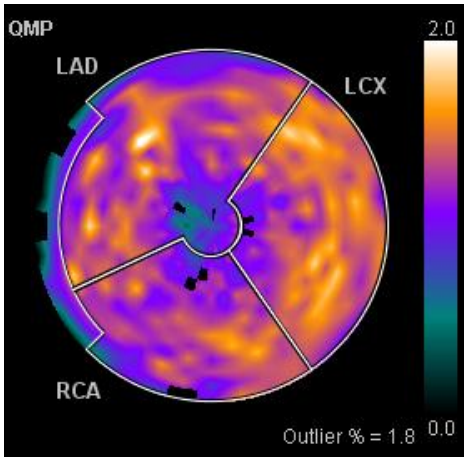

(d) Polar plot of the estimated flow values using motion corrected data using the OSEM-TOF reconstruction algorithm

Figure 5.10: Flow analysis from Siemens Syngo using a 2mm FWHM Gaussian filter

In the above polar plots are the bars indicating the flow values in ml/g/min. Furthermore the black squares are representing outliers, which are having flows that are outside the normal range. These are found by the program, and are not included in the analysis of the estimated mean flow values for each segment.

The polar plot has 540 sub-segments, each representing the mean flow within the given area of the heart. Of the 540 areas are 522 included in the analysis, as the two outer rings marked in the RCA and LAD area are excluded from the analysis. This is due to these areas are mainly connective tissues, which has a low uptake. The flow in these areas are excluded as these will reduce the mean activity measured within the given regions. Each of the segments are having different sizes, the LAD area is having 274 areas, the LCX 132 and the RCA is based on the average of 116 areas. These are based on how great part of the heart the respective coronary arteries are supplying with blood.

In the polar plots shown in figure 5.10 one is able to see the effects of the change in estimated flow values when varying the reconstruction algorithm and the gating set-up. Below is the most interesting changes analysed.

The flow values are found to change when using the different reconstruction algorithms (OSEM and OSEM-TOF). In the OSEM reconstructed data, the flow values are found to be higher in the entire ventricle than the flow values estimated when using the OSEM-TOF reconstruction. These changes are explained in greater details when the input functions (IFs) and Time-activity-curves (TAC's) are analysed. Furthermore it can be seen that the area with Takotsubo are changing size, and appearance when applying the breath gating on the OSEM reconstruction algorithm. In this case is the area determined to be greater when correcting for the breath induced movement. The change of size can be explained by the motion of the heart has been stabilised, giving that the TT area is having no spill-in effects from the neighbouring voxels. A such spill-in is induced by the shift of the hearts position, giving the high flow areas are within the area of the TT area for a fraction of the breath-cycle which increases the mean activity found for this area. This is thought to occur in the non-gated set-up. When analyzing the OSEM-TOF reconstructed images are the OSEM-TOF area found have the same appearance in the two images. In table 5.3, the measured mean flows in the 3 segments, and the global flows shown, are shown.

	Flow values in ml/g/min			
	Normal Reconstruction		TOF Reconstruction	
Region	Non gated	Breath Gated	Non Gated	Breath Gated
LAD	1.79	1.60	1.14	1.14
LCX	1.96	1.87	1.34	1.37
RCA	1.88	1.79	1.20	1.23
Global	1.86	1.72	1.21	1.22

Table 5.3: Flow values for 2mm filtered data shown in figure 5.10

In table 5.3 it can be seen that the flow-values found for the different reconstruction algorithms differ rather much. Furthermore it can be seen that the flow values are reduced for the breath gated set-up when compared to the non-gated set-up for the OSEM reconstructed data. The origins of these changes can be found when analyzing the IF's and the TAC's for the different set-ups. These are shown in figure 5.11, below.

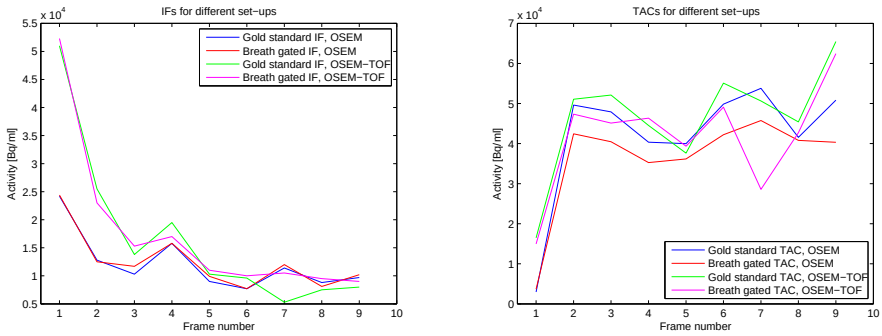

(a) Input functions for the images reconstructed using the conventional and the OSEM-TOF re-construction

(b) Time-activity curves for 25 voxels in the apical part of the heart

Figure 5.11: Input functions and Time-Activity-Curves for the patient using a 2mm filtration

In the above figure it can be seen that both the IF's and the TAC's are having different outlines depending on the reconstruction algorithm. When analyzing the IF's in the initial frames it can be seen that the activity estimates differs depending on the reconstruction algorithms. The difference is seen to be a factor of two between the two reconstructions, which has a major impact on the estimated flow as the OSEM-TOF reconstructions estimates a higher amount of tracer present in the blood. The relative uptake in the tissue are greater for the OSEM-reconstructions, giving a higher flow estimate when analysed. When analyzing the initial activity for the IF's it can be seen that the OSEM reconstructions are having a low amplitude, which are only 10000 Bq/ml higher than the later frames. This is known to be erroneous, as the input functions are extracted from the blood in the basal part of the heart. The patient is given a continuous infusion of the activity over a period of 30 seconds, which gives that the activity measured in the heart is expected to be more than 25000 Bq/ml in the initial frame. When analyzing the IF's from the OSEM-TOF reconstructions it is seen that the initial frames are estimated to have a high activity, which is having a higher correlation to the theoretical input functions. From this it is estimated that the OSEM-TOF reconstructed images are having a more correct estimate of the activity in the initial frames.

When analyzing the TAC's the same patterns are seen for this patient in the first frame. Here it is seen that the OSEM-TOF reconstructed images are estimated to have an activity of approximately 15000 Bq/ml, where the images from the OSEM reconstructions are estimated to have an activity of 3000Bq/ml. In the later frames it is seen that the activity levels are approximately the same. However it is noticed that the breath gated images are having a tendency to have a lower activity than the non-gated images. Due to this tendency the flow estimates for the breath gated data using the OSEM reconstruction method are estimated to have a reduced flow, when compared to the non-gated set-up. When analyzing the OSEM-TOF reconstruction algorithm it can be seen that the flow values are highly identical, which is reflected in the IF's and the measured TAC's. It can be seen that the two curves for the OSEM-TOF reconstruction algorithm are interchanging throughout the entire scan, which gives the similarity in the flow estimates.

From this analysis it can concluded that the OSEM-TOF reconstructions are thought to give the best estimates for this patient. The difference between the breath-gating and the non-gating is found to be minimal for this patient. This is correlated to the deformation fields found for this patient were exceptionally low, as the motion were almost not detected. However the motion was great enough to be able to measure some minor deformations giving some changes in the estimated flow values.

The patient was also analysed using a 4mm filtration on the same images in order to optimize the analysis. It is of great interest to investigate which filtration that gives the most clinical correct flow values. In a paper wrote by Chen et al. [19] it was estimated that one should use a filter with filtration that gave correct flow values, and not use a filter with a too high FWHM blurring effect. The polar plot for the 4mm filtered data is shown in figure 5.12, shown on the next page. In these images it can be seen that the outline of the Takotsubo area is changing both size, and appearance depending on the gating and the reconstruction algorithm. Analyzing the non-gated set-up without breath-gating it can be seen that the flow values are estimated to be high in all segments, where the Takotsubo area is the only area, except the very basal part of the heart, which are having flow values below 1.8 ml/min/g. When applying the breath gating, it can be seen that the general flow-estimate is reduced in all three segments. The Takotsubo is estimated to have the same flow-values, as for the non-gated set-up, while the surrounding area is estimated to have a reduced perfusion. This estimates the outline of Takotsubo area to be larger, which is implying a great defect in the heart.

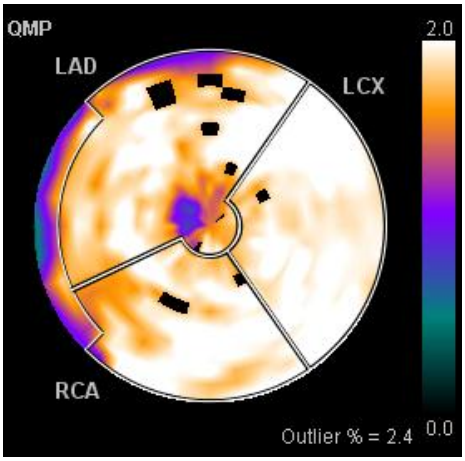

(a) Polar plot of the estimated flow values using the non-gated set-up

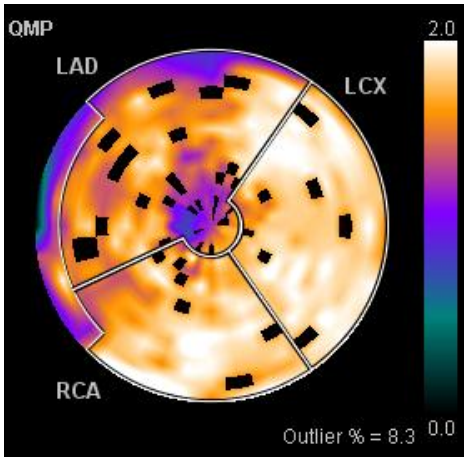

(b) Polar plot of the estimated flow values using motion corrected data

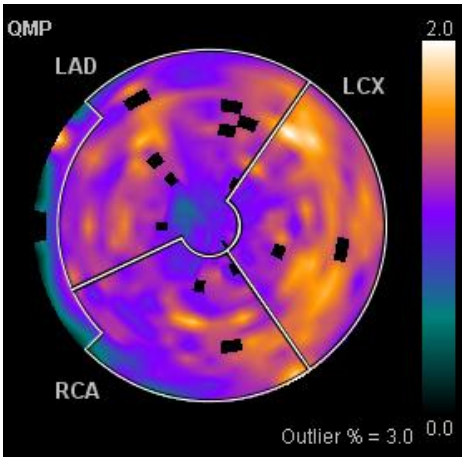

(c) Polar plot of the estimated flow values using the non-gated set-up with the OSEM-TOF reconstruction algorithm

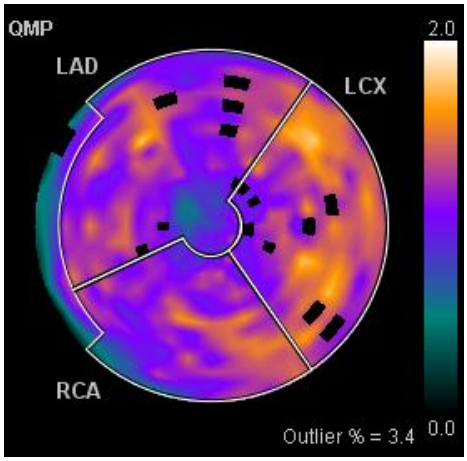

(d) Polar plot of the estimated flow values using motion corrected data using the OSEM-TOF reconstruction algorithm

Figure 5.12: Polar plots from Siemens Syngo using a 4mm Gaussian filtration.

A completely different outline of the flow values are seen when one is using the OSEM-TOF reconstruction algorithms. For these images the flow values are estimated to be within the normal range, around 1-1.2 ml/min/g. The Takotsubo area is in these images defined to have a hypo-perfusion value which is estimated to be around 0.4 ml/min/g. The estimated flow values are shown in table 5.4 , shown on the next page.

	Flow values in ml/g/min			
	Normal Reconstruction		OSEM-TOF Reconstruction	
Region	Non gated	Breath Gated	Non Gated	Breath Gated
LAD	1.72	1.49	1.14	1.08
LCX	1.97	1.85	1.34	1.32
RCA	1.91	1.78	1.19	1.17
Global	1.83	1.67	1.21	1.16

Table 5.4: Flow values for the examination using a 4mm filtration, as shown in figure 5.12

In the above table it can be seen that the flow analysis using the OSEM reconstruction algorithm will classify the patient to suffer from Takotsubo, while the images reconstructed using OSEM-TOF will classify the patient to have recovered from the Takotsubo cardiomyopathy. The TT area will in these images be estimated to have a reduced flow indicating that the patient is recovering from the Takotsubo cardiomyopathy.

It is of great interest to analyse the IFs and the TACs for the 4mm filtered images, as the diagnosis of the patient is based on these curves. The curves are shown in figure 5.13, below.

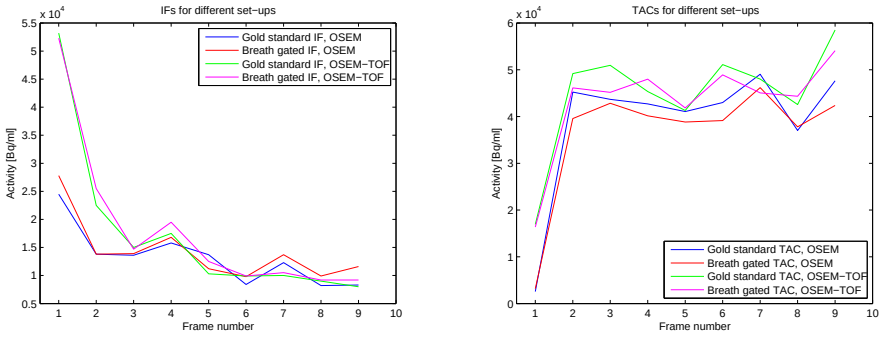

(a) Input functions for the images reconstructed using the conventional and the OSEM-TOF re-construction

(b) Time-activity curves for 25 voxels in the apical part of the heart

Figure 5.13: Input functions and Time-Activity-Curves for the patient using a 4mm Gaussian filtration

In the above figures it is seen that both the IF's and the TAC's are having the same appearance as it was seen for the data having a 2mm filtration. For the 2mm filtered images it was analysed that the OSEM-TOF was having the best

estimate of the activity in the initial frame, due to the known distribution of the bolus. Based on these conclusions it is estimated that the same is valid when using the 4mm filtration. When analyzing the estimated flow values for both the filtrations and the reconstruction algorithms, it is seen that the same pattern is visible in both cases. The flow values are estimated to be reduced for the 4mm filtration, when compared to the flow values for the 2mm filtration. This reduction in the flow values can be introduced in two ways, either by the outliers which are estimated by the software or the difference in the filtration. The difference in the percentage of outliers may reduce the mean flow values a bit for some of the regions, depending on the numbers of the estimated outliers. The second change, the filtration, is known to give reduce the variance in the estimated activity and thereby giving a more homogeneous flow-estimate in the regions. The differences in the estimates are found to be of no significance, when analyzing the 2mm or the 4mm filtration. The effects of the different set-ups will be analysed in the statical analysis in section 5.10.

Analyzing the OSEM-TOF against the OSEM reconstruction algorithm, it can be seen that the flow values changes greatly. Using the OSEM reconstruction it can be seen that the patient is suffering form Takotsubo, while the OSEM-TOF reconstructions are estimating the patient to have a minor increase in the flow in the LCX segment. The other segments are estimated to have normal flow-values, which changes the diagnosis from acute Takotsubo to a recovery of the Takotsubo cardiomyopathy. Based on the found IF's and TAC's it is estimated that the conventional reconstruction algorithm is underestimating the activity in the first 2 frames, which gives a non-correct high flow estimate in all 3 segments. By this analysis it is estimated that the OSEM-TOF reconstruction algorithm is giving the best estimate for this patient.

5.7.1 Flow values for the different patients

5.7.1.1 Patient number 1

This patient is a 71 year old woman having a 3 months control scan after being diagnosed with Takotsubo cardiomyopathy. She had a rest-scan performed at the Siemens Biograph 64 PET/CT scanner. The normal rest-flows are within the range 0.6-1.2 ml/g/min. This scanner are only able to reconstruct the data using the OSEM-reconstruction. The flow values found for this patient is shown in the table below.

	Flow values in ml/g/min			
	2mm Gaussian filtration		4mm Gaussian filtration	
Region	Non gated	Breath Gated	Non Gated	Breath Gated
LAD	1.58	1.78	1.52	1.69
LCX	1.51	1.64	1.44	1.57
RCA	1.71	1.90	1.65	1.84
Global	1.59	1.77	1.53	1.70

Table 5.5: Flow values for a rest study using either a 2mm or a 4mm filtration on the Siemens biograph 64 scanner

Analyzing the above table, it can be seen that all the flow values are exceeding the normal limits for the rest-studies. The flow values are estimated to be correct from the thoroughly analysis of the measured flow analysis, which can be found in appendix B.1. This implies that the patient has not recovered completely from the Takotsubo cardiomyopathy.

5.7.1.2 Patient 2

This patient is a 41 year old woman having a 3 months follow-up scan after being diagnosed with Takotsubo cardiomyopathy. The patient was scanned in the Siemens Biograph 64 scanner, hence only the OSEM-reconstruction is available. The estimated flow values for this patient is listed below.

	Flow values in ml/g/min			
	2mm Gaussian filtration		4mm Gaussian filtration	
Region	Non gated	Breath Gated	Non Gated	Breath Gated
LAD	1.38	1.05	1.36	1.04
LCX	1.60	1.31	1.62	1.35
RCA	1.11	0.91	1.14	0.90
Global	1.38	1.09	1.38	1.09

Table 5.6: Flow values for a rest study using either a 2mm or a 4mm filtration on the Siemens biograph 64 scanner

When analyzing the estimated flow values above, it can be seen that the majority of the flows are within the normal range for the breath-gated set-up. The flow values for the non-gated set-up are however estimating the LAD and the LCX to have a hyper-perfusion. This implies, when using the breath-gated data, that the patient has nearly recovered from the disease. The same conclusion cannot be drawn from the analysis for the non-gated set-up, as these analysis are estimating the flow values to be too high for two of the three segments.

5.7.1.3 Patient 3

This patient is a 74 year old woman having a 3 months follow-up scan after being diagnosed with Takotsubo cardiomyopathy. This scan was performed in the Siemens mCT scanner where it is possible to reconstruct the images using the OSEM reconstruction and the OSEM-TOF reconstruction. For this patient the flow were estimated using both reconstruction algorithms, using both a 2mm and a 4mm FWHM Gaussian filtration. The first table covers the flow estimates using the OSEM-reconstruction, while the second table shows the OSEM-TOF flow estimates.

	Flow values in ml/g/min			
	2mm Gaussian filtration		4mm Gaussian filtration	
Region	Non gated	Breath Gated	Non Gated	Breath Gated
LAD	1.01	0.94	1.05	0.95
LCX	0.98	0.92	1.03	0.97
RCA	0.93	0.88	0.98	0.94
Global	0.98	0.92	1.03	0.96

Table 5.7: Flow values for a rest study using either a 2mm or a 4mm filtration on the Siemens mCT scanner, using a OSEM reconstruction method

	Flow values in ml/g/min			
	2mm Gaussian filtration		4mm Gaussian filtration	
Region	Non gated	Breath Gated	Non Gated	Breath Gated
LAD	1.12	1.05	1.11	1.06
LCX	1.09	1.02	1.09	1.05
RCA	1.01	0.96	1.02	1.01
Global	1.09	1.02	1.08	1.04

Table 5.8: Flow values for a rest study using either a 2mm or a 4mm filtration on the Siemens mCT scanner, using a OSEM-TOF reconstruction method

Analyzing the flows for both the OSEM - and the OSEM-TOF reconstructions it can be seen that the flow values has stabilised to within the normal range. It is, however, seen that the OSEM-TOF reconstructed data is estimated to have a higher flow than the OSEM reconstructed data. Furthermore it is seen that the breath gated data seems to have a tendency to have a reduced flow estimate, when comparing to the respective flow estimates for the non-gated set-up. A further analysis of this is carried out in appendix B.3.

5.7.1.4 Patient 4

This patient is a 54 year old female, who is thought to have ischemic heart disease. Due to this is the patient having both a rest and a stress scan carried out. From the two scans are the doctors able to estimate if the patient is suffering from IHD. The doctors are able to give the diagnose IHD if the flow-reserve (flow in stress divided by the flow in rest) is below a factor of 2.5. Both the scans were carried out at the Siemens mCT scanner, from which an analysis using both OSEM and OSEM-TOF reconstructed data was analysed. Due to the differences in the flows in the rest and the stress are the flows for the rest-scan situation shown below. The flows for the stress scan are analysed on the next page.

	Flow values in ml/g/min			
	2mm Gaussian filtration		4mm Gaussian filtration	
Region	Non gated	Breath Gated	Non Gated	Breath Gated
LAD	0.94	1.11	1.00	1.15
LCX	0.95	1.09	1.00	1.12
RCA	0.93	1.08	0.99	1.12
Global	0.94	1.10	1.00	1.14

Table 5.9: Flow values for a rest study using either a 2mm or a 4mm filtration on the Siemens mCT scanner, using the OSEM reconstruction method

The estimated flows for the OSEM-TOF reconstruction method is shown in the following tables:

	Flow values in ml/g/min			
	2mm Gaussian filtration		4mm Gaussian filtration	
Region	Non gated	Breath Gated	Non Gated	Breath Gated
LAD	1.09	1.13	1.10	1.15
LCX	1.07	1.11	1.07	1.14
RCA	1.10	1.15	1.08	1.18
Global	1.08	1.13	1.09	1.16

Table 5.10: Flow values for a rest study using either a 2mm or a 4mm filtration on the Siemens mCT scanner, using a OSEM-TOF reconstruction method

Analyzing the flows above it can be seen that all the flows are within the normal range for the rest-studies. Furthermore it can be seen that the OSEM-TOF reconstructions are having a tendency to have a higher flow estimate, than the respective flow estimates for the OSEM reconstruction. A further analysis of this will be carried out in appendix B.4.

Below is shown the flow analysis for the patient. The stress scans are having normal flow values, when the blood flow exceeds 2.5ml/g/min.
Below is the flow values from the OSEM reconstructed data shown first, followed by the flow values from the OSEM-TOF reconstruction.

	Flow values in ml/g/min			
	2mm Gaussian filtration		4mm Gaussian filtration	
Region	Non gated	Breath Gated	Non Gated	Breath Gated
LAD	3.44	3.36	3.66	3.66
LCX	3.73	3.66	3.85	3.77
RCA	3.58	3.63	3.80	3.81
Global	3.55	3.51	3.75	3.73

Table 5.11: Flow values for a stress study using either a 2mm or a 4mm filtration on the Siemens mCT scanner, using the OSEM reconstruction method

	Flow values in ml/g/min			
	2mm Gaussian filtration		4mm Gaussian filtration	
Region	Non gated	Breath Gated	Non Gated	Breath Gated
LAD	3.36	3.38	3.29	3.31
LCX	3.52	3.55	3.43	3.49
RCA	3.32	3.39	3.18	3.28
Global	3.39	3.43	3.30	3.35

Table 5.12: Flow values for a stress study using either a 2mm or a 4mm filtration on the Siemens mCT scanner, using the OSEM-TOF reconstruction method

All the flow values are found to meet the criteria sat up for the stress scan. From this it can be seen that eventual ischemic areas are affecting only a minor part of the heart. A further analysis of this patient is found in appendix B.4.

5.7.1.5 Patient 5

This is a 67 year old woman, who were examined to estimate whether or not she suffers from ischemic heart disease. Due to this was she having both a rest and a stress study. She were, however, falling asleep during the rest scan. This altered the breath cycle throughout the scan, leading to a non-measurable breathing pattern, hence the breath-gating from the rest scan was impossible. She was scanned at the Siemens mCT scanner, hence she had an analysis using both the OSEM and the OSEM-TOF reconstruction. The estimated flows, using the OSEM reconstruction is shown first, followed by the flows for the OSEM-TOF reconstruction.

	Flow values in ml/g/min			
	2mm Gaussian filtration		4mm Gaussian filtration	
Region	Non gated	Breath Gated	Non Gated	Breath Gated
LAD	2.40	2.29	1.97	1.92
LCX	3.29	3.10	2.19	2.12
RCA	3.16	3.08	2.30	2.25
Global	2.82	2.70	2.11	2.06

Table 5.13: Flow values for a stress study using either a 2mm or a 4mm filtration on the Siemens mCT scanner, using the OSEM reconstruction method

	Flow values in ml/g/min			
	2mm Gaussian filtration		4mm Gaussian filtration	
Region	Non gated	Breath Gated	Non Gated	Breath Gated
LAD	2.08	2.63	1.97	1.83
LCX	3.11	3.26	2.07	2.01
RCA	2.82	3.60	2.16	2.09
Global	2.54	3.03	2.04	1.95

Table 5.14: Flow values for a stress study using either a 2mm or a 4mm filtration on the Siemens mCT scanner, using the OSEM-TOF reconstruction method

For this patient, it is seen that she do not fulfil the criteria sat up for the stress scan for all the reconstructions but one. This implies she may suffer from ischemic heart disease. The flow values are analysed further in appendix B.5, where the flows will be analysed.

5.7.1.6 Patient 6

This patient is a 40 year old woman, who was scanned to check if she had either a myocardial infarction or the Takotsubo cardiomyopathy. Due to this was the patient only having a rest scan. The scan was performed at the mCT scanner, hence both a OSEM and OSEM-TOF reconstruction was done for this patient. The flow values for the different set-ups are shown below.

	Flow values in ml/g/min			
	2mm Gaussian filtration		4mm Gaussian filtration	
Region	Non gated	Breath Gated	Non Gated	Breath Gated
LAD	1.79	1.60	1.72	1.49
LCX	1.96	1.87	1.97	1.85
RCA	1.88	1.79	1.91	1.78
Global	1.86	1.72	1.83	1.67

Table 5.15: Flow values for a rest study using either a 2mm or a 4mm filtration on the Siemens mCT scanner, using a conventional reconstruction method

	Flow values in ml/g/min			
	2mm Gaussian filtration		4mm Gaussian filtration	
Region	Non gated	Breath Gated	Non Gated	Breath Gated
LAD	1.14	1.14	1.14	1.08
LCX	1.34	1.37	1.34	1.32
RCA	1.20	1.23	1.19	1.17
Global	1.21	1.22	1.21	1.16

Table 5.16: Flow values for a rest study using either a 2mm or a 4mm filtration on the Siemens mCT scanner, using a OSEM-TOF reconstruction method

In the above table, it is seen that the patient is estimated to have a increased flow for the normal filtration, indicating Takotsubo cardiomyopathy. The flow values for the OSEM-TOF are, however, indicating a normal flow. A further analysis of the flow values are needed to give the diagnosis for the patient. This analysis were carried out in the previous section.

5.8 Flow values using a restricted respiratory rate

The flow estimates listed in section 5.7 were estimated using all the measured breath cycles. This is known to introduce some errors in the measured activity, as the sensory head is very sensible to minor changes in the pressure. The errors can be introduced by minor motions of the arms during the scan, or coughing which will alter the translation of the heart while coughing. On the mCT scanner one is able to see a bar plot, showing the respiratory rates. From this plot it is possible to determine which breath-cycles that are within the normal interval. By analysing the normal respiratory rate, it is possible to discard outliers, which are introduced by the above described problems. When discarding the outliers, one is reducing the number of respiratory rates which can be used to reconstruct the images. Furthermore is the reconstruction program (LM-replay) discarding the sub-sequential 3 breath cycles after each discarded breath-cycle. This can give huge problems, which is described below.
Using the restricted set-up on a patient having 12 breath cycles per minute, where one outlier is detected within the first frames, results in the estimated flow is based on data collected for 40 seconds. The loss of 20 seconds of data is having a huge influence on the estimated activity in the initial frames, where the most of the kinetic information is present. Unfortunately the patients are having most of the erroneous measurements in the initial and the ending minutes of the scan. The errors in the initial phase of the scan is due to nervousness and the need to adjust the position to lay more comfortable. The later is also the reason for the increased erroneous measured breath cycles in the latter minutes of the scan.

A patient scanned on the mCT scanner will be analysed using a restriction on the accepted respiratory rate. The patient analysed here (number 3) is a patient who had a erroneous estimate of the breath-pattern in the first frame, which has a major impact on the estimated flow values. Another patient (Patient number 6) is also analysed with a restricted set-up. The analysis for this patient can be found in appendix C.1

In the polar plots below, it can be seen that the flow estimates are erroneous as all the flows are above 2ml/min/g. These flow values are exceeding the normal range by a factor of 1.5, indicating that the restricted respiratory rate has introduced further errors.

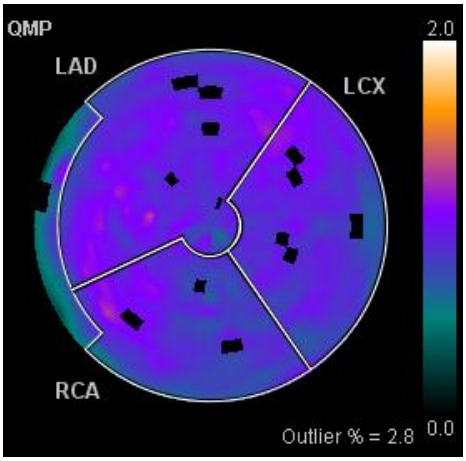

(a) Polar plot using the breath-gated data from the 2mm OSEM-reconstructed data.

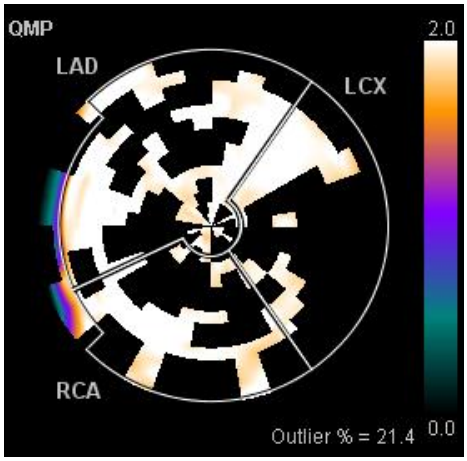

(b) Polar plot using the breath gated data from the 2mm OSEM-reconstructed data using a restricted respiratory rate.

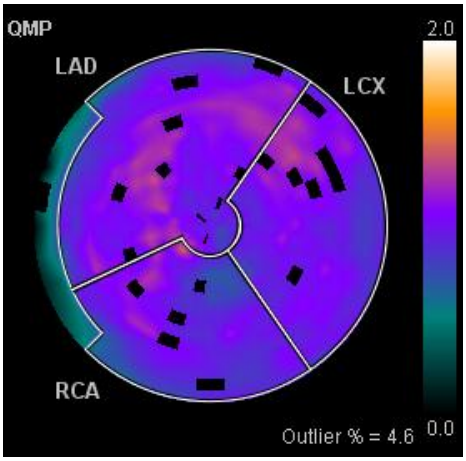

(c) Polar plot using the breath-gated data from the 2mm OSEM-TOF reconstructed data.

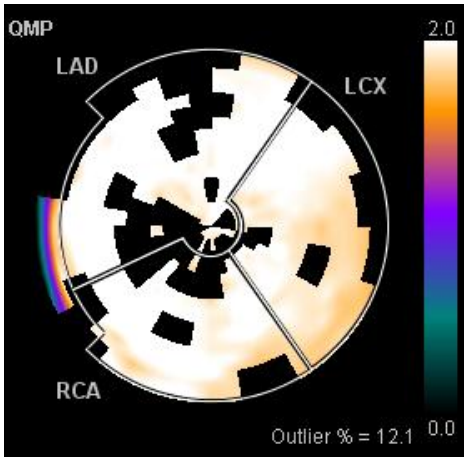

(d) Polar plot using the breath-gated data from the 2mm OSEM-TOF reconstructed data using a restricted respiratory rate.

Figure 5.14: Flow analysis from Siemens Syngo comparing the breath gated data and the restricted breath-gated data

In the polar plots in figure 5.14, it can be seen that the flow values for the reconstructions using either OSEM or OSEM-TOF differs greatly. Furthermore it can be seen that the outlier rate is increasing, when using the restricted breath-gating. The measured respiratory rates for this patient is shown in figure 5.15, below.

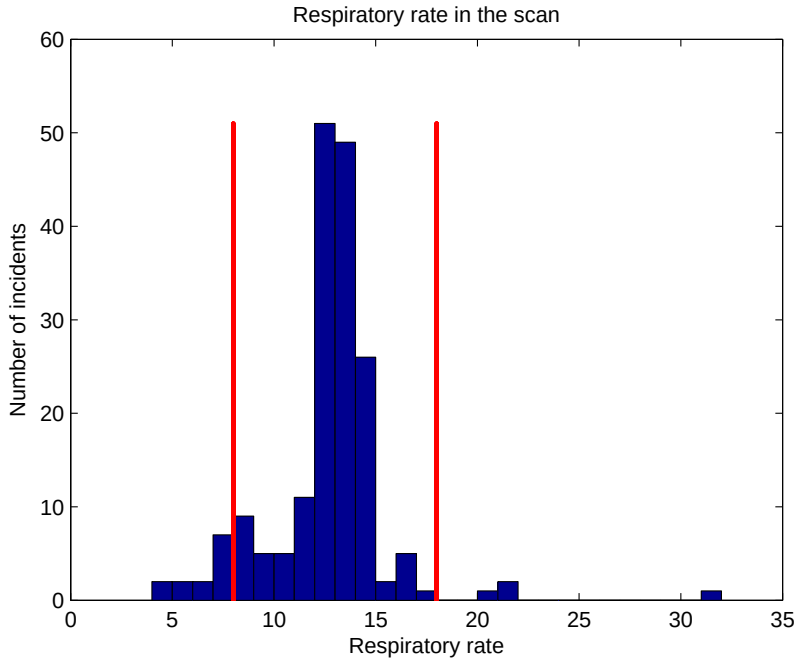

Figure 5.15: Respiratory rate for patient number 3

In figure 5.15 it can be seen that the respiratory rate is having a sort of a normal distribution of the respiratory rates, centred around 12 breath cycles per minute. Furthermore it is seen that the respiratory rate is having outliers, both below and above the cut-off. The outliers above the cut-off, represented by the red lines, are introduced by minor motions in the arms of the patient. These are measured due to the high sensitivity in the sensory head monitored inside the belt. The respiratory rates below the cut-off are estimated to occur from deep respirations. This error will introduce a greater dislocation of the heart, giving the flow analysis would benefit from leaving these breath cycles out of the analysis.

On the next pages the effects of leaving out breath cycles will be analyzed. A plot showing the respiratory measurements are shown for all the frames analysed. These plots are having three sub-plots, as seen in figure 5.16.

The leftmost plot are showing the measured breath cycles, with the gating measurements shown as the red bars. From this one is able to estimate which breath-cycles that has been discarded due to some non-accepted events. The upper-right image shows the respiratory rates in form of a bar-plot, showing the total number of respiratory rates that are outside the accepted interval. There might be more non-accepted measurements, than the summed number of breath cycles discarded(4 per non-accepted breath cycle). This is introduced as only the first of two consecutive measurements are used when discarding the breath cycles, giving a total of 4 rejected breath cycles. The lower right plot shows the measured breath cycles which are discarded within the given frame. The number of respiratory cycle shown on the x-axis is based on the number of red bins shown in the left-most subfigure. From this it is possible to see which breath-cycles one is loosing information from when applying the restrictions.

The first frame has been found to be inflected by the restriction on the respiratory rate, as one breath cycle did not reach the trigger level. This is shown in the figure 5.16, below.

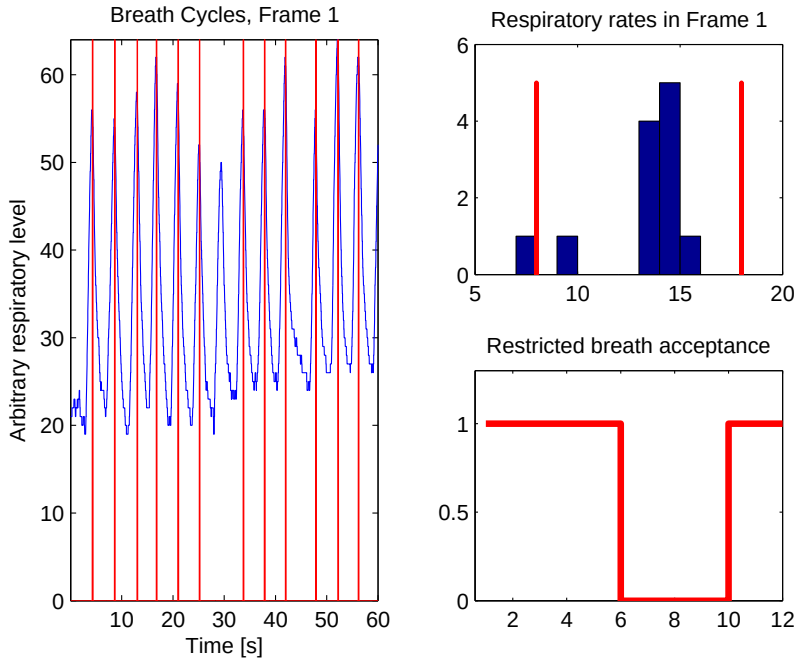

Figure 5.16: Respiratory rate for the first frame

In the above figure it is seen that the wave-analyser missed a breath-cycle at 30 seconds, which introduced a too long temporal distance between the two measured breathing cycles. By restricting the respiratory rate, it is seen that the reconstructed data is lacking information for breath-cycle 6-9, both included. This can be seen in the lower right image of the figure. This is a crucial time to miss information, as the bolus is arriving to the heart in this time interval. This will result in a reduced peak activity for the IF's, which eventually will lead to an increased flow estimate for this patient. The IF's will be shown later in this section, where they will be compared to the TAC's.

Besides the first frame is frame number 5, 6, 7 and 9 also inflected by the restriction on the breath gating. These frames are analysed on the next pages.

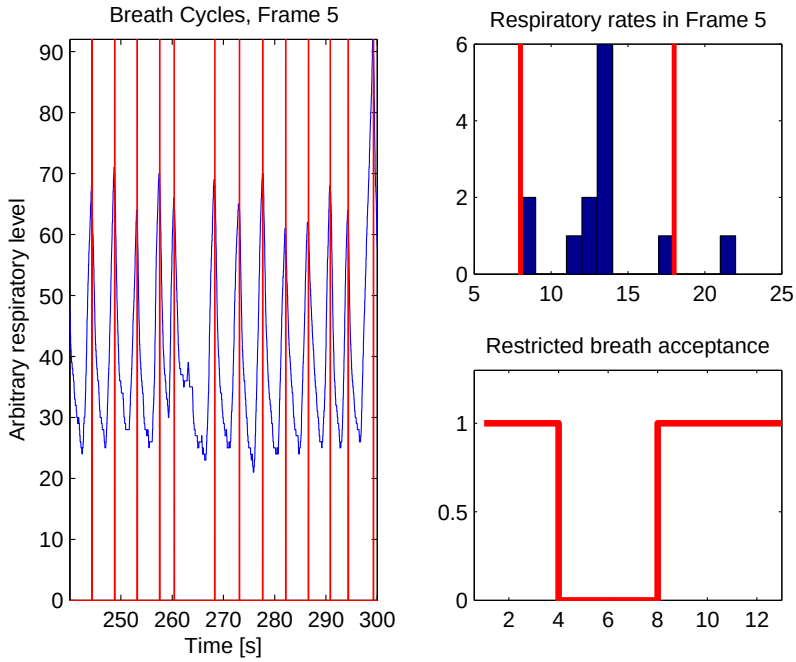

Figure 5.17: Respiratory rate for the fifth frame

In the above figure it can be seen that one of the breath-cycles are having a too high respiratory rate, which occurs between breath cycle number 4 and 5. This is, opposite the first frame, introduced by a too fast respiration. This indicates that the patient might be hyper-ventilating in this period. This is furthermore seen as the following breath-cycle are longer than the normal respiratory rate, but still within the accepted rates. From this it can be seen that the estimated activity in this frame is based on the first 18 seconds and the last 22 seconds, leaving the activity for each bin to be estimated on basis of data from 10 seconds. This is a rather short time-interval to gather information in, which can be seen in the IF and TAC for the patient.

On the next pages the 6th and the 7th frame are analysed.

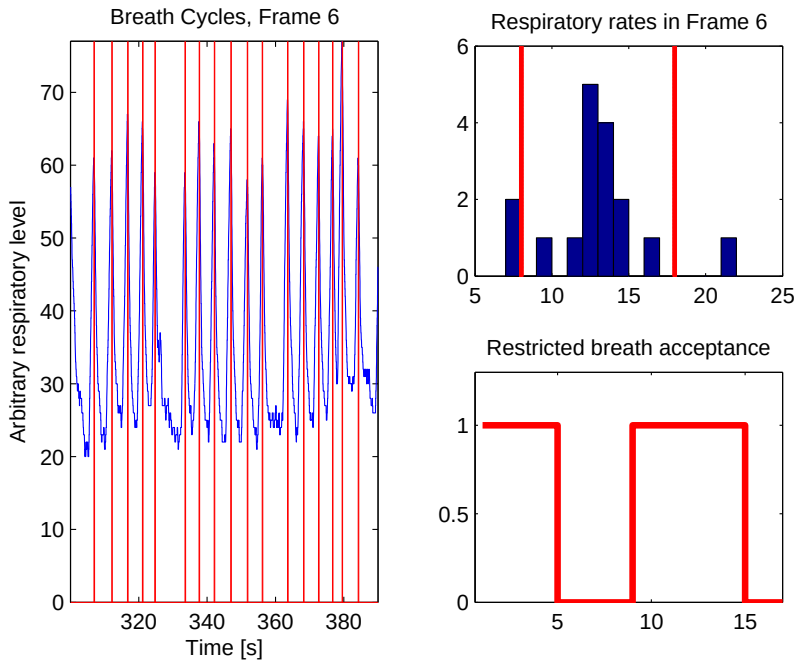

Figure 5.18: Respiratory rate for the sixth frame

In the above figure it can be seen that the breath pattern in this frame is restricting the frame to contain data for approximately 60 seconds, leaving each bin to contain data for 15 seconds. This is not much, as this frame is recorded after a half- half life of the tracer. From this knowledge it is known that the data is more noisy than in the initial frames, which leads to a higher error rate. In this frame it can be seen that there are two breath-cycles which are having a rate outside the restriction. The first rejection occurs from a too long breath-interval, which indicates a breath hold. This leads to a too high translation of the heart, which gives that this restriction would increase the effect of the breath-gating. Unfortunately it is seen that the following respiratory cycles is discarded as well, which lowers the positive effect of the restriction.

The second rejection is found at the end of the frame, and where there are measured two breath-cycles within a short time frame. This indicates a hyper-ventilating occurrence, which leads to a reduced translation of the heart. From this it is estimated that the breath-gating would have gained benefit from rejecting this breath-cycle. Unfortunately are the following 3 breath-cycles discarded as well, which are affecting frame number 7 as well. Here the first breath-cycle is discarded too. However are the remaining breath-cycles accepted, from which it

is estimated that frame number 7 is as good as the analysis without restrictions. Below is shown the restricted breath-pattern for frame number 9.

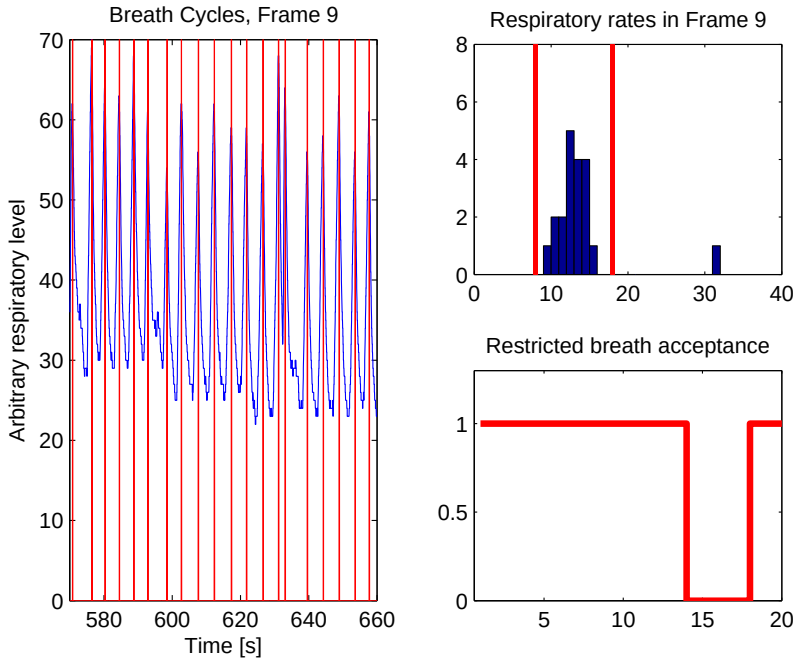

Figure 5.19: Respiratory rate for the ninth frame

In the above figure it is seen that the breath-cycle number 15 is having a too short distance from breath cycle number 14. This indicates that this patient is hyperventilating in this time-period, leaving the translation in of the heart to be minimized. This rejection would have helped the analysis, if the reconstruction program did not reject the 3 consecutive breath cycles too. By restricting this frame it is seen that the image is containing data for a total of 65 seconds, which is thought to be a too short time interval as these data are recorded approximately a half-life after the injection. This gives that the activity within the patient is on 350 MBq, which are distributed throughout the body.

The effect of the restriction of the breath-cycles is easily seen in the analysis of the TAC's and the IF's for this patient. The flow estimates in this section is based on a 2mm FWHM Gaussian filtration. There will be no estimates of the 4mm filtered data, as these analyses are demonstrating the loss of using the restrictions.

The IF's and TAC's are found below.

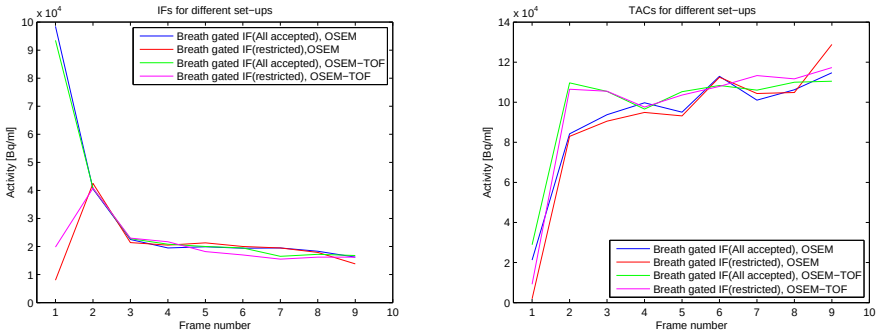

(a) Input function for the restricted set-up compared to the non-restricted set-up.

(b) Time-Activity-Curves for the restricted set-up, compared to the non-restricted set-up

Figure 5.20: Input functions and Time-Activity-Curves for the restricted set-up, compared to the non-restricted set-up

One is able to see the effect of the strict requirements, when analyzing both the IF's and the TAC's in the figure above. Analyzing the IF's first, it is seen that the restriction on the reconstruction is having a huge impact on the activity estimate in the first frame. Analyzing the OSEM-reconstructed data first, it is seen that the restricted data are estimating an activity of a factor 10 below the non-restricted set-up. This witnesses on the restriction leaves out the bolus for this patient. The reduction of the estimated amount of tracer in the initial frame will lead to an increase in the flow estimates. This is due to the TAC will have a contain a higher fraction of the tracer available, which indicates a high perfusion in the myocardial tissues.
This is known to be erroneous, which gives that the restriction on the first frames will lead to a wrong flow estimate. The same pattern is seen for the OSEM-TOF images, however is the difference in the first frame reduced to have a difference of a factor of 4.5. As for the OSEM-reconstructed images will this imply too high flow values throughout the entire ventricle. From the second frame and forth are no significant differences seen, which could alter the flow estimates in the restricted set-up.

When analyzing the TAC's for the patients one is able to notice one tendency which affects the measured perfusion in the heart. This error is manifested in the first frame, where one is able to notice the relation between the restricted and the non-restricted data. For the non-restricted data it is seen that the activities are above 20000Bq/ml for both reconstruction algorithms, with the OSEM-TOF

reconstruction having the highest activity. For the restricted set-up it is seen that both the activity estimates in the first frame are below 10000Bq/ml, again with the OSEM-TOF reconstruction having the highest activity. This reduced activity estimate is introduced to the images, as the data left out from this frame is from the time the bolus passes the heart. From this the activity measurements in the heart are reduced, hence the activity estimates in the first frame. Besides the error in the first frame are no events noticeable, even though there are data missing from frames number 5, 6, 7 and 9. The non-measured activity drop in these frames are thought to be due to the stabilized activity in the heart, which gives a steady activity estimate even though data is missing.

From this it can be concluded that the restricted gating set-up are not improving the analysis, even thought it would improve the analysis from the hypothesis. It is, however, estimated that a correction for the loss of 4 breath cycles to only losing the single breath cycle might improve the analysis.

5.8.1 Flow values for the different patients when using a restricted respiratory rate

In this section are flow values for the two patients having an analysis on the restricted respiratory rate analysed. The analysis on patient number 3 are found in the section 5.8, while the analysis for patient number 6 is found in appendix C.1. These patients were only analysed using a 2mm filtration, as the same tendencies are expected for the 4mm filtration.

5.8.1.1 Patient 3

The restriction on the respiratory rates gave some extreme flow values, which were seen in the polar plots in section 5.8. The flow values found for the restricted breath cycles are compared to the flow values found for the non-restricted set-up, both shown in the table below.

	Flow values in ml/g/min			
	OSEM reconstructions		OSEM-TOF reconstructions	
Region	Breath gated	Restricted breath gated	Breath gated	Restricted breath gated
LAD	0.94	2.01	1.05	2.01
LCX	0.92	1.96	1.02	1.95
RCA	0.88	2.01	0.96	2.00
Global	0.92	2.00	1.02	1.99

Table 5.17: Flow values for the images reconstruction using a restriction on the breath cycles compared to the flow values found for the patients using all the breath cycles.

In the above found flow values it can be seen that the flow values for the restricted set-ups are estimated to be non-physiological high. From this it can be concluded that the restriction on the breath gating has not improved the analysis for this patient.

5.8.1.2 Patient 6

The restrictions on the breath cycles are having a minimal effect on the estimated flow values for this patient. This is due to the time in which the non-accepted breath cycles occur. For this patient the breath cycles are not accepted in the very beginning of the first frame, before the bolus has arrived to the heart. Furthermore are the majority of the non-accepted breath cycles occurring in the last frames, which is thought to give a minor change in the estimated flow values. The flow values are shown in the table below.

	Flow values in ml/g/min			
	OSEM reconstructions		OSEM-TOF reconstructions	
Region	Breath gated	Restricted breath gated	Breath gated	Restricted breath gated
LAD	1.60	1.64	1.14	1.43
LCX	1.87	1.88	1.37	1.73
RCA	1.79	1.79	1.23	1.54
Global	1.72	1.74	1.22	1.53

Table 5.18: Flow values for the images reconstruction using a restriction on the breath cycles compared to the flow values found for the patients using all the breath cycles.

Analyzing the flow estimates for this patient, it is estimated that the restriction on the breath cycles does not change the analysis for the OSEM reconstructed data. The flow values for this reconstruction algorithm were, however, estimated to be too high in section 5.7. From this it is not possible to determine if the restriction is having a negative effect on the estimated flow values.
Analyzing the OSEM-TOF reconstructed flow values, it can be seen that the flow values has increased, as it was seen for patient number 3. For this patient is the flow values increased greatly but still within the physiological limits. This indicates that the patient is suffering from acute TT, where the non-restricted set-up is estimating that the patient is in recovery. For this patient is the restriction of the breath gating thought to have a negative effect on the estimated flow values as the patient is having many outliers. These many outliers decrease the number of measured coincidence events, hence a poor estimate on the activities in each frame.

From this it is estimated that one is getting better results by using the non-restricted set-up, even though this is known to introduce errors.

5.9 Blind test of the reconstructed data

The flow values varies from the different reconstruction algorithms, and filtrations as shown in the previous sections. The estimated flow values are all giving different images, which can be used when the doctors are reading the patients. All the above flow values are only describing the patients flow in the heart using the physics and mathematics and are not correlated to the patients symptoms. The symptoms, and physiological changes are two major areas of interest while analyzing the patient when the diagnosis is given. Due to these parameters the flow values are not viable as stand-alone results, but must be compared with the doctors impression. In order to do this 4 doctors were asked to give their saying on which images they would prefer to use for diagnostic purposes, while blinded for the different set-ups. They were all given the images reconstructed with and without breath-gating and with and without OSEM-TOF where it was available. The doctors were asked to rate the image/images they thought gave the best analysis of the patient based on the medical history of the patient. The scores for the patients are listed in the table below. In the table are PN resembling Patient number, 2/4 resembles the filtration, No/TOF represents OSEM and OSEM-TOF, respectively. Finally are NG representing Non gated and BG represents breath gated data.

Blind test scores				
PN	2NoNG	2NoBG	4NoNG	4NoBG
1	0	0	0	4
2	0	4	0	3
3	3	2	3	3
4	0	1	0	0
5	0	2	0	0
6	0	0	0	0
PN	2TOFNG	2TOFBG	4TOFNG	4TOFBG
1	NA	NA	NA	NA
2	NA	NA	NA	NA
3	1	1	1	2
4	2	2	3	3
5	2	1	4	0
6	1	1	1	4

Table 5.19: Blind test scores for the rest studies.

In the above table are several things visible. The first two patients were not scanned in the mCT-scanner, which gave it was not possible to reconstruct the data using the OSEM-TOF reconstruction algorithm, hence the NA in the OSEM-TOF scores. By analyzing the cumulative scores for the OSEM recon-

struction, the OSEM-TOF reconstruction and the both one is able to extract the preferred set-up. The scores for these tests are analysed below. In the tables are the normalized scores normalized to the maximum number of points, which the given reconstruction could score. In this set-up the maximum scores available for the OSEM-reconstruction is 24, and for the OSEM-TOF reconstructed data 16.

Analyzing the OSEM reconstructed data, it is seen that the cumulative scores are found to be:

Blind test scores				
Calculation	2NoNG	2NoBG	4NoNG	4NoBG
Cumulative	3	9	3	10
Normalized cumulative	0.125	0.375	0.125	0.417

Table 5.20: Analysis of the scores for the OSEM reconstruction

In the above table it can be seen that the majority of the doctors prefer the breath-gated data. From this it is estimated that the breath gating is improving the doctors reading on the images.

Analyzing the OSEM-TOF reconstructions one is seeing a different pattern, in which the distinction between the breath gated data and the non-gated data is not present. These scores are shown in the table below.

Blind test scores				
Calculation	2TOFNG	2TOFBG	4TOFNG	4TOFBG
Cumulative	6	5	9	9
Normalized cumulative	0.375	0.313	0.563	0.563

Table 5.21: Analysis of the scores for the OSEM-TOF reconstruction

In the above table, it can be seen that the distinction between the non-gated and the gated set-up has disappeared, as all the reconstructions have gotten similar scores. From this it is impossible to distinct whether the doctors prefer the breath gated set-up or not. By analyzing the normalized scores it can, however, be seen that the doctors prefers the OSEM-TOF reconstructions over the OSEM reconstructed images. This may be described by the increased contrast in the images, and the better estimate of the activities measured within the heart.

5.10 Statistical analysis

In this section both a 3-way one-sided ANOVA for each region and a 3-way MANOVA will be carried out. The ANOVAs are carried out in order to analyze the main effects, and the interaction hereof. In this project the optimization was done on 3 parameters; the three parameters being.

- Filtering.
  In this project the filtering of the data is analyzed to check if the filtration changes the flow estimates. This is tested as Chen et al has described that the flow estimates might change significantly with large filtering kernels. In this project the data are reconstructed using a 2mm and a 4mm FWHM Gaussian kernel.

- The gating of the data.
  Half the scans are reconstructed using the non-gated set-up which is the gold standard, and half the data is reconstructed using the breath gating. It is of great interest to analyze if the breath-gating has a major impact on the estimated flows.

- The reconstruction algorithm.
  The reconstruction algorithm is the last variable in this project. It is of great interest to analyze if the reconstruction has a major impact on the estimated flow values, as the OSEM-TOF reconstruction is estimated to be superior to the OSEM-reconstruction.

By analyzing these effects in the different segments of the heart, one is able to estimate which parameters that affects the individual regions. There might be significant differences of the various parameters within the respective segments, as the patients are examined for an underlying disease. The flow values are however estimated to be normal within all regions. Finally the data is analyzed in a MANOVA analysis, which is used to analyze if the variables are independent, or if they affect each other. This cannot be tested in a ANOVA analysis, as this only analyzes the main effects and the interactions of those. When doing a multi-dimensional analysis it is possible to analyze how the different parameters affects each other, as the MANOVA is using a variance-covariance matrix. In this matrix the covariances for the different parameters are found in the off-diagonal. Furthermore one is able to analyze if the regional differs from each other. This is of great interest, as the flows in all the segments are estimated to be normal and homogeneous.
On the next pages are the ANOVA analysis for the different regions carried out.

5.10.1 ANOVA's

Two patients who are assumed to have a normal flow in the ventricle are analyzed in this section. The two patients are having a three months follow-up scan and an analysis for IHD, respectively. Both patients were estimated to have normal flows within all three regions. All the statistical analyzes in this section are carried out in the free statistical software tool, R (GNU project).

5.10.1.1 LAD mean flow

The main effects for the two patients are analyzed in this section. A box-plot are generated to get a descriptive plot on how the different parameters affect the estimated flows. From the plot it is possible to estimate which parameters one should expect to have a significance.

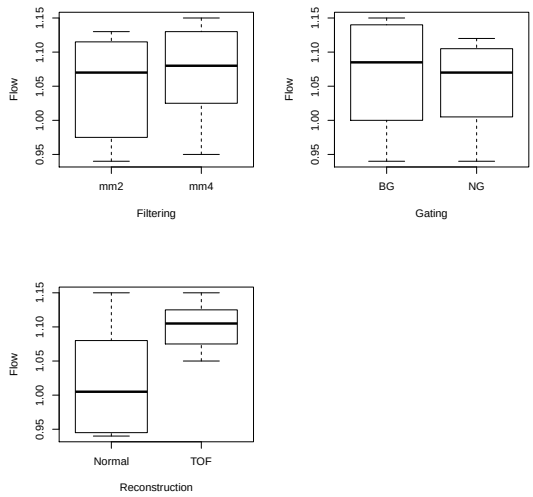

Figure 5.21: Boxplot of the different parameters

Analyzing the box-plots it can be seen that the filtering is estimated to have a great influence on the flow estimates. The effects of the remaining factors are not seen to be significant. This analysis is based on the means of the respective box-plots. The ANOVA table is shown on the next page.

```
> LAD
   Flow Filtering Gating Reconstruction
1  1.01       mm2     NG         Normal
2  1.05       mm4     NG         Normal
3  0.94       mm2     BG         Normal
4  0.95       mm4     BG         Normal
5  1.12       mm2     NG            TOF
6  1.11       mm4     NG            TOF
7  1.05       mm2     BG            TOF
8  1.06       mm4     BG            TOF
9  0.94       mm2     NG         Normal
10 1.00       mm4     NG         Normal
11 1.11       mm2     BG         Normal
12 1.15       mm4     BG         Normal
13 1.09       mm2     NG            TOF
14 1.10       mm4     NG            TOF
15 1.13       mm2     BG            TOF
16 1.15       mm4     BG            TOF
> LADfit <- lm(Flow~Filtering+Gating+Reconstruction,LAD)
> anova(LADfit)
Analysis of Variance Table

Response: Flow
               Df   Sum Sq   Mean Sq F value  Pr(>F)
Filtering       1 0.002025 0.0020250  0.4934 0.49581
Gating          1 0.000900 0.0009000  0.2193 0.64797
Reconstruction  1 0.027225 0.0272250  6.6335 0.02430 *
Residuals      12 0.049250 0.0041042
---
Signif. codes:  0 '***' 0.001 '**' 0.01 '*' 0.05 '.' 0.1 ' ' 1
>
```

Figure 5.22: ANOVA analysis of the parameters in the LAD section

In the above ANOVA table it is seen that the variables Filtering and Gating are having a non-significant effect on the measured blood flow. The reconstruction algorithm, however, is found to be significant. This was expected from the box-plot in figure 5.21. The model was also analyzed using interaction effects. This model was reduced fully by removing the non-significant interactions. The only parameter found significant, after reducing the model fully, were the reconstruction. Due to these findings are the ANOVA analysis using the interaction effects excluded from this section. From the analysis it can be concluded that both the breath-gating and the filtering are having no effect on the estimated flows. This was not expected, as the hypothesis was that both factors were having great effects on the estimated flows. One possible explanation for these findings might be that both parameters are affecting the flow estimates in small regions. If this explanation is correct one is able to estimate significant the two parameters as significant when analyzing patients having either TT or MI. To investigate for this hypothesis are the patient diagnosed with TT analyzed later on.

5.10.1.2 LCX mean flow

In this subsection the ANOVA for the LCX region is carried out. A descriptive box-plot of the parameter effects are shown below, from which it can be analyzed if any of the parameter effects are thought to be significant.

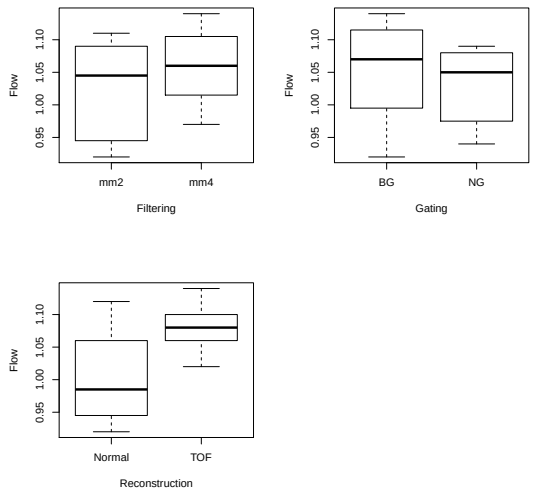

Figure 5.23: Boxplot of the different parameters

In figure 5.23 it can be seen that the post-filtering of the data and the breath-gating does not seem to have a great effect on the estimated flow values, as for the LAD-region. Again it is seen that the reconstruction algorithm seems to have a great effect on the estimated flow values. These hypotheses are analyzed in the ANOVA table on the next page.

```
> LCX
   Flow Filtering Gating Reconstruction
1  0.94       mm2     NG          Normal
2  1.03       mm4     NG          Normal
3  0.92       mm2     BG          Normal
4  0.97       mm4     BG          Normal
5  1.09       mm2     NG             TOF
6  1.09       mm4     NG             TOF
7  1.02       mm2     BG             TOF
8  1.05       mm4     BG             TOF
9  0.95       mm2     NG          Normal
10 1.00       mm4     NG          Normal
11 1.09       mm2     BG          Normal
12 1.12       mm4     BG          Normal
13 1.07       mm2     NG             TOF
14 1.07       mm4     NG             TOF
15 1.11       mm2     BG             TOF
16 1.14       mm4     BG             TOF
> LCXfit <- lm(Flow~Filtering+Gating+Reconstruction,LCX)
> anova(LCXfit)
Analysis of Variance Table

Response: Flow
               Df   Sum Sq   Mean Sq F value  Pr(>F)
Filtering       1 0.004900 0.0049000  1.4990 0.24431
Gating          1 0.002025 0.0020250  0.6195 0.44650
Reconstruction  1 0.024025 0.0240250  7.3499 0.01892 *
Residuals      12 0.039225 0.0032688
---
Signif. codes:  0 '***' 0.001 '**' 0.01 '*' 0.05 '.' 0.1 ' ' 1
>
```

Figure 5.24: ANOVA analysis of the parameters in the LCX section

In the above ANOVA analysis it is seen that the filtering and the gating are found to be non-significant. This was expected from the hypothesis sat up for the LAD-area. An ANOVA with interaction effects were sat up for this region too. The ANOVA was fully reduced, and it gave that the reconstruction algorithm was the only parameter of significance. Due to this finding is this ANOVA not shown in this section.

5.10.1.3 RCA mean flow

The analysis for the RCA is carried out in the same way, as it was in the LAD and the LCX regions. The boxplot for the RCA region is shown in the below figure.

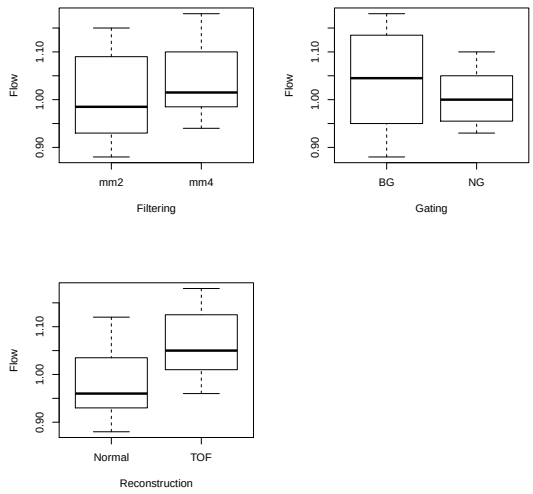

Figure 5.25: Boxplot of the different parameters

In the above figure it can be seen that the 2mm and the 4mm filtrations are having similar flow values, as it was seen for the other regions. For the gating set-up it is seen that the medians for the flows are within the same interval. The means are thought to be in the same interval too, giving that one cannot differentiate between the two set-ups. Analyzing the reconstruction parameter, it is seen that the difference between the two methods are reduced, when compared to the other regions. This might give a reduced significance for the reconstruction parameter in this section.
The analysis is carried out on the next page.

```
> RCA
   Flow Filtering Gating Reconstruction
1  0.93       mm2     NG         Normal
2  0.98       mm4     NG         Normal
3  0.88       mm2     BG         Normal
4  0.94       mm4     BG         Normal
5  1.01       mm2     NG            TOF
6  1.02       mm4     NG            TOF
7  0.96       mm2     BG            TOF
8  1.01       mm4     BG            TOF
9  0.93       mm2     NG         Normal
10 0.99       mm4     NG         Normal
11 1.08       mm2     BG         Normal
12 1.12       mm4     BG         Normal
13 1.10       mm2     NG            TOF
14 1.08       mm4     NG            TOF
15 1.15       mm2     BG            TOF
16 1.18       mm4     BG            TOF
> RCAfit <- lm(Flow~Filtering+Gating+Reconstruction,RCA)
> anova(RCAfit)
Analysis of Variance Table

Response: Flow
               Df   Sum Sq   Mean Sq F value  Pr(>F)
Filtering       1 0.004900 0.0049000  0.7590 0.40075
Gating          1 0.004900 0.0049000  0.7590 0.40075
Reconstruction  1 0.027225 0.0272250  4.2168 0.06248 .
Residuals      12 0.077475 0.0064563
---
Signif. codes:  0 '***' 0.001 '**' 0.01 '*' 0.05 '.' 0.1 ' ' 1
>
```

Figure 5.26: ANOVA analysis of the parameters in the RCA section

The above ANOVA is estimating that none of the variables are significant for this region. The reconstruction algorithm are found to be significant within a 10% significant level, which can have occurred by pure coincidence. The findings in this region might be due to none of the patients are having any problems in the RCA region, giving highly similar flow values.

5.10.1.4 Global mean flow

The global flow values are analyzed here. The global flow is a weighed mean of all the flow values estimated within the left ventricle. By analyzing this, one is able to see if reconstruction algorithm, which has been found to be significant in two of the three regions, is significant when analyzing the left ventricle in total. A box-plot for explanatory purposes is shown below.

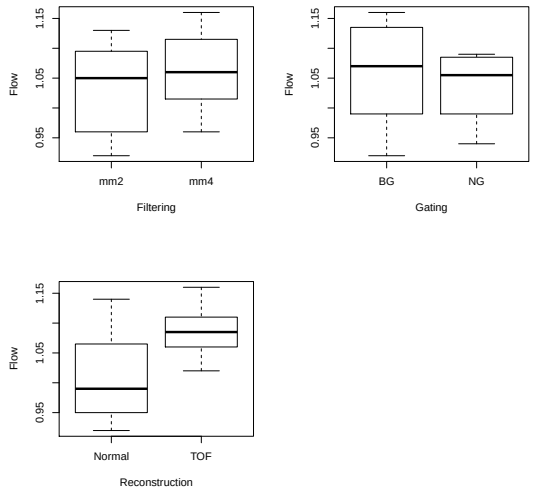

Figure 5.27: Boxplot of the different parameters

Analyzing the above main effects it is seen that the median for the 2 filterings are the same. This indicates that the mean activity might be deviating less than it requires to obtain a significant difference. The same is seen when analyzing the effect of the gating. Analyzing the effect of the reconstruction algorithms it is seen that the two methods differ greatly. This is seen as the upper quartile for the OSEM reconstructed data are at the same level as the lower quartile for the OSEM-TOF reconstructed data. From this, one is able to differentiate between the flow values found for the respective set-ups, giving this parameter is significant. This is tested in the ANOVA analysis on the next page.

```
> Global
   Flow Filtering Gating Reconstruction
1  0.98       mm2     NG         Normal
2  1.03       mm4     NG         Normal
3  0.92       mm2     BG         Normal
4  0.96       mm4     BG         Normal
5  1.09       mm2     NG            TOF
6  1.08       mm4     NG            TOF
7  1.02       mm2     BG            TOF
8  1.04       mm4     BG            TOF
9  0.94       mm2     NG         Normal
10 1.00       mm4     NG         Normal
11 1.10       mm2     BG         Normal
12 1.14       mm4     BG         Normal
13 1.08       mm2     NG            TOF
14 1.09       mm4     NG            TOF
15 1.13       mm2     BG            TOF
16 1.16       mm4     BG            TOF
> Globalfit <- lm(Flow~Filtering+Gating+Reconstruction,Global)
> anova(Globalfit)
Analysis of Variance Table

Response: Flow
               Df   Sum Sq   Mean Sq F value  Pr(>F)
Filtering       1 0.003600 0.0036000  0.8597 0.37210
Gating          1 0.002025 0.0020250  0.4836 0.50005
Reconstruction  1 0.024025 0.0240250  5.7373 0.03381 *
Residuals      12 0.050250 0.0041875
---
Signif. codes:  0 '***' 0.001 '**' 0.01 '*' 0.05 '.' 0.1 ' ' 1
>
```

Figure 5.28: ANOVA analysis of the parameters in the heart in general

In the above figure it is seen that the filtering and the gating are found to be non-significant, as explained on the previous page. The reconstruction algorithm is however found to be significant with a p-value on 0.03381. From this it can be concluded that the reconstruction algorithm is having a significant change on the estimated flow values, even though the parameter was found to be non-significant in one segment.

5.10.2 MANOVA

The MANOVA analysis is carried out to analyze if the flow values differ from the different areas, when comparing the flow values found for each area. By using a MANOVA analysis one is analyzing the interaction effects if the different parameters in a multivariate space. From this, one is able to analyze how the different parameters interacts, and affect other parameters. This is not possible in the ANOVA analysis, as this analysis only tests the main effects, and the interactions hereof.
The MANOVA analysis is shown below.

```
> summary.aov(MANOVA.ana,test="Pillai")
 Response Filtering :
            Df  Sum Sq Mean Sq F value Pr(>F)
Flow         1  0.4972 0.49723  1.9884 0.1652
Residuals   46 11.5028 0.25006

 Response Gating :
            Df  Sum Sq Mean Sq F value Pr(>F)
Flow         1  0.3055 0.30546  1.2015 0.2787
Residuals   46 11.6945 0.25423

 Response Reconstruction :
            Df Sum Sq Mean Sq F value    Pr(>F)
Flow         1 3.4174  3.4174  18.316 9.388e-05 ***
Residuals   46 8.5826  0.1866
---
Signif. codes:  0 '***' 0.001 '**' 0.01 '*' 0.05 '.' 0.1 ' ' 1

 Response Area :
            Df  Sum Sq Mean Sq F value Pr(>F)
Flow         1  1.3075 1.30755  1.9597 0.1683
Residuals   46 30.6925 0.66723

>
```

Figure 5.29: MANOVA analysis on the flow values for the patients

Analyzing the MANOVA results above, it is seen that only the reconstruction algorithm has been found to be significant. This factor is, however, only found to have a significance on the flow values measured in total, and not on the flow values found in the respective regions. From the above results it is possible to conclude that the reconstruction are having a significance on the measured flow values for the patients having a normal flow estimate in the heart. It is, however, seen that the breath-gating does not have a significance for these patients. These findings might be explained by the hypothesis sat up in the ANOVA analysis for the LAD region.

5.10.3 ANOVA analysis for a patient

In the previous section it was found that the breath gating was found to be non-significant for the patients having a normal flow. A hypothesis on the non-significant findings were sat up. The hypothesis stated that the non-significant changes might have been introduced as the breath gating is thought to have local effects on the non-normal flow areas, such as TT and MI areas. To test this hypothesis the only patient having a non-normal flow is analysed in this section. This patient (number 6) was estimated to have a TT-area in the left ventricle which has been estimated to affect approximately 2% of the LCA area for the respective set-ups. The TT area were seen to change both size and flow values in section 5.7. From this it is estimated that one is able to see an effect of the breath gating, as this is thought to be the main contributor to change in the TT-area.
The hypothesis is tested for all the regions, as it was for the patients estimated to have a normal flow.
The respective flow analyses are done on the next pages.

5.10.3.1 LAD area

The breath gating is thought to be significant for this region, as the patient is having the TT area covering approximately 2% of the region. To get an estimate on whether the breath gating has improved the analysis or not are a explanatory box-plot is shown below.

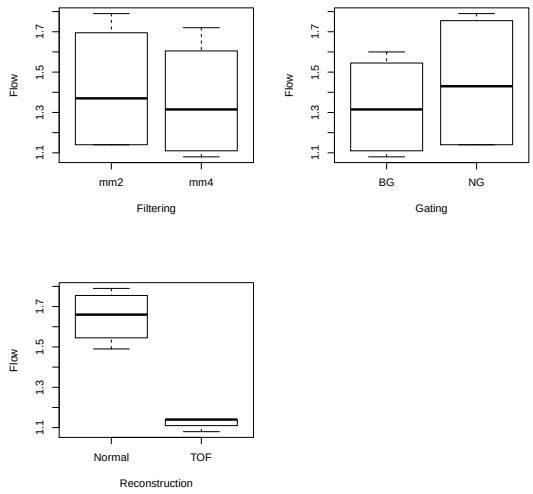

Figure 5.30: Boxplot of the different parameters

When analyzing the effects of the different parameters in the above box-plot one is able to estimate which parameters that are estimated to be significant. The reconstruction parameter is highly significant, as the flow estimates from the two reconstruction algorithms differ greatly. It is seen that the 2 different filterings are having the same estimate on the median flows, giving that this factor might be non-significant. The gating, however, is found to have a difference in the estimated median flow values. The difference might be found to be significant on a 5% significance level. This is tested in the ANOVA on the next page.

```
> anova(LADfitPt)
Analysis of Variance Table

Response: Flow
                      Df  Sum Sq Mean Sq  F value    Pr(>F)
Filtering              1 0.00720 0.00720   6.9677 0.0776794 .
Gating                 1 0.02880 0.02880  27.8710 0.0132528 *
Reconstruction         1 0.55125 0.55125 533.4677 0.0001778 ***
Gating:Reconstruction  1 0.01620 0.01620  15.6774 0.0287640 *
Residuals              3 0.00310 0.00103
---
Signif. codes:  0 '***' 0.001 '**' 0.01 '*' 0.05 '.' 0.1 ' ' 1
>
```

Figure 5.31: ANOVA analysis of the parameters in the LAD section

In the above ANOVA it can be seen that both the gating, the reconstruction and the interaction hereof are found to be significant when analyzing patient number 6. The interaction tells that one is getting a different estimate on the flow values, when varying on both parameters simultaneously. From this it is seen that one is getting the best flow analysis by using both a breath-gated set-up and a OSEM-TOF reconstruction algorithm within this region. The filtering is furthermore found to be significant on a 10% level, which is a low significance.

The above findings might be explained from the hypothesis sat up in the LAD analysis for the patients having normal flow values. The explanation might be that the size of the TT and the flow values inside the TT area has changed, which alters the estimated flow values for the gated set-ups.

One should, however, not put to much weight into the analyses carried out in this section as only one patient is analysed here. The poor number of measurements might indicate that one might estimate the different parameter effects on an erroneous estimate.

5.10.3.2 LCX area

The significance of the three parameters for the LCX region are analysed here. From the box-plot shown below one is able to estimate that the reconstruction algorithm is having a major significance on the flow estimates within this region. The filtering is thought to have a non-significant impact on the estimated flows, which can be seen as the two boxes are estimating the flows to lay within the same interval. Analyzing the gating it is seen that the non-gated set-up is estimated to have a higher variance in the estimated flows, which might indicate a significance for the gating.

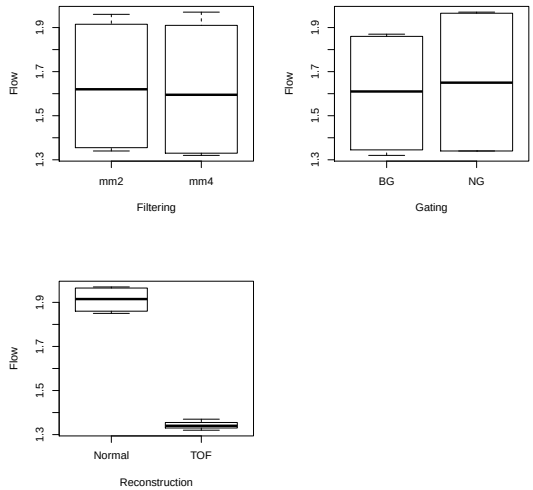

Figure 5.32: Boxplot of the different parameters

The significance of the breath-gating is estimated in the ANOVA on the next page.

```
> anova(LCXfitPt)
Analysis of Variance Table

Response: Flow
                     Df  Sum Sq Mean Sq  F value    Pr(>F)
Gating                1 0.00500 0.00500   13.333   0.02174 *
Reconstruction        1 0.64980 0.64980 1732.800 1.991e-06 ***
Gating:Reconstruction 1 0.00605 0.00605   16.133   0.01591 *
Residuals             4 0.00150 0.00038
---
Signif. codes:  0 '***' 0.001 '**' 0.01 '*' 0.05 '.' 0.1 ' ' 1
>
```

Figure 5.33: ANOVA analysis of the parameters in the LCX section

Analyzing the ANOVA results above it can be seen that both the gating, the reconstruction and the interaction hereof are significant. This concludes that both the parameters affects the estimated flow. The effect of the breath-gating is thought to be positive from the analyses carried out in the other result sections. This gives that the breath gating is necessary in order to obtain the most correct flow values. It is furthermore possible to conclude that the OSEM-TOF reconstructions are giving a better flow estimate, which are based on the analysis done in section 5.7.

The findings in this section are, as for the other estimates within this section, based on an analysis for a single patient. From this one is able to find some parameters to be significant, which might have occurred by an error in the reconstruction of the images. Due to this one is not able to tell if this is the tendency for a larger population.

5.10.3.3 RCA area

The analysis of this region is of great interest as the reconstruction parameter was found to be non-significant for the two patients having a normal flow. This finding is not thought to occur for the patient, as the flow values for the different reconstruction algorithms varies greatly. A box-plot showing the main-effects are shown below, as it has been for the other regions.

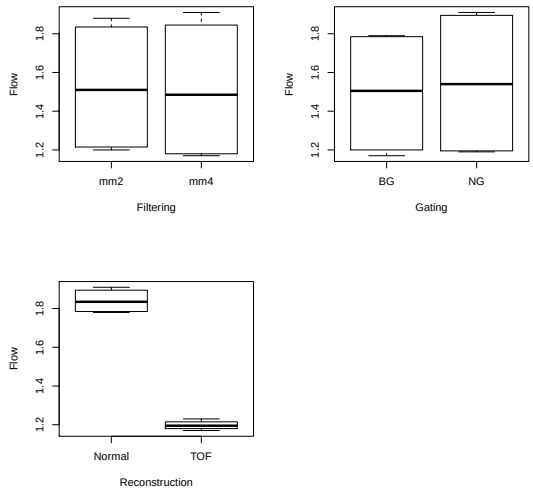

Figure 5.34: Boxplot of the different parameters

In the above figure it can be seen that the reconstruction parameter is highly significant as the means are differing greatly. Again it is seen that the filtering is estimating the same flow values, which gives that this parameter is thought to be non-significant. Analyzing the effects of the gating indicates that the mean flows might be different. The significance of the breath gating is analysed in the ANOVA table on the next page.

```
> anova(RCAfitPt)
Analysis of Variance Table

Response: Flow
                     Df  Sum Sq Mean Sq  F value    Pr(>F)
Gating                1 0.00551 0.00551    9.383   0.03754 *
Reconstruction        1 0.82561 0.82561 1405.298 3.024e-06 ***
Gating:Reconstruction 1 0.00661 0.00661   11.255   0.02844 *
Residuals             4 0.00235 0.00059
---
Signif. codes:  0 '***' 0.001 '**' 0.01 '*' 0.05 '.' 0.1 ' ' 1
>
```

Figure 5.35: ANOVA analysis of the parameters in the RCA section

In the above ANOVA analysis it is seen that the gating factor is found to be significant. Furthermore the interaction between the reconstruction algorithm and the gating is found to be significant. This indicates that the gating are having some effects on the RCA region. The polar plots showing these flow values are found in section 5.7. From these analyses are the gating and the reconstruction algorithms estimated to be significant for the global analysis carried out on the next page. The filtering however, is estimated to be non-significant as none of the regions found this parameter to be significant.

5.10.3.4 Global flow analysis

The findings in this region was described in the previous sub-section. The estimated flow values for this region is based on a weighed mean of the estimated flow values for all the regions. Due to this the box-plot is not shown here, as these will contain the same information as the boxplots for the respective regions. The ANOVA table for the global flow is shown below.

```
> anova(GlofitPt)
Analysis of Variance Table

Response: Flow
                      Df  Sum Sq Mean Sq  F value    Pr(>F)
Filtering              1 0.00245 0.00245    7.000  0.077274 .
Gating                 1 0.01445 0.01445   41.286  0.007641 **
Reconstruction         1 0.64980 0.64980 1856.571 2.751e-05 ***
Gating:Reconstruction  1 0.00845 0.00845   24.143  0.016145 *
Residuals              3 0.00105 0.00035
---
Signif. codes:  0 '***' 0.001 '**' 0.01 '*' 0.05 '.' 0.1 ' ' 1
>
```

Figure 5.36: ANOVA analysis of the parameters for the global mean flows

The above ANOVA gave the results as expected. It is seen that both the breath-gating, the reconstruction and the interaction hereof are found significant. From this it can be concluded that one should use the OSEM-TOF reconstruction and the breath-gating, as it was in for the LAD-region. However is the filtering of the images found to be non-significant. From this it can be concluded that the two filterings are not giving any change in the estimated flows.

5.10.4 MANOVA analysis for the patient

The previous analyses for the patient estimated the gating protocol to be significant, when analyzing the main effects. In this section is investigated if the gating is found significant for the MANOVA analysis, where the interaction effects for the respective factors are included. The MANOVA analysis for the patient is shown below.

```
> MANOVA.anaPT <- manova(cbind(Filtering,Gating,Reconstruction,Region)~Flow,
+ data=flowsPT)
> summary.aov(MANOVA.anaPT,test="Pillai")
 Response Filtering :
            Df Sum Sq  Mean Sq F value Pr(>F)
Flow         1 0.0131 0.013087  0.0481 0.8284
Residuals   22 5.9869 0.272132

 Response Gating :
            Df Sum Sq  Mean Sq F value Pr(>F)
Flow         1 0.0846 0.084624  0.3147 0.5805
Residuals   22 5.9154 0.268881

 Response Reconstruction :
            Df Sum Sq Mean Sq F value    Pr(>F)
Flow         1 5.1604  5.1604  135.22 7.258e-11 ***
Residuals   22 0.8396  0.0382
---
Signif. codes:  0 '***' 0.001 '**' 0.01 '*' 0.05 '.' 0.1 ' ' 1

 Response Region :
            Df  Sum Sq Mean Sq F value Pr(>F)
Flow         1  0.4711 0.47114  0.6675 0.4227
Residuals   22 15.5289 0.70586

> |
```

Figure 5.37: MANOVA analysis on the flow values for the patient

In the above analysis it is seen that the reconstruction is the only factor that is found significant. When analyzing the gating it is seen that the MANOVA analysis does not find this factor to be significant. This was not expected, as the ANOVA's for the respective regions did find this to be significant. From this it is concluded that more tests are necessary in order to determine whether or not the breath gating is significant for the flow estimates. A such test may be a series of ANOVA's and a MANOVA for multiple patients, all having a TT area.

Chapter 6

Discussion

6.1 Quality Control

The breath gating is estimated to improve the contrast between the myocardial tissue and the blood as the position of the heart is kept constant throughout the analysis. In this section the effect of breath gating will be analysed for a patient who are having a 3-months follow-up scan. The analysis will furthermore cover the filtration.

The filtration was found to be non-significant in the previous sections. Even though the filtration was found to have a non-significant effect on the estimated flow values, there is a certain possibility that the filtration is having a great effect on the still images. The still-images are used for clinical analysis, as these can be used to analyse the respective uptake rates in the heart. An example on this are analyses using ^{18}F-FDG as a tracer, which gives information on the metabolic activity within the heart. The filtration is known to give more homogeneous images when the filtration kernel is increased in size. From this it is estimated that one obtains a more homogeneous image when using a 4mm filtration.

The effects of the breath gating of a 2mm filtered image will be analysed first. The image shown on the next page is a time-weighted sum image for 11 minutes

(5 frames 60 seconds followed by 4 frames of 90 seconds).

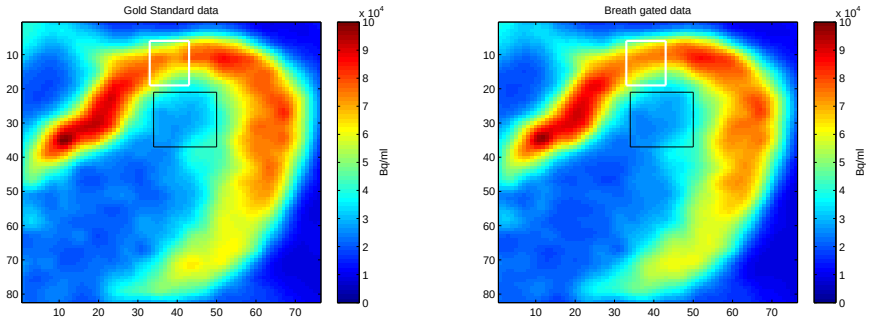

(a) Gold Standard (Non-gated image) (b) Breath gated data using a 2mm filtration

Figure 6.1: Time weighted activities for a tomogram using either non-gated data or breath gated data

In the above images, one is able to see several changes in the estimated activities for the two set-ups. The first difference analyzed here is the activity estimate within the lumen of the ventricle. Inside the lumen, a black box is shown, covering one area of interest. One is able to see two changes when applying the breath gating to the image-reconstruction.
The first thing seen, is that the low-activity areas within the black box has increased. It is furthermore seen that the estimated activities within the low-activity area are estimated to be higher in the non-gated set-up. This higher uptake is estimated to be erroneous, as the activity in the blood is seen to be low in the basal parts of the heart.
Both these effects are thought to be introduced by the continuous motion of the heart in the non-gated set-up. The motion of the heart will increase the estimated activity within the lumen if the heart is having a high cranio-caudal translation. One is getting a more homogeneous position of the heart by correcting for this motion. This will reduce the activity estimate within the lumen, as it is seen in figure 6.1b.
In this project the breath cycles are divided into 4 bins, which gives a little blurring of the hearts activity as the heart moves a bit within each second. This together with the path length of the tracer gives an aura, which is seen as the turquoise colors surrounding the high-activity areas. The aura however, is seen to have been decreased when applying the breath gating. This tells that the breath-gating has improved the image-quality.

When analyzing the cardiac wall within the white square it can be seen that the breath gating has changed the activity estimate. The gated set-up is having a more homogeneous appearance than the non-gated, which might indicate that the non-gated set-up is having an erroneous estimate. This conclusion is based on the knowledge on this patient should have a normal flow in the entire ventricle. The reduced uptake for the non-gated image might have been introduced by the 3D-motion, which has been corrected for in the breath gated set-up. The deformation fields for this patient (patient number 1) is shown in appendix A.

The effect of the 4mm filtration is shown in the image below.

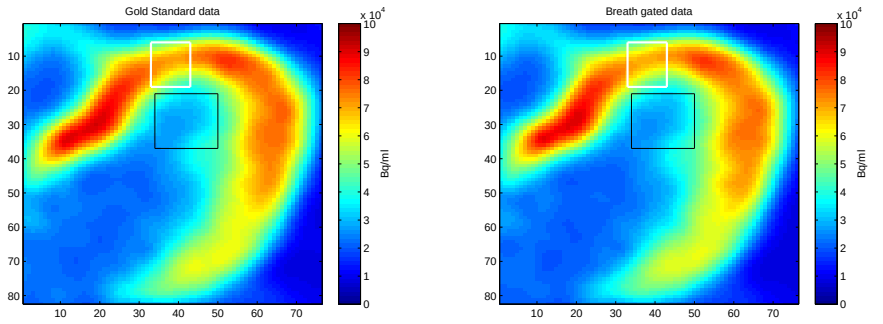

(a) Gold Standard (Non-gated image) (b) Breath gated data using a 4mm filtration

Figure 6.2: Time weighted activities for a tomogram using either non-gated data or breath gated data

In figure 6.2 it can be seen that the activity in the lumen inside the black box has been increased, and thereby reduced the contrast between the myocardium and the surrounding tissues. This effect was expected, as the 4mm Gaussian filter will blur out the high-activity areas found in the cardiac wall into the lumen of the left ventricle. This will introduce some falsely high activities in the lumen, which might introduce some non-correct estimates on the hearts position when analyzing the heart in the clinical software.

The low-uptake area found inside the white box on figure 6.1a is blurred out on figure 6.2a. This indicates that the greater filtration of the images is having the same effect as the breath-gating has, at least for this patient. This might raise the question on how important the breath-gating is, as one might just use a larger filtration kernel instead.

The answer to the above question is found within the very same images from which the question was raised. By using a larger filtration kernel one is reducing the high-activity areas found locally inside the myocardium. These phenomena are shown in the four images in the basal part on the left-hand side of the ventricle. In the 2mm filtered images the activity is estimated to be approximately $9.5{\cdot}10^4$Bq/ml in the area around $(x = 15; y = 35)$. The activities for the 4mm filtered images are found to be $8.5 \cdot 10^4$Bq/ml within the same area. This shows that the larger filtration is giving more appealing images on behalf of the activity estimates. This however, is not affecting the estimated flow values, which indicates that the this effect is more critical when analyzing the still-images of the heart.

The statistical non-significant change in the flow values, when changing the filtration kernel is analyzed in the IF's and TAC's- below.

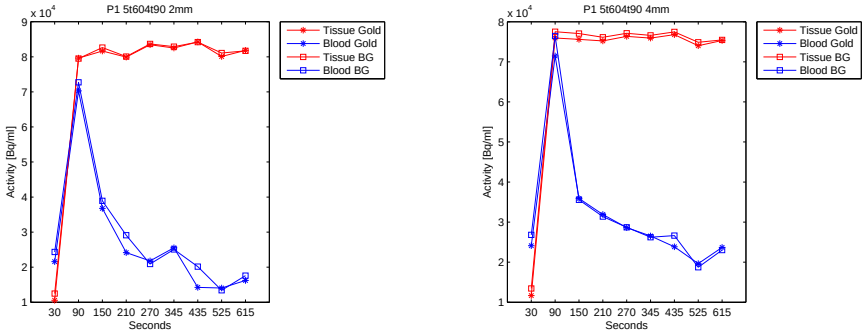

(a) IF and TAC using a 2mm filtration

(b) IF and TAC using a 4mm filtration

Figure 6.3: IFs and TACs for both a 2mm filtration and a 4mm filtration

The analysis of the two images will be divided into an analysis on the breath gating and an analysis of the filtration.

By analyzing the effect of the breath-gating, one is able to see the breath gating has increased the activity estimate for the IF for the 2mm filtered data. The same tendency can be found within the first frames for the 4mm filtration. This indicates that the flows for the specific region analyzed here, is estimated to have a reduced flow, as the TAC's are having the same activities discarding the gating-protocol. Analyzing the relative uptake rates of the TAC's, it can be seen that the 2mm filtered data are taking up more tracer, than the IF is estimating. This might be explained by the late occurrence of the peak. For this patient it is estimated that the peak might physically occur in the first seconds of the second frame, giving that the heart is having a long time to take in the tracer. When

filtering the images with a 4mm filter, one is blurring the estimated activity over a large area. This gives a reduced activity estimate, which has been estimated to be the same as the IF for this patient. From this analysis it is estimated that the 2mm filtered data will be expected to have a higher flow estimate than the 4mm filtered data for this specific area in the apical region. This is determined by the same activity estimates in the TAC's, while the 2mm filtered data has taken up a larger fraction of the tracer available.

From the above analysis it was seen that the two flow estimates might be explained by the breath-gating, which was also seen in the statistical analyses. The effect of the filtering is not as significant as breath-gating when analyzing the curves above. Here, it is seen that the activity estimates for the IF's are within the same levels, indicating that the filtering has no effect on the IF's. This was expected as the IF's are estimated within the lumen in the basal region of the heart. This area is known to be somewhat stable, giving that no tissue-components are affecting the activity estimate here. Analyzing the filtering effect on the TAC's it is seen that the estimated activities for the 2mm filtering are estimated to be higher than the 4mm filtering. This phenomenon is explained by increased blur of the high-activity voxels, which is decreasing the high-activity areas. This was seen in the figures 6.1 and 6.2. The effect is, however, not big enough to be found in a statistical analysis, which indicates that the flow values are not changing significantly by the improved activity estimates within the wall.

6.2 Measured flows using the gated set-up

The flow values are estimated on the input-functions and the time-activity-curves, as seen in the result section. In section 5.7 it was seen that the two estimates, using the OSEM and the OSEM-TOF reconstructions gave different results. These changes in the flow values were estimated to occur from the changes in the activity estimates within the first two frames. The activity within these frames were estimated the best for the OSEM-TOF reconstructions for the patient analyzed in sectopm 5.7.

Findings like these gives rise to multiple questions which all relate to the estimated flow values. The first, and most important questions are:

- Are we sure that the measured flow values are correct? If not, how far are the results from the actual flow values in the body?
- Does non-exact flow values have an effect on the diagnosis of the patient?
- Which reconstruction is the best, the OSEM or the OSEM-TOF?

Additional questions on breath-gating appear in the same sentence.

- Is the breath-gating improving the analysis? - If so, does it then have any effects on the diagnosis of the patients?
- Are we able to tell anything on the patient's disease based on the mean flows for the three segments?

All of these questions are of great importance to answer as they are based on the very foundation of the analysis. Answers to all of these questions will be discussed in this section.

The first question to be discussed is which reconstruction algorithm that is the best, the OSEM or the OSEM-TOF?
In the statistical analysis it was found that the choice of reconstruction algorithm was significant for both the patients who are estimated to have a normal flow, and the patient with known TT. From these analyses it is seen that the choice of reconstruction algorithm is having a huge impact on the flow values, which might change the diagnostic purposes of the images.

The findings in the statistical analyses were easily seen in the analysis of the IF's and TAC's too. These changes were most significant in the analysis for patient number 6.
The peak deviations between the two reconstruction methods were found to be more than 50% , while the deviations for the remaining patients were found to be 17.67%. The peak activities for the rest studies are shown in the figure 6.4 - below.

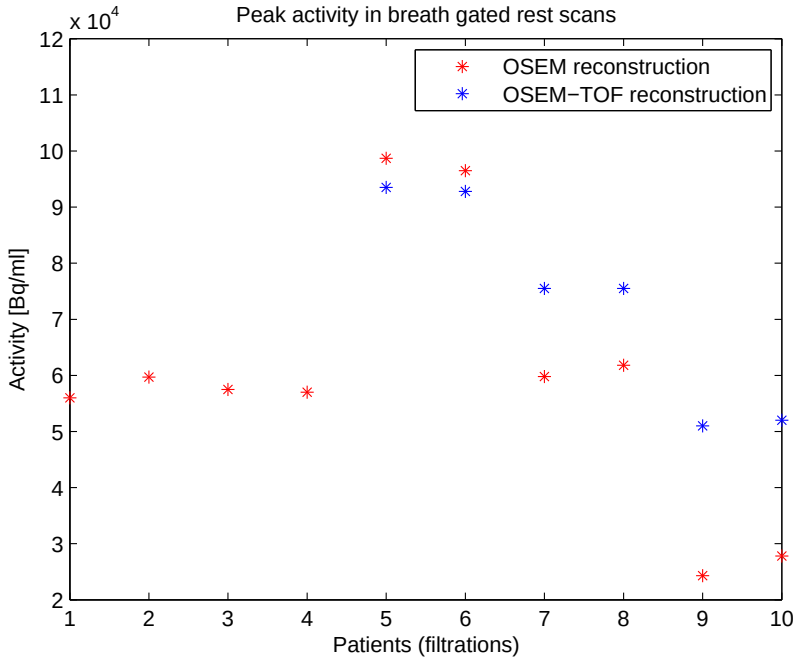

Figure 6.4: Peak activities for the rest studies

In the above figure, the peak values for the respective patients are analyzed one by one. The odd numbers on the x-axis represents a 2mm filtration of the images, while the even numbers represents a 4mm filtration.
When analyzing the graph it can be seen that the general peak activity is estimated to be greater than or equal to 50000 Bq/ml. It is, however, noticed that the last patient (patient number 6) is having a peak activity estimate below 30000 Bq/ml for the OSEM reconstructions. This suggests that the OSEM-reconstructions for this patient is having an erroneously low peak-estimate, which eventually leads to an erroneous high flow for the entire left ventricle. When analyzing the IF's for the initial frame(fig. 5.11 and 5.13) for this patient it is seen that the peak activity is not having a great difference from the activity

in the fourth frame. For this patient it is seen that the deviation is on 54%, whereof the other reconstructions are having an average deviation on 271% for the rest scans. This means that the apical region is estimated to have a high fractional uptake of the tracer. This gives a high flow estimate for the apical region. These findings are seen both in the polar plots, and the tables containing the flow values in section 5.7.
When analyzing the fractional difference between the first and the fourth frame for the OSEM-TOF reconstructed data, it is seen that the deviation is large, which leads to the fact that the flow estimated for this region is found to be reduced when compared to the OSEM reconstructed data. From the above analysis it is concluded that the OSEM-TOF reconstruction is giving the best result.

As seen in figure 6.4 the majority of the OSEM-TOF reconstructions are increasing the peak-activity. This elevation in the peak-activity relates to the improved estimate on where the annihilation event has occurred. The reason for this is that the activity within the first frames are high due to the continuous infusion of the tracer. Furthermore the activity estimates throughout the scans are estimated to have a higher activity for the OSEM-TOF reconstructions in general. This is, however, not affecting the flow-estimates as the flows are based on the tracer available(IFs), and the activity measured in the myocardial cells (TAC). From this it is estimated that the most correct flow estimates are based on the OSEM-TOF reconstructions.

The above discussion leads to the question on; has the breath-gating improved the flow-analysis? There are many ways to answer this question. One is able to answer the question by using the results from the blind test and the statistical analysis. Another way to answer the question is to analyse the IF's and the TAC's for the individual patients. The question will be answered from the statistical point of view first, followed by the analysis of the IF's and TAC's.

In the blind test a group of doctors were asked to choose the image or images he/she would prefer, when doing a clinical analysis on the patients. The doctors were blinded for the variable factors, meaning that the doctors were not able to choose the usual set-up by heart. In the analysis it was found that the doctors preferred the breath-gated data when using the OSEM reconstructed data. This was expected as the breath gating were thought to improve the SNR in the OSEM reconstructed data, hence improve the flow analysis. The same pattern was not recognized when analyzing the OSEM-TOF reconstructed data as all the factorial set-ups were scored equivalently.
This non-significant result might be explained by the statistical analysis of the data, where the reconstruction parameters were highly significant for all the set-ups. From this, it is seen that reconstruction algorithm is having the greatest impact on the flow estimates, hence the breath gating might be found non-

significant for the doctors. The statistical analyses of the patient having TT were the only analyses where breath gating was seen to be significant. This might imply that the effect of the breath gating cannot be seen in the OSEM-TOF reconstructed data in total.
When analyzing the blind-test for the patient having TT, it was seen that doctors preferred the OSEM-TOF reconstructed data with a 4mm filtration and breath-gating. This might indicate that one should use the breath gating when analyzing patients. This finding was not expected as Chen et al warned about using a too high filtration.[19] The finding in this analysis might indicate that one should not use a too low filtering either, as this might give an increase in the level of noise in the polar plots. It is, however, not possible to conclude which filtration is best, as this analysis is performed on a single patient.

When analyzing the ANOVA tables for the patient it can be seen that the breath gating is found to be significant for all the regions. The same was not found when analyzing the results in the MANOVA analysis. This implies that the statistical analyses carried out in this thesis cannot determine whether or not the breath gating improves the analysis. To analyse this, one is required to do more analyses on the measured flow values. The first step might be to include more patients in the analysis, as only a single patient having a flow-defect in the heart was analyzed in this thesis. One might be able to find the effects significant or non-significant by including more patients having a TT within the apical region.
One plausible explanation on why the ANOVAs for the patient find the breath gating to be significant is that the effects of the gating are measured on a regional basis. As the TT area is small, the effects are most easily seen here, while the normal flow estimates might not benefit for the gating. This, however, does not explain the reason the breath gating is not significant in the MANOVA analysis. When analyzing the patients having a normal flow, one is not able to find any significant changes in the flow values when using the breath gating. This might imply that the breath gating is not having the expected effect on patients having normal flows.

The lack of significance for all the regions might be explained by the poor translatory effects found for the patients in this thesis. The translatory effects in this thesis was found to be only 1.55 ± 0.82 mm for the patients having a rest scan. Such low translatory effects will not induce any significant changes in the flow estimates for basal parts of the heart, as these regions are thick and muscular. A translation on 1.55 mm will only translate the heart 1.55 voxels, giving a non-significant change in the activity estimate in the basal parts of the heart. It is estimated that patients that have deep breathing cycles have a greater translatory effect as the diaphragm are pushing and pulling the heart more. This could be obtained by instructing the patients to have a monotone

breath-cycle every 6th second. Introducing this set-up will not only improve the significance of the breath-gating, but it might also improve the clinical tests. Currently, all patients are breathing at their own rate, hence the breath pattern is superficial for some patients. These superficial breath cycles leads to a deep breath cycle a couple of times during the scan which stuns the sensory head. This is seen in the analysis of the restricted breath-gating for patient number 6 (see. C.1). Here it is seen that the patient is both coughing and having deep breath-cycles which gives a high translatory effect on the heart, while the breath-gating is impossible. This might be avoided by instructing the patients to breathe in a certain way. One might set up different breath-patterns for the patients, depending on their age. It is estimated that younger patients might be able to have a respiratory rate on 8, while elderly patients might have a rate on 12. To improve the analysis it is estimated that a screen which shows when they are allowed to breathe, might improve the breath-pattern significantly.

The question on how the breath gating is improving the analysis can also be answered by analyzing the IF's and the TAC's.
For the majority of the patients it seems that the breath-gating has improved the estimates of the activity. This is based on the TAC-curves, which in general, are more stable than the non-gated set-ups. The TAC's are found on basis of the mean activity for 25 neighbouring voxels in the apex. The total of 25 voxels were chosen to reduce the noise in the activity-estimates for each frame, as the noise is varying from frame to frame in each voxel. This stabilized TAC's when using the breath gated set-up are especially visible for patients number 1, 2 and 5 (see appendix B.1, B.2 and B.5). For patient number 5 it can be seen that the breath-gated data is having less fluctuation in the activity from frame to frame, especially for the 2mm filtration. The reason that the 2mm filtration is giving a better result is that the blurring effect is smaller, hence one is getting a more correct activity estimate in each voxel. For this particular set-up, the flow is analyzed using a 5 by 5mm grid, giving that the activity estimates using a 4mm Gaussian filtration will blur the activity within the entire grid. For patient number 5 it can be seen that the breath-gating is increasing the activity estimate for the OSEM-TOF reconstruction to a higher level than the non-gated set-up. This is thought to be due to a lower dislocation of the heart throughout the scan, which gives a more stable activity estimate in each frame. From this, it is estimated that the breath-gating has improved the flow-estimates for the patients.

In this project, the patients were analyzed in the Siemens Cardiac PET, which has been approved by the FDA for clinical analysis. When analyzing the patients, all analyses are done in three segments, on which a mean flow for each region is estimated. These flow estimates are used in the statistical analysis, which is thought to give misleading conclusions due to the large areas on which the mean flows are estimated. The large regions gives a high variety in the

estimated flows, which is especially seen for patients having TT or MI. In these patients, a part of the area is determined to have a lower flow than the healthy regions. This is seen as a reduced flow estimate within the region. The flow reduction, however, is minimal when the patient is having a small TT/MI area. By analyzing the means, one is not able to determine which disease the patient suffers from. This is thought to give the non-significant findings in the statistical analysis. The statistical analysis is, however, thought to be improved when using a 17 segment model. This is due to the larger ratio which the TT/MI areas are taking up within the smaller segments. From this it can be concluded that the statistical indications on a significant change when using the breath-gating, might be significant in the MANOVA analysis when analyzing the heart in 17 segments.

The above discussion leads to the question: Are we able to rely on the flows estimated in this project? If not how far are we from the correct flow values? These questions are fundamental, as the flow values are seen to change a lot when changing the analytical set-up.

The questions are difficult to answer, as only six patients were analyzed in this project. Three of these patients were having follow-up scans, meaning the flow values for the patients should be normal if their treatment has had the wanted effect. Of the remaining three patients, one was analyzed and diagnosed, with Takotsubo. From this disease it is not possible to estimate whether the flows are correct or not as the flows are known to be raised above the normal levels. The last two patients were analyzed for IHD. Areas with ischema will have a reduced flow, which makes it impossible to estimate whether or not the flow is correct. The best way to check the flow estimates is to analyse patients having MI as these patients are known to have a flow on 0 ml/g/min due to the fact that the tissue is dead. From this it is thought possible to estimate the size of the infarction, and compare this with the ECG analysis. By correlating these findings it is thought possible to estimate if the area is estimated to be correct when using the ECG. As no patients having a MI were analyzed in this project, this question is difficult to answer.

One possible way to answer the question is to analyse the IF's and the TAC's as the flow values are based on these. Analyzing the IF's and TAC's for the individual patients (see 5.7 and appendix B.1 through B.5), it is seen that the IF's are having two different outlines. These are shown on the next page.

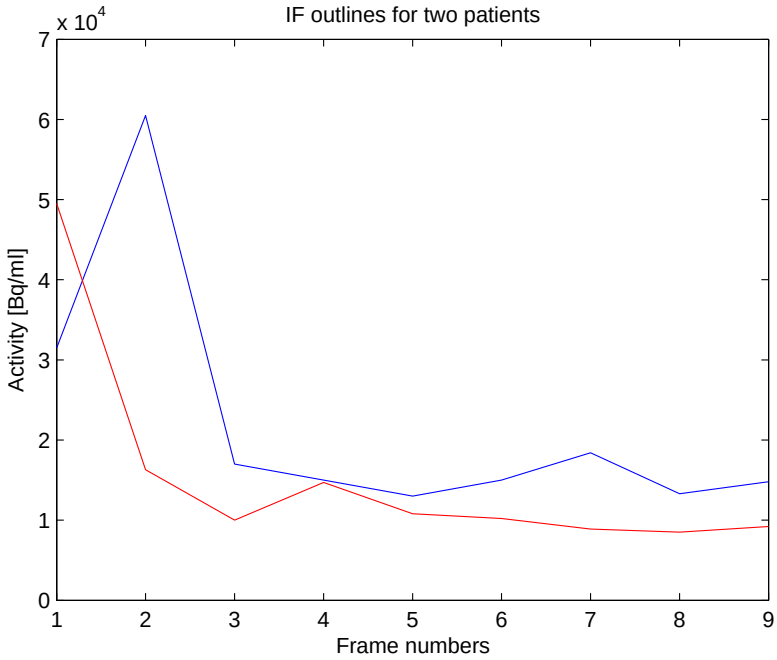

Figure 6.5: Input functions for two patients

Figure 6.5 shows the two possible occurrences of the input functions found for the patients analyzed in this project. It can be seen that the outlines are different, as the peak activity occurs at frame one and two, respectively. The two different outlines may lead to the conclusion that the red IF is erroneous, as it only decays. This conclusion is not correct, as the IF is depending on several physical factors within the patient. The patients are all having the scans started at the time of the injection, meaning that the peak is thought to occur at the same time. The patients, however, are having different physical factors influencing on how fast the tracer is transported to the heart. These are factors as stress-levels and the pulse, which affects the blood circulation. Due to these physiological differences the two occurrences of input-functions are estimated to be correct. This is furthermore based on the fact that the tracer is injected over a 30 seconds interval, meaning that one should not expect a sudden rise and fall in the input function. The continuous injection of the tracer is thought to improve the analysis, as one is getting a more stable estimate on the activity in the blood-phase, when using a 60 seconds frame. In general the peak-estimates are estimated to have an activity on 50000Bq/ml or more, hence one may conclude that if the IF reaches this level, it is correct. This has been estimated by analyzing the peak activities for the majority of the patients. When analyzing

the TAC's for all the patients all the curves are reaching a plateau. The plateau is reached as the myocardial tissue takes up all the tracer available in the blood, while some of the tracer molecules are diffusing back into the blood. The patients flow estimates for the apical region seem correct, as the TAC's are all reaching the plateau. The flow values might, however, be physiological incorrect. This cannot be determined in the patients as this requires a investigation on the heart during the scan. This is not possible, as this would require an autopsy, where the heart is analyzed. A possible method to check if the flows are correct would be to do an analysis on a custom made phantom, simulating the hearts motion and contraction. From such a phantom it would be possible to know the exact flow in the phantom, and correlate the known flows to the estimated flows. By doing this, one would be able to correct the estimated flows to the correct flow. The correct flow values might not be necessary to know, as the doctors are used to look at a certain set-up for the estimated flows. When analyzing new patients the doctors are looking for any pathological changes, which might describe the symptoms the patient has. From this, it can be concluded that the exact flows are not necessary to know, as long as the doctors are able to correlate the flows found for the patient to the diseases they are investigated for.

6.3 Restricted - Non-restricted flows

The patient's breathing pattern is known to have a huge impact on the translation of the heart during the breath-cycle. This is a well known issue, as the diaphragm is pushing and pulling in the respective parts of the breath cycle. A superficial breathing pattern will result in a minimal translation of the heart, while a profound breathing pattern will give a large translation. Due to this, the breath-pattern is vital when doing the motion correction on the breath-gated data. As seen in section 5.8, the breath-pattern is not homogeneous throughout the scan. This might reduce the effect of the breath-gating if all the breath-cycles are accepted because one allows some non-normal translations to affect the estimated activity in the respective frames. There are two possible ways these errors can occur.
The first way is motion in the arms, which is causing a trigger event just before or after a true trigger event. A such event will cause two different non-true binnings of data, which will be described below:

The case with a motion trigger before the breath-induced trigger will cause the last part of the breath-cycle to be divided into 4 bins, even though the event is occurring in the inhaling period of the breath-cycle.

- The data from the extra trigger event will mean that a part of the inhalation data will be analysed as being a part of the other bins.
- This will give a reduction in the activity estimated in the inhalation bin (bin 4), which might give a reduced SNR for the given frame.
- Furthermore, the other bins are introduced to a minor increase of blurring, as the data from the inhilation period are located in other positions than the remaining bins.

The case of a motion trigger just after the breath-induced trigger will cause a similar error to the one just described. In this case, the start of the exhaling will be divided into 4 bins, which will be aligned with the true bins. Furthermore, the remaining part of the breath-cycle will be divided into 4 temporal-equal bins, which will introduce an error in the translation for each of the 4 bins.

The effects of these two wrongly triggered events will decrease both the SNR, and the breath-gating for the 2 affected breath cycles. This can be corrected by setting an upper limit for the respiratory rate for the patient, determined by the average respiratory rate for the patient.

The second non-normal breath cycle that is accepted, if no restrictions are used, is the possibility that the wave-generator does not send out a trigger event at the respiratory peak. This can be caused by two different events.
The first is introduced if the respiratory peak does not reach 50 percent or more on the calibrated scale (as seen in figure 5.16). This will cause that the previous measured breath-cycle is estimated to last 2 breath-cycles, giving the 4 bins will contain half a breath cycle each. This will introduce blurring effects on the estimated binned data, as this will contain data from two bins for the correct breath-gated data. This will furthermore reduce the estimated activity in the averaged bin image, hence the image used for the final frame.
The other possibility is that the patient is having a deep inhalation before a non-normal event. This can be a cough, or just a deep breath due to the fact that the patient is relaxed. A such event is visible in figure C.6(in appendix C.1), where the patient might be relaxed. In this figure, it is seen that the following 10 breath-cycles are not having any trigger events. This is partly caused by a non-sufficient amplitude, and that the wave-generator is stunned for some seconds due to this event. In this case, this will cause the last breath-cycle from frame number 6 to last for about 30 seconds, meaning that it contains data for 10 breath-cycles within the normal breath-pattern for this patient. This leads to each bin contains data for 2.5 breath-cycles which is blurring out the effect of the breath-gating as this is equal to the non-gated set-up. The remaining part of the frame will only contain data for about 60 seconds using this scanning protocol, giving a lowered SNR due to the decay of the tracer. One is able to correct for these errors by excluding breath-cycles having a too low respiratory rate, when compared to the average respiratory rate for the patient.

In a hypothetical setup these restrictions would improve the analysis of the patient, as one would only use data for homogeneous breath-cycles. This is however not the case for the current reconstruction methods, where the reconstruction tool is excluding the following 3 breath cycles from an breath-cycle without the accepted cut-off rates. This is done to ensure that the breath-cycle is stabilized before one is accepting data again. The setup will be accepted when analyzing the breath-gating effect from a steady-state image ("still-image") of the heart, where one is trying to estimate various parameters. This is the case when using ^{18}F-FluroDeoxyGlucose(FDG), which tells on metabolism in the heart. However, this precaution is thought to reduce the effectiveness when doing a dynamic analysis. This has been tried analyzed in this report in both the result section, and the appendix. In both cases the flow is estimated to change to either non-physiological flow values, or flow values close to the flow estimated using all the breath cycles. The change in the flow is determined by the time for the non-accepted events, as the flow is based on the peak activity for the dynamic analysis. This gives that a non-accepted event within the first frames will have a high influence on the flow, which might cause it to rise if the non-accepted event happens when the first pass of the tracer is occurring.

This gives that the breath-gated setup using a restriction on the breath-cycles is giving non-true flows, which cannot be used for clinical analysis, even though it would hypothetically improve the analysis. A change in the reconstruction protocol would improve the flow analysis for the patients, if only the non-accepted respiratory rates were discarded. This would however introduce some non-stable breath-cycles for the consecutive breath-cycles, which cannot be corrected for. However, the flow values based on all the breath-cycles, is not giving the correct flow estimate, even though it is close to the non-gated set-up. This is due to the non-monotone breathing patterns for the patient, which is introducing breath-cycles to contain data from multiple breaths, as discussed previously. The flows from these affected frames will contain more blurring, and not necessarily have the same deformation field as the remaining frames. This will require that the affected frames had to be corrected to the reference image on an individual basis in order to establish the best flow estimates possible. This has however not been tested in this thesis, as this is outside the scope of this analysis.

From the above discussion it is shown that one cannot trust the estimated flow values, as it was discussed in the previous section. However, it is estimated that one can rely more on the reconstructions using all the breath-cycles than on the restricted reconstructions at the moment. An improvement in the reconstruction protocol might change the conclusion. When such a change is possible, one is obliged to check which cut-off rates that is giving the most correct flow estimates. It is however thought that the accepted respiratory rate should cover the majority of the histogram, as shown in figure 5.15. It is furthermore thought that accepting only one respiratory rate might give the best results from a theoretical approach. This is, however, not thought to be the case when reconstructing the images as this will reduce the number of events in the histograms for the images. This will give more noise in the images, and thereby reducing the effectiveness of the breath-gating.

Chapter 7

Conclusion

In this project the dynamic cardiac analysis was tried optimized by introducing a breath-gated set-up. Besides the gating, the analysis was tried optimized by changing the filtering of the images and the reconstruction algorithms. From the respective analyses in this report it is possible to conclude several things.

It can be concluded that the used frame set-up estimates flow values, which are comparable to the gold standard used at the hospital currently.

It was found that the filtration did not give any significant changes in the estimated flow values. From this, it is concluded that the 4mm filtration is giving valid results. This filtration might be of benefit in the analysis for the doctors, as the heart appears more homogeneous.

The reconstruction algorithm was found to be highly significant in the statistical analyses. The same pattern was found in the blind test performed by the doctors. From the analyses of the input functions it is concluded that one obtains the best results by using the OSEM-TOF reconstruction algorithm.

The breath gating protocol was introduced by using a reference image generated for each individual patient. The statistical analyses indicates that the breath-gating does not have any significant impact on the flow estimates for patients having a normal flow. When analyzing a patient having a flow-altering disease it was found that the breath-gating was significant in the ANOVA analyses. The same was not found when analysing the data in a MANOVA. From this it can be concluded that a further analysis is required before concluding on the effect of the breath-gating.
When analyzing the estimated flow values, it can be seen that the values from the breath-gated set-ups have different flow values from the non-gated set-up. From this it can be concluded that the breath-gating is having an effect on the analysis, even though it might be found statistically.

The breath-gating was found to have improved the contrasts between the cardiac wall and the lumen in the left ventricle. From this it can be concluded that the breath-gated set-up is improving the analyses on the static images.

From the conclusions above, it was possible to set up a list of recommendations, which is meant to improve the dynamic analysis for the cardiac PET scans. These recommendations are found on pp. 136.

7.1 Future work

In the conclusion it can be seen that one is able to optimize the dynamic analysis by changing the current scanning protocol. The improvements found in this thesis does not give the exact flow estimates for the heart. By analyzing different aspects of the cardiac analysis, it is thought possible to find the optimum analysis. Below are listed two possible approaches one could use for optimizing the cardiac analysis.

Analyse the flow using a cardiac gating

In this project was the dynamic analysis tried optimized by correcting for the breath induced translations of the heart. The average translations were found to be minor for the majority of the patients. Though the minor translations, it was still possible to estimate flow changes for all the patients. By analyzing the flow values using a cardiac gating, one is able to determine which correction that benefits the analysis the most. The cardiac gating might give the same improvements as the breath gating, as the heart is having its own translation during the contraction. By only using the diastolic part of the cardiac cycle, one is thought able to estimate the effects of the cardiac gating. From the results found for the cardiac gating one is able to estimate which correction that benefits the cardiac analysis the most.

It is however not possible to do both the corrections simultaneously as this would generate to many bins, e.g. one would have to low signal in each bin.

Correct the hearts motion by correcting in the listmode file

One is able to improve the analysis further by correcting for both the cardiac motion and the breath motion in the listmode file. This is thought possible as the mCT scanner is having a dual gating scanning protocol, in which both measurements are analysed. The two trigger signals are stored within the listmode file, which enables a correction on both motions. By doing this one is able thought to improve the diagnostic value of the analysis.

7.2 Recommendations

This section will point out the recommendations for the dynamical PET analysis of the heart using ^{13}N-NH_3. The recommendations below are divided into a general optimization of the dynamic analysis, and the recommendatory set-up for the breath-gating protocol. The general optimizations are shown below.

- Use the OSEM-TOF reconstruction with 2 iterations and 21 subsets in order to obtain the most correct activity estimates.
- Reduce the scan time to 10 minutes, as the kinetic model are based on the activity within the first 8 minutes.
- Check if the input functions and time-activity-curves for the different regions seems acceptable, before relying on the correctness of the flows.

The optimizations regarding the breath gating is shown below.

- Use a 4-bin set-up as this is thought to give the best results, when not correcting for the cardiac motion.
- Use all the measured breath-cycles until an improvement of the reconstruction protocol has been released. When one is able to exclude the single non-accepted breath cycles, then use a restricted set-up. If the patients are not instructed to have a certain breath-pattern, then the restrictions must be made on a personal basis.
- Make sure that the patient have a somewhat monotone breath cycle throughout the scanning, e.g. keep the patient awake if the patient starts to slumber.
- Use a great amplification of the breath-cycle which covers the entire scale, if possible. If this is not possible, then make sure that the respiratory peaks are well above the 50% line, otherwise are the risks that the patients altered respiratory level may drop below the trigger level.
- Make sure that the respiratory belt is tightened properly, which is shown on the connector box. If tightened too little one is risking not to measure the breath-cycles, and tightened too much might give too many triggers.
- Instruct the patient to breathe in a certain way in order to have better breath-measurements.
- If the estimated flows does not seem correct, then analyse the measured breath-pattern for the patient as this might affect the flow values.

Appendix A

Measured deformation fields for patients scanned in the Siemens Biograph 64

In this section are the deformation fields for the different reconstructions analysed. The scans are, as mentioned in the report, carried out on two scanners. The first two patients were scanned at the Siemens Biograph 64 scanner, which only has the possibility of reconstruct the data using the OSEM algorithm. The remaining four patients had their scans carried out at the Siemens mCT scanner. This scanner has the possibility of reconstructing the images using both the OSEM and the OSEM-TOF reconstruction algorithms. The four patients are analysed using both reconstruction algorithms. The deformation fields for the last patient was last due to some clean up processes on the pc on which the reconstructions were performed.

The tables shows the translation which are given in mm, the rotation which are given in degrees.

Patient number 1

Transformation parameters using a 2mm Filtration						
	Bin 1			Bin 2		
Affine parameter	X	Y	Z	X	Y	Z
Translation	1.20	-0.32	0.43	0.00	0.00	0.00
Rotation	-0.10	0.03	0.05	0.00	0.00	0.00
Scale	1.01	1.00	1.00	1.00	1.00	1.00
Shear	-0.01	0.00	0.00	0.00	0.00	0.00
	Bin 3			Bin 4		
Affine parameter	X	Y	Z	X	Y	Z
Translation	0.00	0.00	0.00	1.02	0.84	0.53
Rotation	0.00	0.00	0.00	0.07	-0.04	-0.06
Scale	1.00	1.00	1.00	1.00	1.00	1.00
Shear	0.00	0.00	0.00	0.00	0.00	0.00

Table A.1: Affine transformation parameters found for the respective bins for patient number 1

Transformation parameters using a 4mm Filtration						
	Bin 1			Bin 2		
Affine parameter	X	Y	Z	X	Y	Z
Translation	0.13	0.17	-0.05	0.00	0.00	0.00
Rotation	-0.10	0.08	-0.06	0.00	0.00	0.00
Scale	1.00	1.00	1.00	1.00	1.00	1.00
Shear	-0.00	0.00	0.00	0.00	0.00	0.00
	Bin 3			Bin 4		
Affine parameter	X	Y	Z	X	Y	Z
Translation	0.00	0.00	0.00	0.73	0.69	0.39
Rotation	0.00	0.00	0.00	0.01	-0.10	0.00
Scale	1.00	1.00	1.00	1.00	1.00	1.00
Shear	0.00	0.00	0.00	0.00	0.00	0.00

Table A.2: Affine transformation parameters found for the respective bins for patient number 1 using a 4mm Gaussian filtration of the data

In table A.1 and A.2 it is seen that the deformation fields applied to the different bins are of low magnitude. From this it is estimated that the flow estimates for both the breath-gated and the non-gated set-up are similar. The estimated flows are analysed in the next appendix.

Patient number 2

Transformation parameters using a 2mm Filtration						
	Bin 1			Bin 2		
Affine parameter	X	Y	Z	X	Y	Z
Translation	0.01	0.37	1.02	1.07	0.12	0.10
Rotation	-0.26	0.18	-0.30	0.02	-0.18	0.15
Scale	1.00	1.00	1.00	1.00	1.00	1.00
Shear	-0.00	0.00	0.00	-0.00	-0.00	0.00
	Bin 3			Bin 4		
Affine parameter	X	Y	Z	X	Y	Z
Translation	0.96	0.52	0.02	0.36	0.65	0.34
Rotation	0.01	0.08	-0.13	-0.08	-0.32	-0.05
Scale	1.00	1.00	1.01	1.01	1.00	1.00
Shear	0.00	0.00	0.01	0.00	0.00	0.00

Table A.3: Affine transformation parameters found for the respective bins for patient number 2

Transformation parameters using a 4mm Filtration						
	Bin 1			Bin 2		
Affine parameter	X	Y	Z	X	Y	Z
Translation	1.12	0.33	2.92	0.69	0.70	-0.10
Rotation	-0.33	0.78	-0.17	-0.33	0.19	0.18
Scale	0.99	1.00	1.02	0.99	1.00	1.02
Shear	0.00	0.01	0.01	-0.01	-0.02	0.00
	Bin 3			Bin 4		
Affine parameter	X	Y	Z	X	Y	Z
Translation	1.18	-0.14	-0.39	1.50	0.65	0.97
Rotation	0.05	0.19	-0.18	-0.16	0.22	-0.25
Scale	1.02	1.00	1.01	1.02	1.00	1.01
Shear	0.00	-0.01	-0.01	0.00	0.00	0.00

Table A.4: Affine transformation parameters found for the respective bins for patient number 2 using a 4mm Gaussian filtration of the data

The deformation fields for this patient is seen to be rather low. It is, however, seen that the craniocaudal motion has been estimated to great for the 4mm reconstructed data. From this it can be estimated that the apical flows are estimated to be more true for breath gated data, than for the non-gated data.

A.1 Measured affine transformation parameters acquired at scans from the Siemens mCT scanner

In this section are the 2mm filtrations shown first, followed by the 4mm filtered data. For both filtration algorithms are the deformation fields for the OSEM reconstruction shown first, followed by the OSEM-TOF reconstructions.

Patient 3

Transformation parameters using a 2mm Filtration						
	Bin 1			Bin 2		
Affine parameter	X	Y	Z	X	Y	Z
Translation	0.36	0.84	0.93	0.42	2.12	-0.84
Rotation	-0.25	0.23	-0.12	0.03	-0.01	-0.10
Scale	1.00	1.00	1.00	1.00	1.00	1.01
Shear	0.01	0.01	0.00	0.00	-0.00	-0.01
	Bin 3			Bin 4		
Affine parameter	X	Y	Z	X	Y	Z
Translation	0.81	1.60	1.23	0.27	-0.07	0.53
Rotation	-0.06	0.42	-0.67	-0.27	-0.05	-0.14
Scale	1.01	1.00	1.02	1.01	1.00	1.00
Shear	-0.01	0.00	-0.01	-0.00	0.00	0.00

Table A.5: Affine transformation parameters found for the respective bins for patient number 3

Transformation parameters using a 2mm Filtration						
	Bin 1			Bin 2		
Affine parameter	X	Y	Z	X	Y	Z
Translation	0.08	-0.31	-0.12	-0.07	0.45	0.42
Rotation	-0.13	0.03	0.10	0.20	-0.07	-0.08
Scale	1.00	1.00	1.00	1.00	1.00	1.02
Shear	-0.00	-0.00	-0.00	-0.00	0.01	-0.01
	Bin 3			Bin 4		
Affine parameter	X	Y	Z	X	Y	Z
Translation	0.25	1.47	1.96	0.07	0.84	-0.03
Rotation	-0.33	-0.34	-0.21	-0.11	0.05	0.09
Scale	1.02	1.00	1.02	1.00	1.00	1.00
Shear	-0.02	0.02	-0.00	-0.00	0.00	-0.00

Table A.6: Affine transformation parameters found for the respective bins for patient number 3, using the TOF reconstruction method

Transformation parameters using a 4mm Filtration						
	Bin 1			Bin 2		
Affine parameter	X	Y	Z	X	Y	Z
Translation	0.18	0.15	1.17	1.27	0.82	-0.41
Rotation	-0.16	0.11	0.13	-0.18	0.26	-0.03
Scale	0.99	1.00	1.00	1.00	1.00	1.01
Shear	-0.00	-0.00	-0.01	-0.02	0.01	-0.00
	Bin 3			Bin 4		
Affine parameter	X	Y	Z	X	Y	Z
Translation	1.32	1.73	0.49	0.14	-1.49	3.25
Rotation	-0.12	0.48	-0.48	-0.37	0.06	-0.21
Scale	1.01	1.00	1.01	1.01	1.01	1.00
Shear	-0.02	0.01	-0.01	-0.01	0.02	-0 01

Table A.7: Affine transformation parameters found for the respective bins for patient number 3

Transformation parameters using a 4mm Filtration						
	Bin 1			Bin 2		
Affine parameter	X	Y	Z	X	Y	Z
Translation	0.1	0.23	-0.30	-0.72	1.77	-0.58
Rotation	-0.05	0.12	0.02	-0.01	-0.01	-0.31
Scale	1.00	1.00	1.00	1.00	0.99	1.02
Shear	0.00	-0.00	-0.00	-0.01	0.01	0.00
	Bin 3			Bin 4		
Affine parameter	X	Y	Z	X	Y	Z
Translation	1.03	2.38	0.43	0.41	0.14	2.81
Rotation	-0.36	0.13	-0.06	-0.35	0.14	-0.06
Scale	1.00	0.99	1.02	1.00	1.00	0.99
Shear	-0.02	0.01	-0.00	-0.01	0.01	-0.01

Table A.8: Affine transformation parameters found for the respective bins for patient number 3, using the TOF reconstruction method

In the above tables it is possible to compare the deformation fields determined for the 3 patient in this study. Common for all the deformation fields is, that the scale and the shear are 1 and 0, respectively. This was expected, as the heart is assumed to have the same size, and torsion throughout the scan, when not correcting for the hearts own motion.

Patient 4

This patient had both a rest and a stress scan carried out. The estimated translations for both the rest, and the stress scan is shown here. The data is presented in the same order as for the other patients, however is the deformation fields for the rest scan shown first followed by the deformation fields for the stress scan.

Transformation parameters using a 2mm Filtration						
	Bin 1			Bin 2		
Affine parameter	X	Y	Z	X	Y	Z
Translation	0.90	1.04	0.97	0.76	0.98	0.77
Rotation	0.04	0.09	0.04	-0.15	-0.20	-0.04
Scale	1.00	1.00	1.00	1.01	1.00	1.01
Shear	0.01	0.00	0.00	0.00	0.02	0.01
	Bin 3			Bin 4		
Affine parameter	X	Y	Z	X	Y	Z
Translation	1.40	1.03	0.47	0.53	0.60	1.09
Rotation	0.19	-0.09	-0.03	0.13	-0.13	-0.35
Scale	1.01	0.99	1.02	1.02	1.00	1.00
Shear	0.00	0.02	0.00	0.00	0.02	-0.00

Table A.9: Affine transformation parameters found for the respective bins for patient number 4

Transformation parameters using a 2mm Filtration						
	Bin 1			Bin 2		
Affine parameter	X	Y	Z	X	Y	Z
Translation	0.77	0.11	0.86	0.70	-0.36	-0.28
Rotation	0.03	-0.12	0.17	0.04	-0.05	0.08
Scale	1.01	1.00	1.00	1.00	1.00	1.01
Shear	0.00	0.00	000	-0.00	0.00	-0.00
	Bin 3			Bin 4		
Affine parameter	X	Y	Z	X	Y	Z
Translation	2.44	-1.05	0.82	1.17	-0.11	-0.69
Rotation	0.26	0.33	0.01	0.09	0.28	-0.10
Scale	1.00	1.01	1.03	1.00	1.00	1.00
Shear	-0.00	0.02	-0.00	-0.00	0.00	-0.00

Table A.10: Affine transformation parameters found for the respective bins for patient number 4, using the TOF reconstruction method

Transformation parameters using a 4mm Filtration						
	Bin 1			Bin 2		
Affine parameter	X	Y	Z	X	Y	Z
Translation	1.73	0.09	1.13	0.83	0.82	0.04
Rotation	-0.02	0.39	0.44	-0.10	-0.06	0.13
Scale	0.99	1.00	1.01	1.00	1.00	1.02
Shear	0.00	-0.00	-0.00	-0.00	0.01	0.01
	Bin 3			Bin 4		
Affine parameter	X	Y	Z	X	Y	Z
Translation	1.63	0.20	0.48	1.24	0.56	-0.32
Rotation	-0.10	-0.06	0.13	0.00	0.10	0.23
Scale	1.00	1.00	1.03	1.01	1.00	1.00
Shear	-0.01	0.01	0.01	0.00	-0.01	-0.01

Table A.11: Affine transformation parameters found for the respective bins for patient number 4

Transformation parameters using a 4mm Filtration						
	Bin 1			Bin 2		
Affine parameter	X	Y	Z	X	Y	Z
Translation	0.44	0.18	0.84	-0.12	-0.38	-0.93
Rotation	-0.00	-0.03	0.04	-0.34	0.13	-0.37
Scale	1.01	1.00	1.00	1.00	1.01	1.02
Shear	0.00	0.01	-0.00	-0.01	0.02	0.02
	Bin 3			Bin 4		
Affine parameter	X	Y	Z	X	Y	Z
Translation	0.19	0.84	0.49	1.58	0.21	-0.03
Rotation	-0.76	-0.03	-0.48	-0.56	0.11	-0.21
Scale	1.01	1.01	1.03	1.02	1.00	0.99
Shear	-0.01	0.02	0.02	-0.02	-0.00	-0.00

Table A.12: Affine transformation parameters found for the respective bins for patient number 4, using the TOF reconstruction method

On the next pages are the deformation fields for the stress scan shown.

Transformation parameters using a 2mm Filtration						
	Bin 1			Bin 2		
Affine parameter	X	Y	Z	X	Y	Z
Translation	2.19	-0.39	0.40	4.38	0.99	0.69
Rotation	0.01	0.42	0.18	-0.11	0.76	-0.07
Scale	1.00	1.00	1.00	1.02	1.00	1.02
Shear	-0.01	0.01	-0.00	-0.01	0.02	0.00
	Bin 3			Bin 4		
Affine parameter	X	Y	Z	X	Y	Z
Translation	3.59	-0.22	0.97	1.60	1.37	-0.34
Rotation	0.21	0.57	-0.26	-0.09	0.15	0.11
Scale	1.02	1.00	1.02	1.00	1.00	1.00
Shear	-0.02	0.03	-0.01	-0.00	0.00	-0.00

Table A.13: Affine transformation parameters found for the respective bins for patient number 4

Transformation parameters using a 2mm Filtration						
	Bin 1			Bin 2		
Affine parameter	X	Y	Z	X	Y	Z
Translation	0.72	-0.52	1.34	1.67	-0.19	0.43
Rotation	-0.04	-0.00	0.11	0.16	0.36	-0.38
Scale	1.00	1.00	1.00	1.01	1.00	1.02
Shear	-0.00	0.00	-0.00	-0.01	0.01	-0.01
	Bin 3			Bin 4		
Affine parameter	X	Y	Z	X	Y	Z
Translation	2.50	-0.44	1.06	0.33	0.28	0.63
Rotation	0.08	0.35	-0.44	0.33	0.28	0.63
Scale	1.02	1.01	1.02	1.02	1.00	1.00
Shear	-0.01	0.01	-0.01	-0.00	0.00	-0.00

Table A.14: Affine transformation parameters found for the respective bins for patient number 4, using the TOF reconstruction method

Transformation parameters using a 4mm Filtration						
	Bin 1			Bin 2		
Affine parameter	X	Y	Z	X	Y	Z
Translation	0.92	-0.52	0.68	1.61	-0.58	0.05
Rotation	0.16	0.21	0.07	0.02	0.50	-0.65
Scale	1.00	1.00	1.00	1.01	1.01	1.02
Shear	0.00	0.01	-0.00	-0.00	0.01	0.00
	Bin 3			Bin 4		
Affine parameter	X	Y	Z	X	Y	Z
Translation	1.37	1.29	0.44	0.95	0.89	0.25
Rotation	-0.28	0.41	-1.02	-0.17	0.35	0.56
Scale	1.02	1.00	1.01	1.02	1.00	1.00
Shear	-0.00	0.01	-0.01	0.01	0.01	-0.01

Table A.15: Affine transformation parameters found for the respective bins for patient number 4

Transformation parameters using a 4mm Filtration						
	Bin 1			Bin 2		
Affine parameter	X	Y	Z	X	Y	Z
Translation	-0.05	0.32	0.63	0.87	0.13	-0.66
Rotation	-0.15	-0.01	0.03	0.08	-0.20	-0.25
Scale	1.00	1.00	1.00	1.01	1.00	1.01
Shear	-0.00	-0.01	-0.01	-0.01	0.01	-0.00
	Bin 3			Bin 4		
Affine parameter	X	Y	Z	X	Y	Z
Translation	1.91	1.18	0.04	0.22	1.81	2.31
Rotation	-0.01	-0.06	-0.37	-0.44	-0.02	-0.51
Scale	1.02	1.0	0 1.02	1.02	1.00	1.00
Shear	-0.01	0.02	-0.00	-0.00	0.01	-0.02

Table A.16: Affine transformation parameters found for the respective bins for patient number 4, using the TOF reconstruction method

When analyzing the deformation fields for the rest and the stress scan, it is seen that there is a tendency to the translatory effects are greater for the stress scan than for the rest. This was expected as the heart is stressed to work harder, and it is known that the drug injected to the patient may give the side effect of nausea. Both these changes will alter the breath-cycle to have a more profound breath-pattern which shows a greater translatory effect.

Patient 5

The deformation fields found for this person are retrieved from a stress study, as the patient did not have a successful breath gating of the rest-scan.

Transformation parameters using a 2mm Filtration						
	Bin 1			Bin 2		
Affine parameter	X	Y	Z	X	Y	Z
Translation	0.23	0.46	0.34	-0.04	1.66	0.86
Rotation	-0.08	0.05	-0.02	-0.35	0.10	-0.30
Scale	1.00	1.00	1.00	1.00	01.00	1.02
Shear	-0.00	0.00	-0.00	-0.00	0.01	0.00
	Bin 3			Bin 4		
Affine parameter	X	Y	Z	X	Y	Z
Translation	1.42	1.69	0.41	0.32	0.76	1.40
Rotation	-0.27	-0.18	0.03	0.08	0.06	0.07
Scale	1.02	1.00	1.00	1.01	1.00	1.00
Shear	-0.01	0.01	0.01	0.01	0.00	-0.00

Table A.17: Affine transformation parameters found for the respective bins for patient number 5

Transformation parameters using a 2mm Filtration						
	Bin 1			Bin 2		
Affine parameter	X	Y	Z	X	Y	Z
Translation	1.65	1.41	1.44	1.2	1.56	1.16
Rotation	-.22	0.21	0.22	-0.43	0.01	-0.18
Scale	1.00	1.00	1.01	1.01	1.01	1.02
Shear	-0.00	0.00	0.01	-0.00	0.02	0.01
	Bin 3			Bin 4		
Affine parameter	X	Y	Z	X	Y	Z
Translation	2.05	0.63	0.84	0.19	0.25	1.00
Rotation	-0.35	-0.02	0.15	0.09	0.04	0.14
Scale	1.01	1.01	1.01	1.00	1.00	1.00
Shear	-0.00	0.02	0.01	0.01	0.00	-0.00

Table A.18: Affine transformation parameters found for the respective bins for patient number 5, using the TOF reconstruction method

Transformation parameters using a 4mm Filtration						
	Bin 1			Bin 2		
Affine parameter	X	Y	Z	X	Y	Z
Translation	0.40	0.60	0.05	0.36	1.19	0.58
Rotation	-0.19	0.11	0.12	-0.10	0.04	-0.14
Scale	1.00	1.00	1.00	1.00	1.00	1.01
Shear	0.00	0.00	0.00	-0.01	0.01	-0.00
	Bin 3			Bin 4		
Affine parameter	X	Y	Z	X	Y	Z
Translation	0.61	0.90	-0.18	0.15	0.09	0.67
Rotation	-0.22	0.25	-0.26	-0.14	0.19	-0.01
Scale	1.01	1.00	1.01	1.00	1.00	1.00
Shear	-0.01	0.01	-0.00	0.01	0.00	0.00

Table A.19: Affine transformation parameters found for the respective bins for patient number 5

Transformation parameters using a 4mm Filtration						
	Bin 1			Bin 2		
Affine parameter	X	Y	Z	X	Y	Z
Translation	1.03	0.78	0.59	2.12	0.79	-0.90
Rotation	-0.22	0.21	0.04	-0.24	0.44	0.08
Scale	1.00	1.00	1.01	1.00	1.00	1.01
Shear	-0.00	-0.00	0.00	-0.01	0.01	0.00
	Bin 3			Bin 4		
Affine parameter	X	Y	Z	X	Y	Z
Translation	1.97	0.60	0.80	1.34	-0.10	1.62
Rotation	-0.47	0.59	0.02	-0.15	0.49	-0.03
Scale	1.01	1.01	1.02	1.01	1.00	1.00
Shear	-0.01	0.01	0.00	0.00	0.00	-0.00

Table A.20: Affine transformation parameters found for the respective bins for patient number 5, using the TOF reconstruction method

The deformation fields for patient number 6 were lost before the measured data was retrieved from the computer. The breath-gating was, however performed which is analysed in section 5.7. Here it can be seen that the breath-gating has changed the input functions and the TAC's for the patient, which indicates that the heart was having a large translatory effect.

Appendix B

Analysis of the measured flow values for all the patients

B.1 Patient 1

This patient were scanned at the PET6-scanner, which is a Siemens Biograph 64 scanner. This scanner does not have the possibility to reconstruct the images using the TOF reconstruction method. Due to this is this patient only analyzed using the 2mm and the 4mm filtration using 4 iterations and 21 subsets. The polar plots analyzing the effects of the breath gating and the filtration are shown in figure B.1 on the next page. The patient were having a three-months follow-up scan after being diagnosed with Takotsubo cardiomyopathy, in order to analyze if the patient has recovered. Due to the ethology of the disease it is expected that the patient has recovered, hence the flow values is expected to be normal.

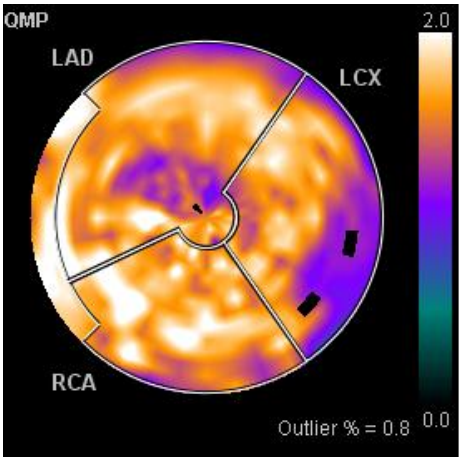

(a) Polar plot of the estimated flow values using the non-gated set-up and a 2mm filtration

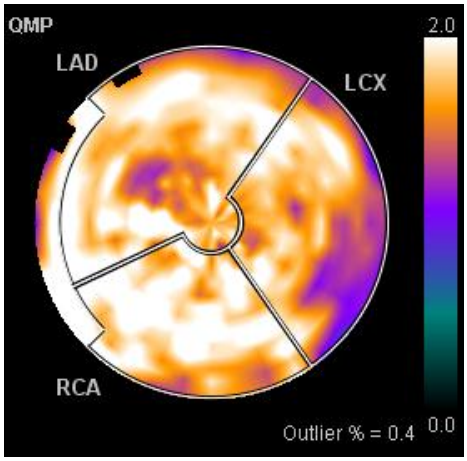

(b) Polar plot of the estimated flow values using motion corrected data

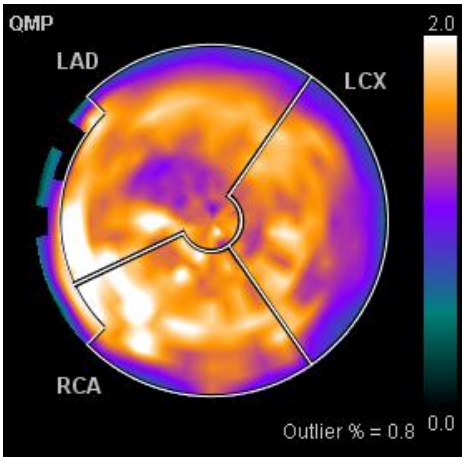

(c) Polar plot of the estimated flow values using the non-gated set-up and a 4mm filtration

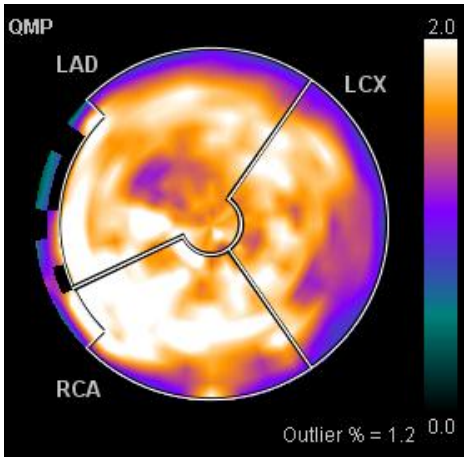

(d) Polar plot of the estimated flow values using motion corrected data

Figure B.1: Flow analysis from Siemens Syngo

In the above images it is seen that the patient is having a reduced uptake in the LAD region, in a otherwise high-perfused area. This might indicate that this patient is still suffering form TT, as the flow is estimated to be approximately 1.1 ml/g/min. The remaining part of the ventricle is seen to have hyper-perfusion values which are close to 2 ml/g/min. These high flow values, along the expected TT area, indicates that the patient is still having emotional stress which causes TT. When analyzing the effect of the breath gating, it is seen that the breath

gating are increasing the estimated flow values, which might indicate that this patient has not recovered yet. The mean flows for the respective segments are shown in the table below.

	Flow values in ml/g/min			
	2mm Gaussian filtration		4mm Gaussian filtration	
Region	Non gated	Breath Gated	Non Gated	Breath Gated
LAD	1.58	1.78	1.52	1.69
LCX	1.51	1.64	1.44	1.57
RCA	1.71	1.90	1.65	1.84
Global	1.59	1.77	1.53	1.70

Table B.1: Flow values for a rest study using either a 2mm or a 4mm filtration on the Siemens biograph 64 scanner

In the above table it can be seen that the tendency is that all the flows are increased when applying the breath-gating. This can be explained by the motion of the heart. The motion has been estimated to be above 1mm in the x-direction for two of the bins, which is equal to a shift of the voxel in the x-direction, and approximately a half voxel in the z-direction when using the 2mm filtration. When using the 4mm filtration the motions are estimated to be reduced, which is due to the larger filtration kernel. A further analysis on the flow analysis is done on the next couple of pages.

The further analysis is based on the input functions and the time-activity-curves, which are shown on the next page. The TAC is estimated from the mean of 25 voxels in the apex. This area has been chosen due to the Takotsubo usually affects this area. In figure B.2 is shown both the input function and the time-activity-curve for the 2mm filtration set-up.

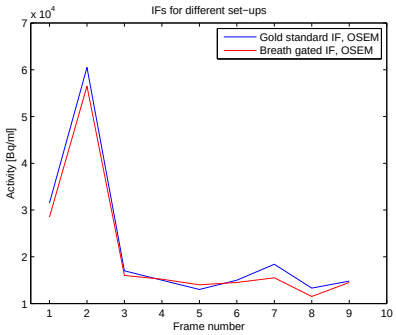

(a) Input functions for patient number 1

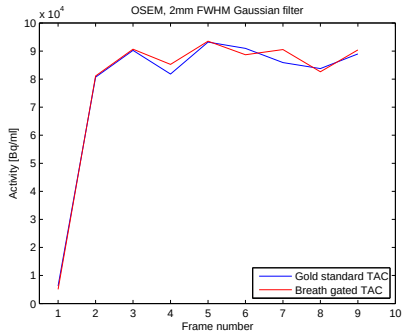

(b) Time-Activity-Curves for patient number 1

Figure B.2: Input function and Time-Activity-Curves for patient number 1

When analyzing the IF's it can be seen that the breath-gated images are having a reduced activity estimate in the IF's in general. This analyzed against the TAC's, where the opposite is found, reveals that the breath-gated data is having a higher up-take of the tracer available. This gives the higher flow-estimates, which are thought to be more accurate. This is estimated on the ANOVA tests carried out for the patient. The same patterns are found for the 4mm filtered data, which are shown on the next page.

From this it is estimated that the flow values found for the breath-gated data are more accurate than the non-gated set-up. On the other hand it is not possible to determine which filtration that gives the best flow-estimate, as it can be seen that the data having 4mm filtrations are estimated to have a higher activity level. This can be explained by the reduction in the low-flow areas when using the larger filtration kernel. At the same time the 4mm filtration is having a more stable TAC, which indicates that this set-up is the best.

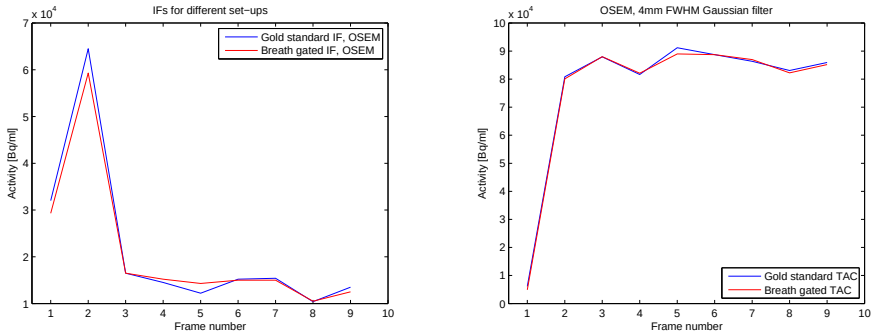

(a) Input functions for patient number 1 (b) Time-Activity-Curves for patient number 1

Figure B.3: Input function and Time-Activity-Curves for patient number 1

B.2 Patient 2

The patient is having a 3-months follow-up scan after being diagnosed with TT. The patient was scanned in the Siemens Biograph 64 scanner, hence the data is only reconstructed using the OSEM reconstruction algorithm. The polar plots for this patient is shown below.

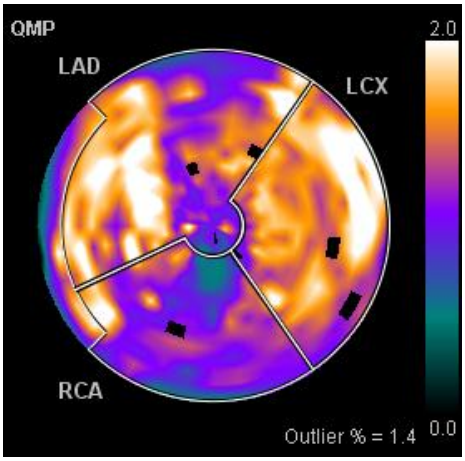

(a) Polar plot of the estimated flow values using the non-gated set-up and a 2mm filtration

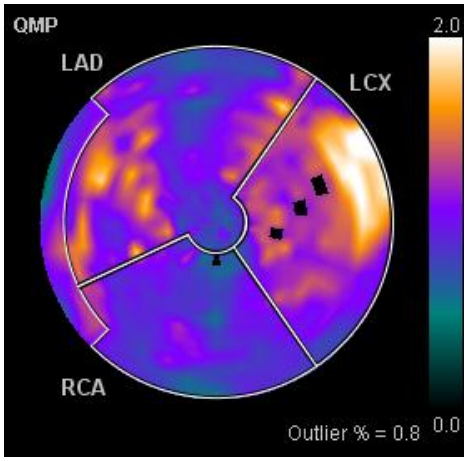

(b) Polar plot of the estimated flow values using motion corrected data

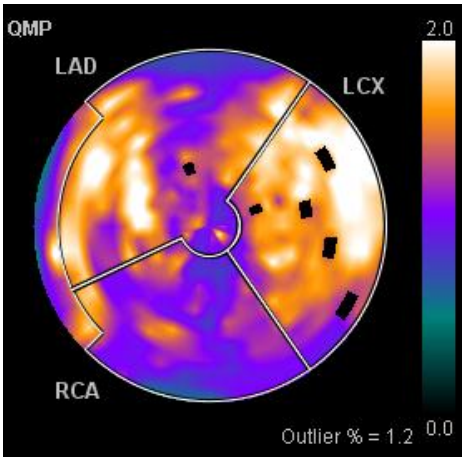

(c) Polar plot of the estimated flow values using the non-gated set-up and a 4mm filtration

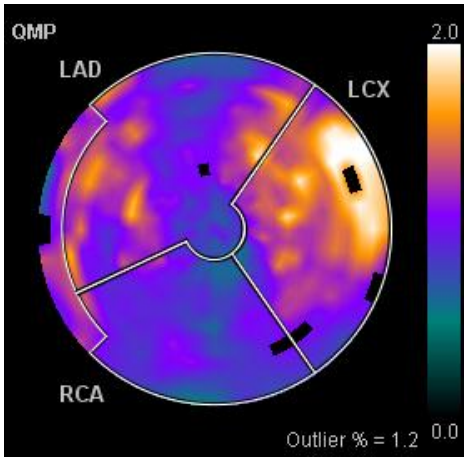

(d) Polar plot of the estimated flow values using motion corrected data

Figure B.4: Flow analysis from Siemens Syngo

In the polar plots on the previous page it can be seen that non-gated set-up is estimating the LAD and the LCX regions to have an increased flow. When applying the breath-gating it is seen that the flows are reduced greatly for the LAD region. The LCX region is, however, still estimated to have a high flow value in the basal region. These findings are seen in the mean flow estimates for the respective regions, shown in the table below.

	Flow values in ml/g/min			
	2mm Gaussian filtration		4mm Gaussian filtration	
Region	Non gated	Breath Gated	Non Gated	Breath Gated
LAD	1.38	1.05	1.36	1.04
LCX	1.60	1.31	1.62	1.35
RCA	1.11	0.91	1.14	0.90
Global	1.38	1.09	1.38	1.09

Table B.2: Flow values for a rest study using either a 2mm or a 4mm filtration on the Siemens biograph 64 scanner

In the above table it can be seen that the flow estimates for the non-gated set-ups are estimating a hyper-perfusion in the LAD and LCX regions, as these areas are above 1.2 ml/min/g. When applying the breath gating, it is seen that the LAD region is estimated to have a normal flow, leaving the LCX region to have a hyper-perfusion. The change in the flow estimates are visible in the IF's and TAC's, which are shown below.

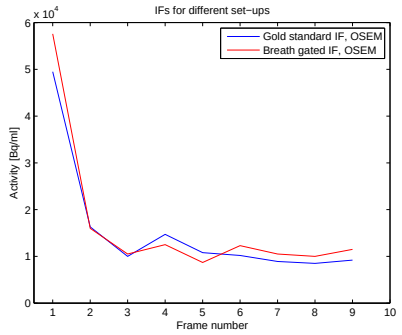

(a) Input functions for patient number 2

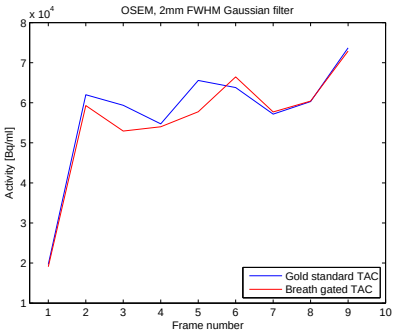

(b) Time-Activity-Curves for patient number 2

Figure B.5: Input function and Time-Activity-Curves for patient number 2

In figure B.5a it can be seen that the breath-gated data is estimated to have a higher activity in the initial frame, than the non-gated set-up. When comparing

this to the TAC's for the respective set-ups it is seen that the OSEM-TOF reconstructed data will have a reduced flow estimate when compared to the OSEM reconstruction. This is due to the TAC activity for the OSEM-TOF images are estimated to be lower, which represents a lower fractional uptake of the tracer available.

The IF's and TAC's for the 4mm filtered data is shown in the figure B.6, below.

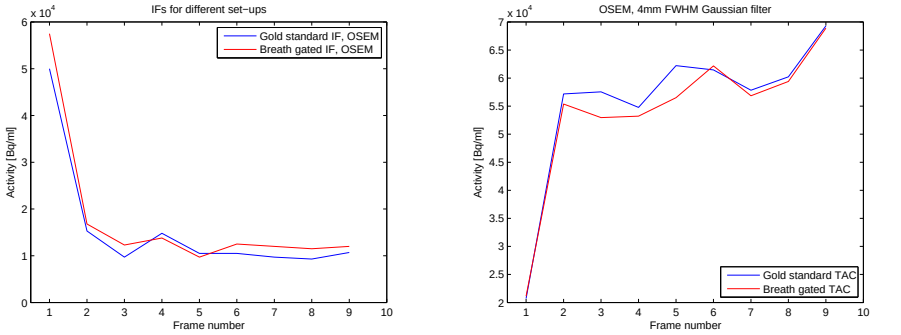

(a) Input functions for patient number 2 (b) Time-Activity-Curves for patient number 2

Figure B.6: Input function and Time-Activity-Curves for patient number 2

In the above figure is the same tendencies seen as for the 2mm filtration set-up. When analyzing the IF's and TAC's in general it is noticed that the breath-gated data is having a lower variance between the estimated activities in the respective frames, which leads to the conclusion that the breath-gating is improving the analysis for this patient. As for patient number 1, it is impossible to determine which of the filtrations that gives the most accurate perfusion estimate, as the polar plots are showing the same areas with reduced uptake. In the 4mm filtration it is seen that the areas are estimated to be larger, but the flow is estimated to be higher than the flow values for the 2mm filter situation. This was expected as the 4mm filtration is known to blur out the data, which will increase the area with a reduced uptake. On the other hand are these areas also interpolated with the neighbouring areas, where the flow estimates are normal, which are increasing the flow estimate in the hypo-perfused area.

B.3 Patient 3

This patient had a 3-months follow-up scan after being diagnosed with TT. The patient was scanned in the Siemens mCT, which gave the opportunity to analyse the patient both with and without the use of the Time-Of-Flight reconstruction method. Due to this opportunity the patient was analysed using both the 2mm and the 4mm Gaussian filtered images for both the conventional OSEM reconstruction and the OSEM-TOF reconstruction. In this section the conventional OSEM reconstruction will be analysed first, followed by the analysis of the OSEM-TOF reconstructed images. In figure C.9 on the next page, the polar plots for the conventional reconstruction is analysed. The polar plots show no evidence on the patient has suffered from TT, hence the patient seems to have recovered from the disease. This is furthermore shown in the flow estimates for the respective regions which are shown below.

	Flow values in ml/g/min			
	2mm Gaussian filtration		4mm Gaussian filtration	
Region	Non gated	Breath Gated	Non Gated	Breath Gated
LAD	1.01	0.94	1.05	0.95
LCX	0.98	0.92	1.03	0.97
RCA	0.93	0.88	0.98	0.94
Global	0.98	0.92	1.03	0.96

Table B.3: Flow values for a rest study using either a 2mm or a 4mm filtration on the Siemens mCT scanner, using a conventional reconstruction method

In the above table it can be seen that the breath-gating is reducing the flow-estimates for the conventional reconstruction method. In all the segments it can be seen that the flow estimates are within the normal range, hence the patient have recovered from Takotsubo cardiomyopathy.

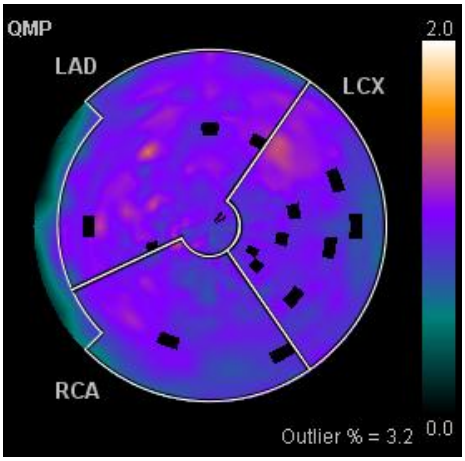

(a) Polar plot of the estimated flow values using the non-gated set-up and a 2mm filtration

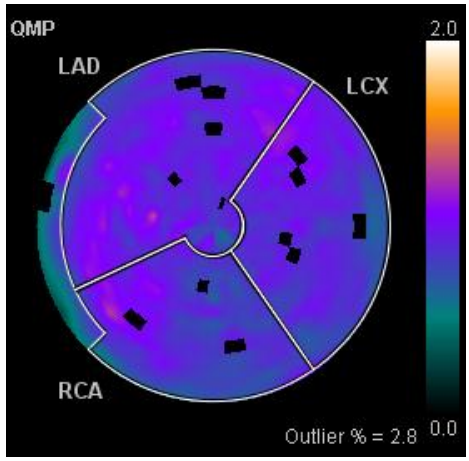

(b) Polar plot of the estimated flow values using motion corrected data

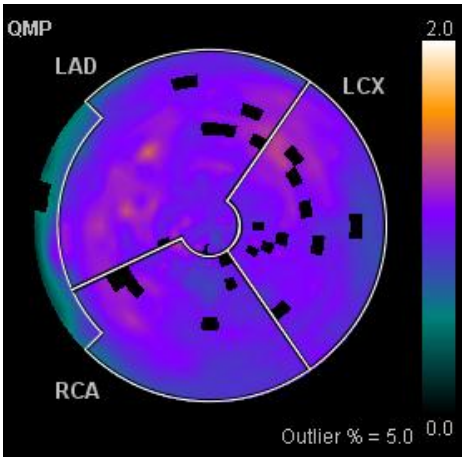

(c) Polar plot of the estimated flow values using the non-gated set-up and a 4mm filtration

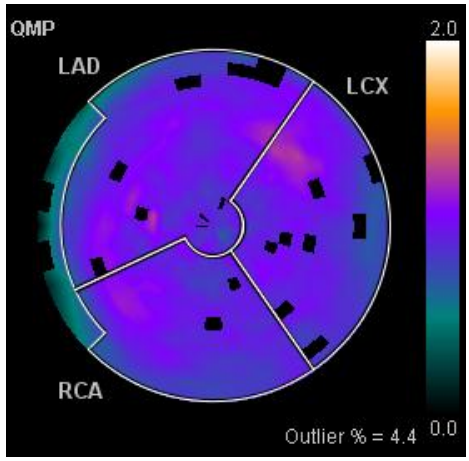

(d) Polar plot of the estimated flow values using motion corrected data

Figure B.7: Flow analysis from Siemens Syngo

The IF's and TAC's for the normal reconstruction are analysed, and compared to the IF's and TAC's for the OSEM-TOF reconstruction on the next pages.

In the flow estimates for the TOF-reconstructions, shown on the next page, it can be seen that all the flow estimates are having a normal perfusion values. Common for all the flow estimates are that no areas with hypo-perfusion is found, except the baso-lateral part of the heart, which is not included in the

analysis. This area is estimated to have low perfusion values, as this part of the heart is mainly connective tissues, which are dividing the left ventricle and the right ventricle. Due to this are these fibres not used for contraction of the heart, hence they do not need to have a high perfusion.

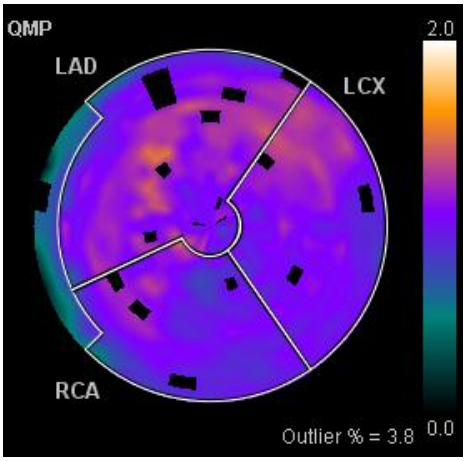

(a) Polar plot of the estimated flow values using the non-gated set-up and a 2mm filtration

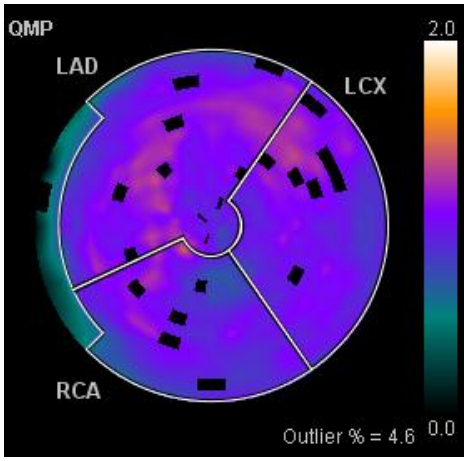

(b) Polar plot of the estimated flow values using motion corrected data

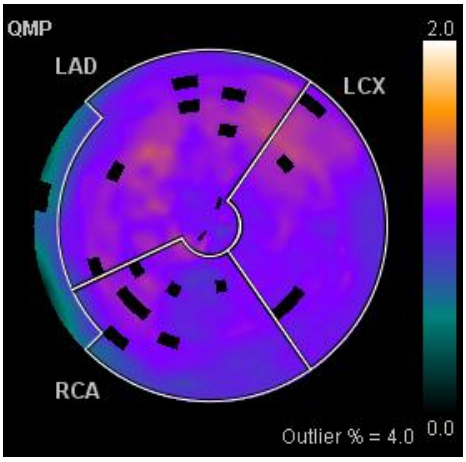

(c) Polar plot of the estimated flow values using the non-gated set-up and a 4mm filtration

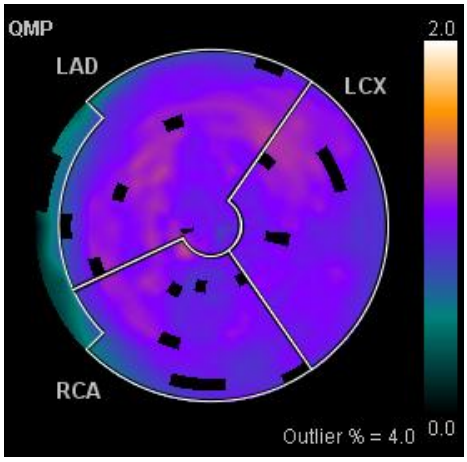

(d) Polar plot of the estimated flow values using motion corrected data

Figure B.8: Flow analysis from Siemens Syngo

The estimated flow values for the OSEM-TOF reconstructed images are shown in the table below. In this table it can be seen that all the flow values are within the range for a normal flow. Furthermore it can be seen that the flow values are estimated to exceed the estimated flow values for the OSEM-reconstruction in general. This change in the flow values are estimated to be introduced by the improved estimate on where the decay occurred in the body. The IF's and the TAC's for both the OSEM and the OSEM-TOF reconstructions using a 2mm filtration are shown in figure B.13, below table B.4.

	Flow values in ml/g/min			
	2mm Gaussian filtration		4mm Gaussian filtration	
Region	Non gated	Breath Gated	Non Gated	Breath Gated
LAD	1.12	1.05	1.11	1.06
LCX	1.09	1.02	1.09	1.05
RCA	1.01	0.96	1.02	1.01
Global	1.09	1.02	1.08	1.04

Table B.4: Flow values for a rest study using either a 2mm or a 4mm filtration on the Siemens mCT scanner, using a TOF reconstruction method

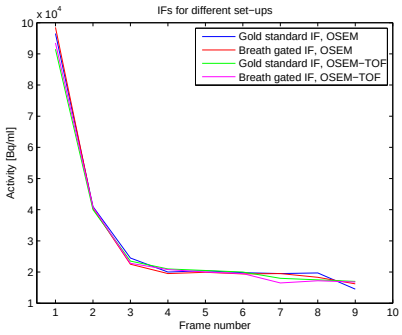

(a) Input functions for patient number 3

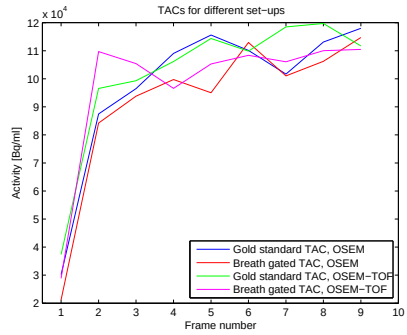

(b) Time-Activity-Curves for patient number 3

Figure B.9: Input function and Time-Activity-Curves for patient number 3

Analyzing the IF's above it can be seen that the activity estimates for all the frames, except the first are the same despite of the reconstruction method. The breath-gated data are here having a higher activity estimate than their respective non-gated data-sets. From this it seen that the flow estimates for the breath-gated set-ups are reduced when compared to the non-gated set-up. This is especially seen for the OSEM-reconstructed data where the TAC for the breath-gated data is having reduced activity levels for the non-gated data for all the frames. This gives that the fractional uptake for the breath gated

is reduced, hence a lower flow estimate. The same is seen for the OSEM-TOF reconstructions from frame 3 and forth. In the first three frames the activity estimates for the breath-gated data are above the activity estimates for the non-gated data. This does not have any effect on the final flow estimates, as seen in table B.3.

The same pattern is seen of the 4mm filtered data. The IF's and TAC's are shown below.

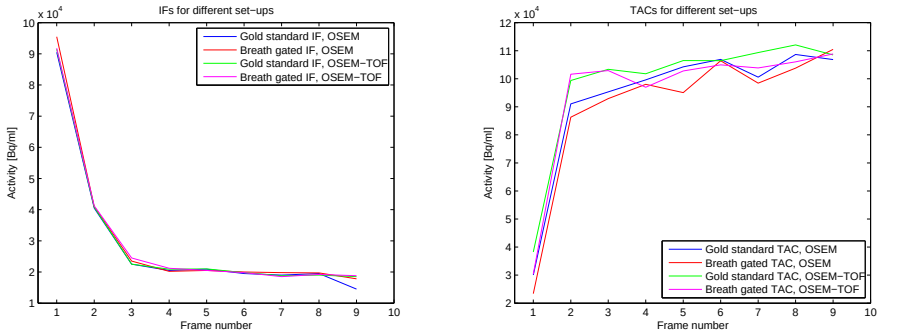

(a) Input functions for patient number 3 (b) Time-Activity-Curves for patient number 3

Figure B.10: Input function and Time-Activity-Curves for patient number 3, using a 4mm filtration

The above analyses indicates that the breath-gated data is having a better flow estimate, than the non-gated data. This is despite the statistical analysis does not find any significant change when using the breath-gating on the healthy subjects.

B.4 Patient 4

This patient was analysed for outlining the possibility of ischemic heart disease. Patients suffering from this disease are known to have a reduced tracer uptake in a part of the heart eg. a reduced flow. This disease may be introduced by various detergents on the heart. The patient had both a rest and a stress scan in the Siemens mCT scanner. In the stress scan is the patient infused with dipyridamole, which elevates the workload in the heart. This is done as the diapyridamole is a vasodilator. The vasodilator relaxes the vessels in the body, which lowers the resistance in the cardiovascular system. More blood capable of staying on the extremities of the body when the peripheral resistance is lowered, hence less blood is returning to the heart. By doing this is the heart required to elevate the ejection rate to stabilize the cardiac output.

By having both a rest and a stress scan one is able to estimate the flow reserve. The flow reserve is used to estimate if the heart is responding properly to the stressing conditions. The flow reserve should be around 2.5 to 3, and is calculated as the fractional increase of the blood flow when inducing the pharmaceutical.

Due to the multiple analysis of this patient, is the analysis of the patient split into multiple subsections. The first section analysed is the conventional OSEM-reconstruction method for the rest scan, using a 2mm and a 4mm Gaussian filter, respectively. This is followed by the analysis of the rest scan, using the OSEM-TOF reconstruction method, using a 2mm and a 4mm filtration, respectively. The same analysis are done for the stress study.

The polar-plots showing the estimated flows for the rest study using the conventional OSEM reconstruction are shown in figure B.11, on the next page.

In the polar plots shown here it can be seen that the breath-gating are increasing the flow values in the heart for the patient. Furthermore are no hypo-perfusion areas detected within the polar-plots, from which it is estimated that the patient does not suffer from ischemic heart disease. The flow values shown in table B.5 is confirming this.

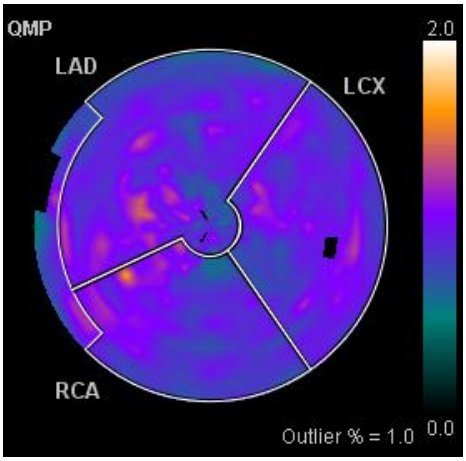

(a) Polar plot of the estimated flow values using the non-gated set-up and a 2mm filtration

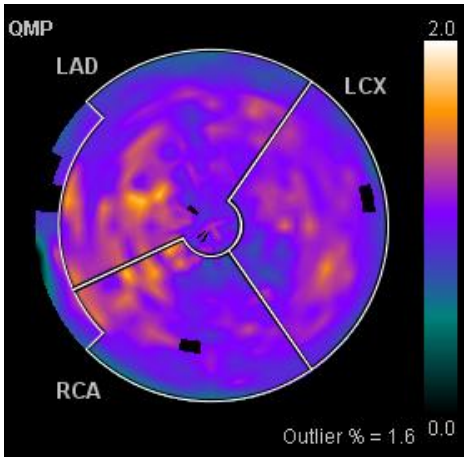

(b) Polar plot of the estimated flow values using motion corrected data

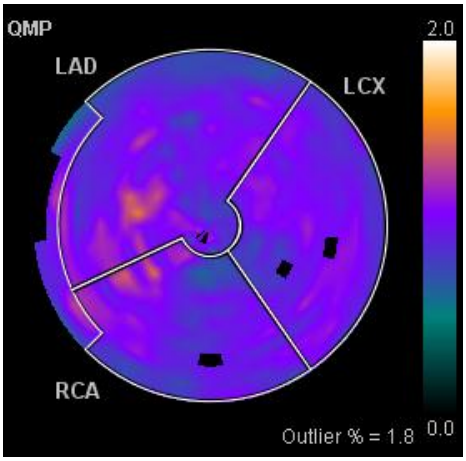

(c) Polar plot of the estimated flow values using the non-gated set-up and a 4mm filtration

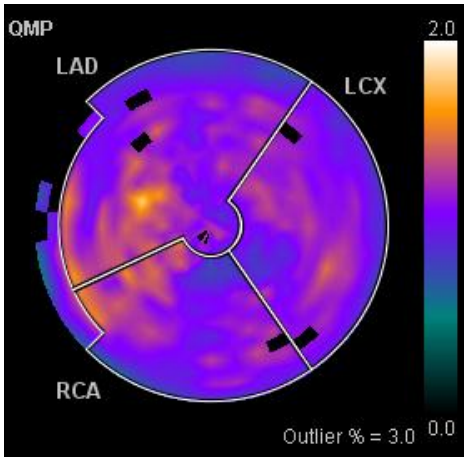

(d) Polar plot of the estimated flow values using motion corrected data

Figure B.11: Flow analysis from Siemens Syngo using the conventional OSEM-reconstruction for the rest scan.

The flow values on the next page are all showing an increase in the flow estimate, when applying the breath gating. The reason for this increase in the flow values are explained by the IF's and TAC's for this set-up. These curves are analysed in figure B.16.

	Flow values in ml/g/min			
	2mm Gaussian filtration		4mm Gaussian filtration	
Region	Non gated	Breath Gated	Non Gated	Breath Gated
LAD	0.94	1.11	1.00	1.15
LCX	0.95	1.09	1.00	1.12
RCA	0.93	1.08	0.99	1.12
Global	0.94	1.10	1.00	1.14

Table B.5: Flow values for a rest study using either a 2mm or a 4mm filtration on the Siemens mCT scanner, using a conventional reconstruction method

The polar plots for the OSEM-TOF rest scan are shown in figure B.12, on the next page. In these plots are no hypo-perfused areas detected, which gives that this patient cannot be diagnosed with ischemic heart disease, while in rest situation. Again it is seen that the breath-gating is increasing the estimated flow values in the 3 segments. This is visualized in the table below.

	Flow values in ml/g/min			
	2mm Gaussian filtration		4mm Gaussian filtration	
Region	Non gated	Breath Gated	Non Gated	Breath Gated
LAD	1.09	1.13	1.10	1.15
LCX	1.07	1.11	1.07	1.14
RCA	1.10	1.15	1.08	1.18
Global	1.08	1.13	1.09	1.16

Table B.6: Flow values for a rest study using either a 2mm or a 4mm filtration on the Siemens mCT scanner, using a TOF reconstruction method

When comparing the flow-estimates for the two reconstruction methods, it is seen that the OSEM-TOF reconstruction method is estimating the flows to be higher, than the conventional OSEM-reconstruction method. This is due to the change in the estimated IF's and TAC's found for the respective reconstruction methods. These are analysed on the next couple of pages.

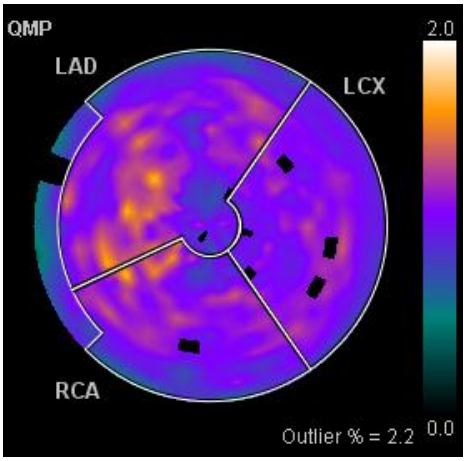

(a) Polar plot of the estimated flow values using the non-gated set-up and a 2mm filtration

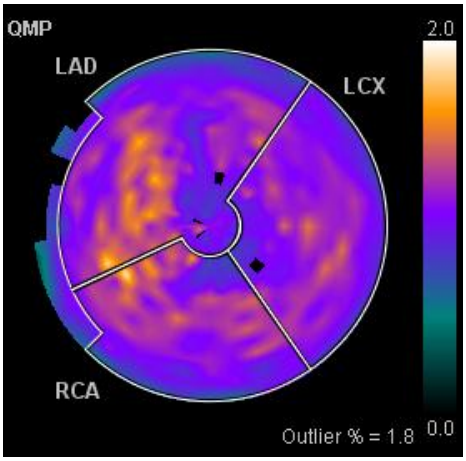

(b) Polar plot of the estimated flow values using motion corrected data

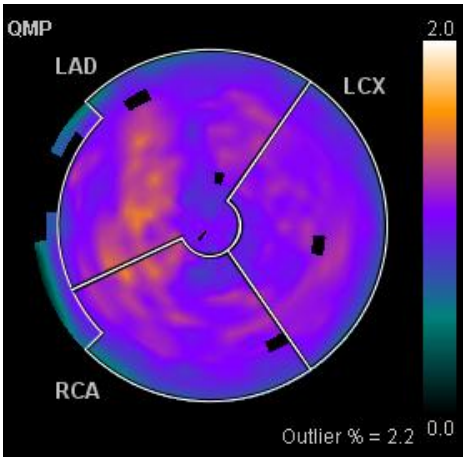

(c) Polar plot of the estimated flow values using the non-gated set-up and a 4mm filtration

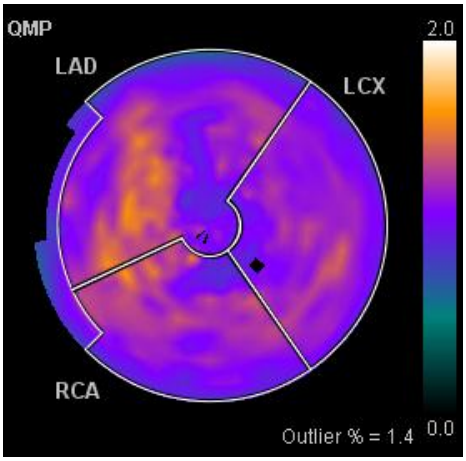

(d) Polar plot of the estimated flow values using motion corrected data

Figure B.12: Flow analysis from Siemens Syngo using the OSEM-TOF reconstruction for the rest scan.

On the next page is shown the IF's and TAC's for the 2mm filtered data, using either the conventional OSEM, or the OSEM-TOF reconstruction method.

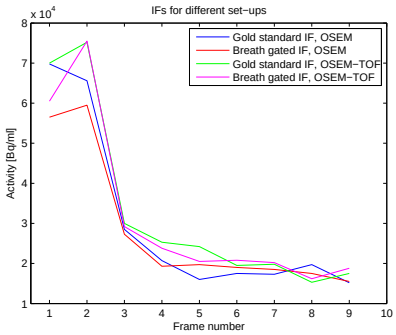

(a) Input functions for patient number 4

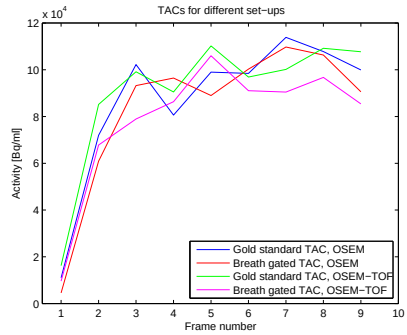

(b) Time-Activity-Curves for patient number 4

Figure B.13: Input function and Time-Activity-Curves for patient number 4, using a 2mm filtration kernel in the rest study.

The IF's are, in general, increasing the activity estimate for the second frame. The non-gated OSEM reconstructed data set is however not having this tendency. This implies that this reconstruction is having an error, when comparing to the other reconstructions. Furthermore it can be seen that the TOF-reconstructions are having higher activities from the 3 frame and forth. This gives that this reconstruction algorithm might compensate for the attenuation within the body. When comparing the IF's to the TAC's (obtained in the apex) for the respective reconstructions, several things are noticed. It is noticed that the breath-gated data for both reconstruction algorithms are estimated to have lower activities than the non-gated set-ups. This gives the respective decrease in the estimated flow values for the breath-gated data, as the heart is taking up less of the tracer available in the blood.

On the next page is the stress scan, using the conventional OSEM-reconstruction method analysed.

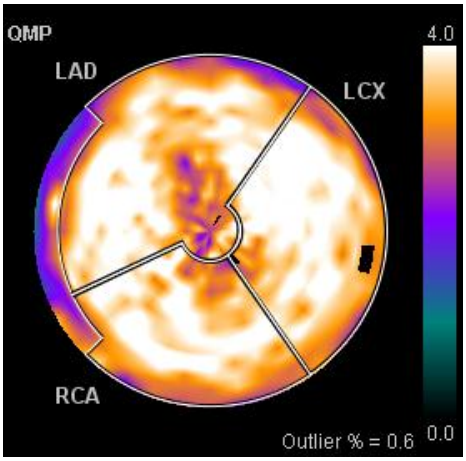

(a) Polar plot of the estimated flow values using the non-gated set-up and a 2mm filtration

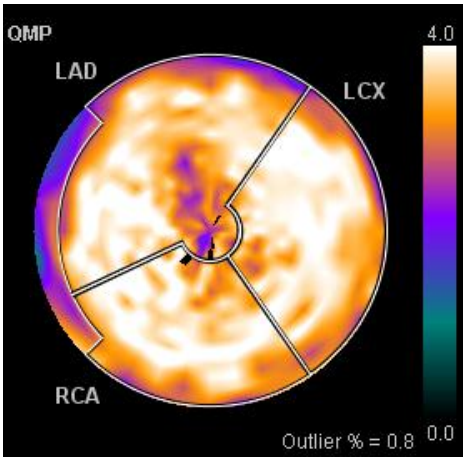

(b) Polar plot of the estimated flow values using motion corrected data

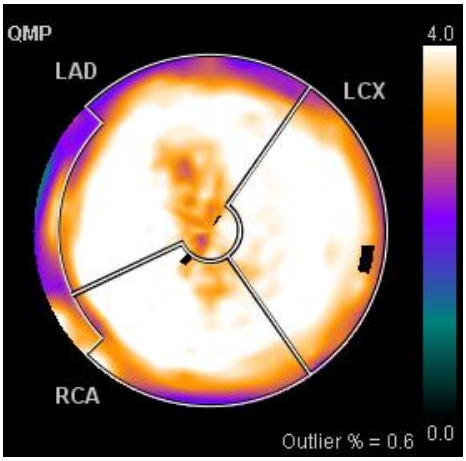

(c) Polar plot of the estimated flow values using the non-gated set-up and a 4mm filtration

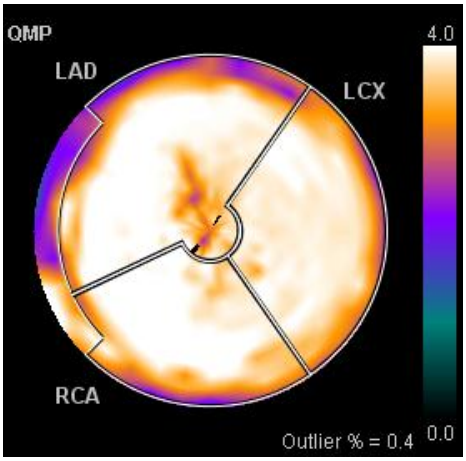

(d) Polar plot of the estimated flow values using motion corrected data

Figure B.14: Flow analysis from Siemens Syngo using the conventional OSEM-reconstruction for the strees scan.

In the above figure it is seen that the flow-values for the stress scan are found to differ greatly between the 2mm - and the 4mm Gaussian filtration. In the 2mm filtered set-up it is seen that the apical, and the apical-lateral part are estimated to have a reduced flow. The same tendency is shown for the 4mm filtration to some extend, as the same areas are shown to have a minor reduction in the estimated flow values. The reduction in the flow estimates were not found to be

of high magnitude for the 4mm filtration, which implies that the 4mm filtration might blur out the information. The change in the polar plot is also shown in the estimated mean flow values for the three segments. These are shown in the table below.

	Flow values in ml/g/min			
	2mm Gaussian filtration		4mm Gaussian filtration	
Region	Non gated	Breath Gated	Non Gated	Breath Gated
LAD	3.44	3.36	3.66	3.66
LCX	3.73	3.66	3.85	3.77
RCA	3.58	3.63	3.80	3.81
Global	3.55	3.51	3.75	3.73

Table B.7: Flow values for a stress study using either a 2mm or a 4mm filtration on the Siemens mCT scanner, using a conventional reconstruction method

In the above table it is seen that the 4mm filtration is estimating the flows to be higher, which can be described by the analysis of the IF's and TAC's for the respective reconstructions. The IF's and TAC's are compared to the IF's and TAC's found for the OSEM-TOF reconstruction algorithm, hence the analysis is performed after the analysis of the OSEM-TOF polar plots. The OSEM-TOF polar plots can be found on the next page. In the 2mm filtered data one is able to detect some hypo-perfused areas in the apical-lateral part of the heart. The hypo-perfused areas are estimated affect a smaller area, and they are not as low as the estimates for the conventional reconstruction method. The same pattern are found for the 4mm filtered data, though are the flow estimates of equivalent measurements as in the 2mm set-up. This gives that the area with reduced flow-estimates might not be as large as first thought, when analysed the conventional reconstruction algorithm. The measured flows for the OSEM-TOF reconstructed images are shown in the table below:

	Flow values in ml/g/min			
	2mm Gaussian filtration		4mm Gaussian filtration	
Region	Non gated	Breath Gated	Non Gated	Breath Gated
LAD	3.36	3.38	3.29	3.31
LCX	3.52	3.55	3.43	3.49
RCA	3.32	3.39	3.18	3.28
Global	3.39	3.43	3.30	3.35

Table B.8: Flow values for a stress study using either a 2mm or a 4mm filtration on the Siemens mCT scanner, using a TOF reconstruction method

In table B.8 it can be seen that the perfusion is estimated to increase, when applying the breath gating. This is the opposite of was seen for the conventional OSEM-reconstruction. An analysis of the IF's and TAC's is needed to estimate which of the two reconstruction methods that gives the most correct flow estimate. This will be conducted on the next page.

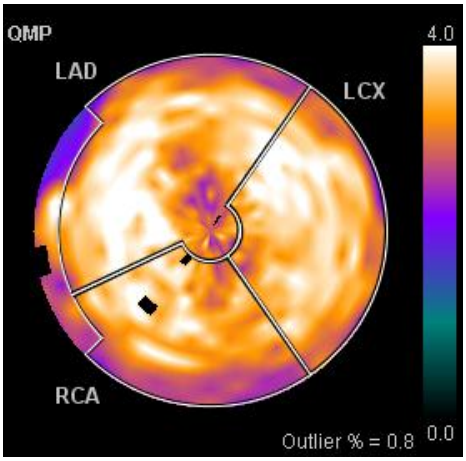

(a) Polar plot of the estimated flow values using the non-gated set-up and a 2mm filtration

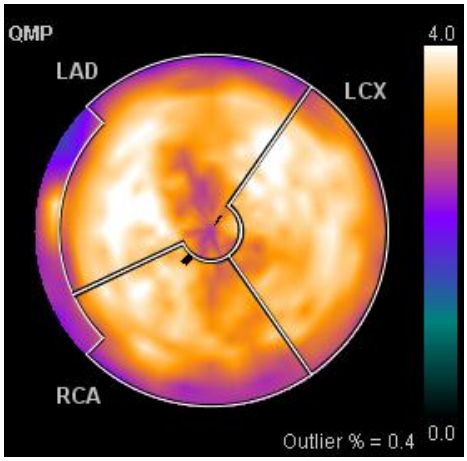

(b) Polar plot of the estimated flow values using motion corrected data

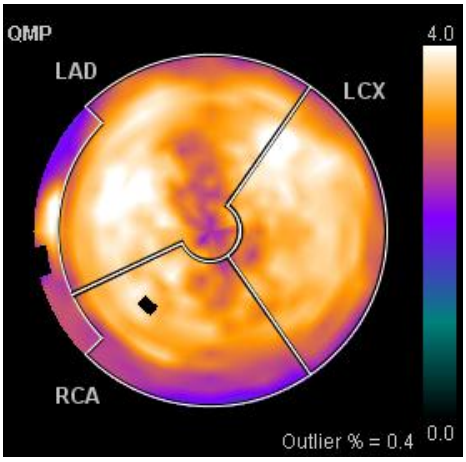

(c) Polar plot of the estimated flow values using the non-gated set-up and a 4mm filtration

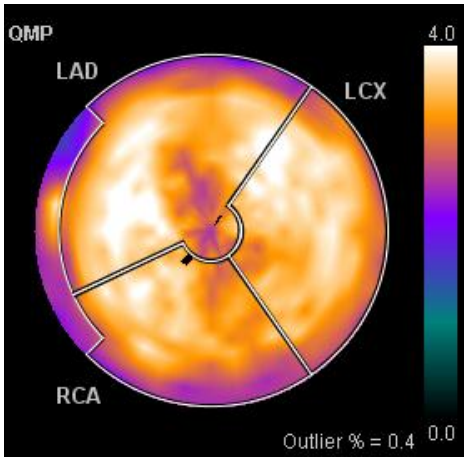

(d) Polar plot of the estimated flow values using motion corrected data

Figure B.15: Flow analysis from Siemens Syngo using the OSEM-TOF reconstruction for the stress scan.

The IF's and the TAC's for the stress scan are analysed in the figure below.

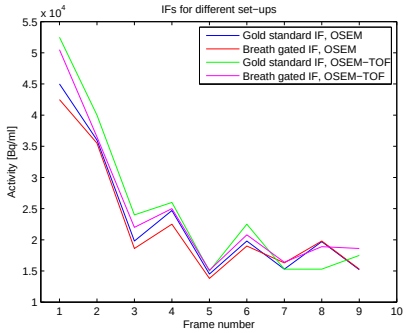

(a) Input functions for patient number 4

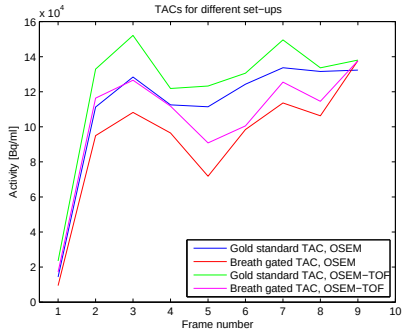

(b) Time-Activity-Curves for patient number 4

Figure B.16: Input function and Time-Activity-Curves for patient number 4, using a 2mm filtration kernel in the stress study.

When analyzing the IF's one is able to notice one important feature of the TOF-reconstructions. The feature is the activity measured in the first frame of the dynamic series. For both the gated and the non-gated set-ups it is noticed that the OSEM-TOF images are having an measured activity that is 7000 Bq/ml higher than the respective images from the OSEM reconstruction. The remaining frames are estimated to have the same activities from frame 3 and forth, giving the kinetic differences are obtained within the first frames.

The TAC's are having the same patterns as the IF's. Again are the gold standard from the OSEM-TOF reconstruction having the highest estimates, and the remaining TAC's are having the same order as in the IF's. The relative increase in the TAC's for the OSEM reconstructions are higher than for the OSEM-TOF reconstructions. From this are the OSEM reconstructed images having a greater flow estimate than the OSEM-TOF images.

It is possible to extract a lot of information from this patient. The first thing being the reconstruction algorithm has a huge influence on the estimated flow values, especially for the stress studies. In one study the patient is estimated to have a major reduction in the flow, while the other images are estimating the reduction in the flow to be of minor importance. Furthermore it is seen that the flow values found for the 4mm filtrations might be erroneous, especially for the conventional OSEM-reconstructed images. From this, and the statistical analysis it is estimated that the OSEM-TOF images gives the best flow estimates.

B.5 Patient 5

The patient analyzed here were examined for analyzing the probability of the patient having ischemic heart disease. The patient had both a rest and a stress study, as patient number 4. This patient felt asleep during the rest-scan which altered the respiratory cycle, which made it impossible to reconstruct the rest scan using the breath-gating. Due to this is the analysis done on the stress study as a single basis.

The study was performed at the Siemens mCT PET-CT scanner, which has the opportunity of reconstructing the images using the TOF information. The analysis were done using both reconstruction methods, in order to compare the flow values. The polar plots for the OSEM-reconstructed images are shown in figure B.17 on the next page. Several differences are seen, when analyzing the polar plots. The most distinct difference that can be noticed is the great difference in the estimates of the flows. The data reconstructed using a 2mm filtration is having a flow-estimate exceeding the flow-estimate expected for the 4mm filtration. The flow values for the two reconstructions is shown in the table below.

	Flow values in ml/g/min			
	2mm Gaussian filtration		4mm Gaussian filtration	
Region	Non gated	Breath Gated	Non Gated	Breath Gated
LAD	2.40	2.29	1.97	1.92
LCX	3.29	3.10	2.19	2.12
RCA	3.16	3.08	2.30	2.25
Global	2.82	2.70	2.11	2.06

Table B.9: Flow values for a stress study using either a 2mm or a 4mm filtration on the Siemens mCT scanner, using a conventional reconstruction method

In the above table it is seen that the flow estimates varies greatly, as seen in the polar plots. It can furthermore be noticed that all the flow values are high, which are introduced by the stressing condition. This gives that the 2mm filtrations are expected to have the most accurate flow estimate, as these plots show high flow values. Before this is concluded, are the IF's and the TAC's for all the set-ups analysed. This analysis can determine which flow value that is most plausible to be correct. As the IF's and TAC's are compared to the OSEM-TOF reconstructions are the analysis not done until the analysis of the polar plots for the OSEM-TOF reconstructions has been done. The analysis for this can be found on the next pages.

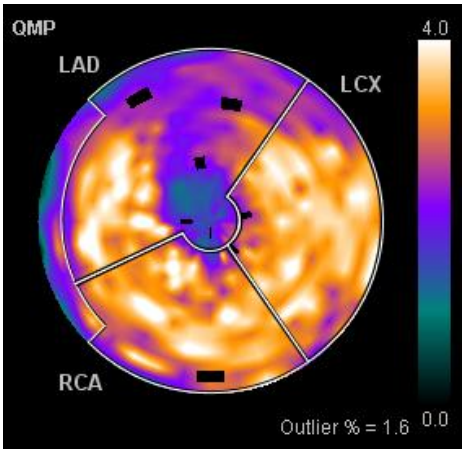

(a) Polar plot of the estimated flow values using the non-gated set-up for a 2mm Gaussian filtration

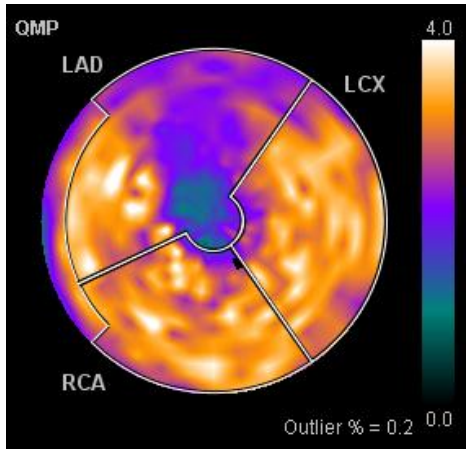

(b) Polar plot of the estimated flow values using motion corrected data

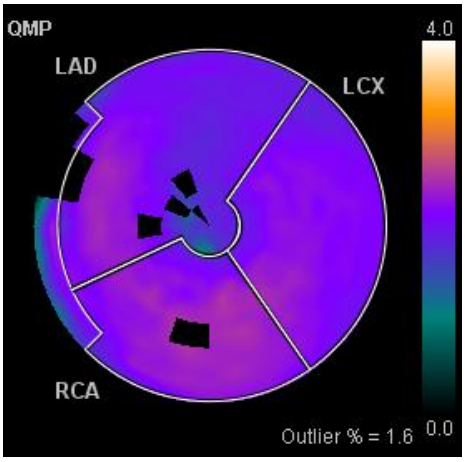

(c) Polar plot of the estimated flow values using the non-gated set-up with a 4mm Gaussian filtration

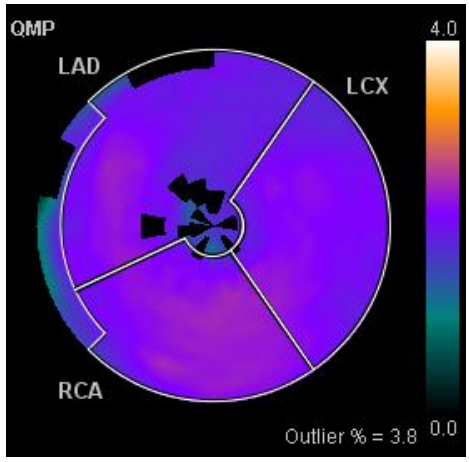

(d) Polar plot of the estimated flow values using motion corrected data

Figure B.17: Flow analysis from Siemens Syngo using the conventional OSEM reconstruction

When analyzing the polar plots generated from the OSEM-TOF reconstruction, it is seen that the plots are having the same properties as the OSEM-reconstructions. This leads to a hypothesis that the 4mm filtration might be erroneous. This hypothesis is to be tested, when analyzing the IF's and TAC's for the reconstructions. The mean flow values found in each segment is shown

in the table on the next page.

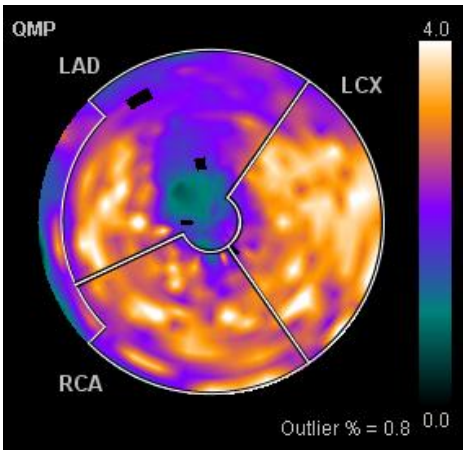

(a) Polar plot of the estimated flow values using the non-gated set-up for a 2mm Gaussian filtration and the TOF-reconstruction method

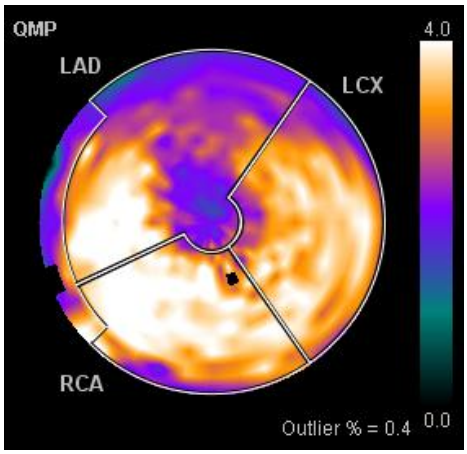

(b) Polar plot of the estimated flow values using tra-motion corrected data

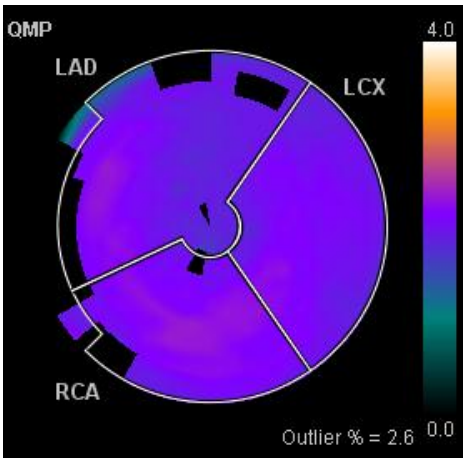

(c) Polar plot of the estimated flow values using the non-gated set-up with a 4mm Gaussian filtration

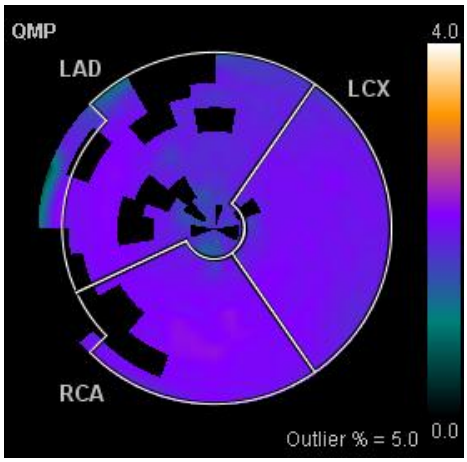

(d) Polar plot of the estimated flow values using motion corrected data

Figure B.18: Flow analysis from Siemens Syngo

Analyzing the flow values, it can be seen that the breath gating is estimated to have a huge impact on the estimated flow values for the 2mm filtration. The flow values are estimated to increase greatly when applying the breath gating. This increase will be analysed in the analysis of the IF's and TAC's on the next pages.

	Flow values in ml/g/min			
	2mm Gaussian filtration		4mm Gaussian filtration	
Region	Non gated	Breath Gated	Non Gated	Breath Gated
LAD	2.08	2.63	1.97	1.83
LCX	3.11	3.26	2.07	2.01
RCA	2.82	3.60	2.16	2.09
Global	2.54	3.03	2.04	1.95

Table B.10: Flow values for a stress study using either a 2mm or a 4mm filtration on the Siemens mCT scanner, using a TOF reconstruction method

The following IF's and TAC's were found for the 2mm filtered data:

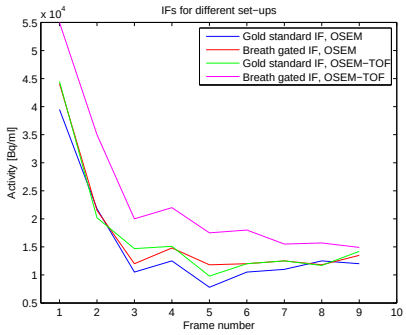

(a) Input functions for patient number 5

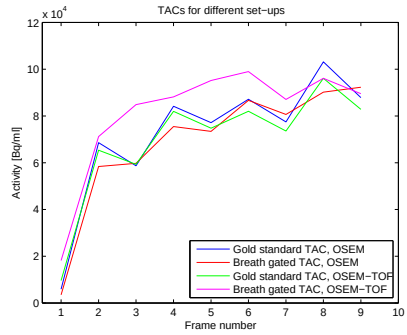

(b) Time-Activity-Curves for patient number 5

Figure B.19: Input function and Time-Activity-Curves for patient number 5, using a 2mm filtration kernel.

In figure B.19a it can be seen that the input functions are having a great deviance in the measured activity levels for the different reconstructions. Analyzing the first frame, it can be seen that the non-gated study for the OSEM reconstruction is giving the lowest activity estimate of all. When the breath gating are applied to the OSEM reconstructed images are the activity estimates seen to be equal to the OSEM-TOF - non-gated images. This implies that the non-gated set-up

for the OSEM-reconstruction is under-estimating the activity. Furthermore it can be seen that the breath-gated set-up using the OSEM-TOF reconstruction gives the highest activity estimate for all the reconstruction algorithms for this patient. This was expected, as the OSEM-TOF is known to give an improved estimate of the actual activity levels in the images, due to its improved accuracy. When analyzing the TAC's for the patients, several things are noticed. The OSEM-TOF images are having the highest estimates, as for the IF's. The remaining TAC's are having a lower offset where they all are developing as expected for the TAC's. Though are the OSEM-TOF breath gated data estimated to be most correct, as the plateau is more homogeneous than the other set-ups. This implies that this activity level found in the body does not vary much, which gives a stable flow analysis.

For the 4mm filtrations were the following IF's and TAC's found.

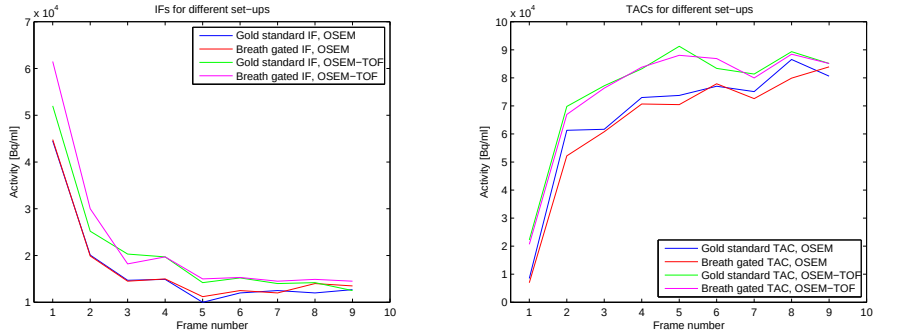

(a) Input functions for patient number 5 (b) Time-Activity-Curves for patient number 5

Figure B.20: Input function and Time-Activity-Curves for patient number 5, using a 4mm filtration kernel.

When analyzing the IF's in figure B.20a, it is seen that the images from the OSEM-reconstruction are having lower estimates than the OSEM-TOF reconstructed data. It is seen that the breath-gating do not seem to improve the OSEM-reconstructed data, as the IF's are similar throughout the entire scan. The OSEM-TOF algorithms differ rather much in the initial frames, which indicates that the breath-gating is having a huge impact in the initial frames. It can be seen that the breath gated data is estimated to have an approximate of 10000 Bq/ml higher activity in the first frame. This will have a huge impact on the measured perfusion values found for this reconstruction, especially when it is compared to the TAC's found for the OSEM-TOF reconstruction. Here it can be seen that the breath-gated and the non-gated data are having the same

TAC-activities. This explains the higher estimate of the flow for the non-gated set-up, than the gated set-up. This is introduced by the relative higher uptake of the tracer available in the blood for the non-gated set-up. When analyzing the OSEM-reconstructed data, it is noticed that the non-gated set-up is having a general higher activity estimate, which leads to a higher flow estimate for the non-gated set-up.

From the estimated IF's and TAC's it can be estimated that the breath-gated data will have a better estimate of the actual flow values, which are based on the findings in the analysis of the 2mm filtered data. Furthermore it can be concluded that the OSEM-TOF reconstructions are estimated to give a more accurate estimate as the TAC's for these reconstructions contains less noise in the plateau, than the OSEM reconstructions. As for the other patients, it is not possible to estimate whether the 2mm or the 4mm filtration gives the best estimate of the actual flow.

B.6 Patient 6

The analysis for this patient can be found in the results section.

Appendix C

Analysis of the measured blood flows using restriction on the measured breath cycles

C.1 Patient 6

This patient were analysed in sec 5.7 in the report. Here it was found that the flow is varying greatly, depending on the reconstruction algorithm and the filtration of the data. The patient is of great interest to analyse, when applying the restricted breath-cycles as this patient has some extreme breathing patterns throughout the examination. The measured respiratory rates, shown on the next page, witnesses on a possible advantage on using the restricted breathing pattern. However one is having the disadvantage of loosing information for multiple breathing cycles, when doing the restriction on the breath-cycle.

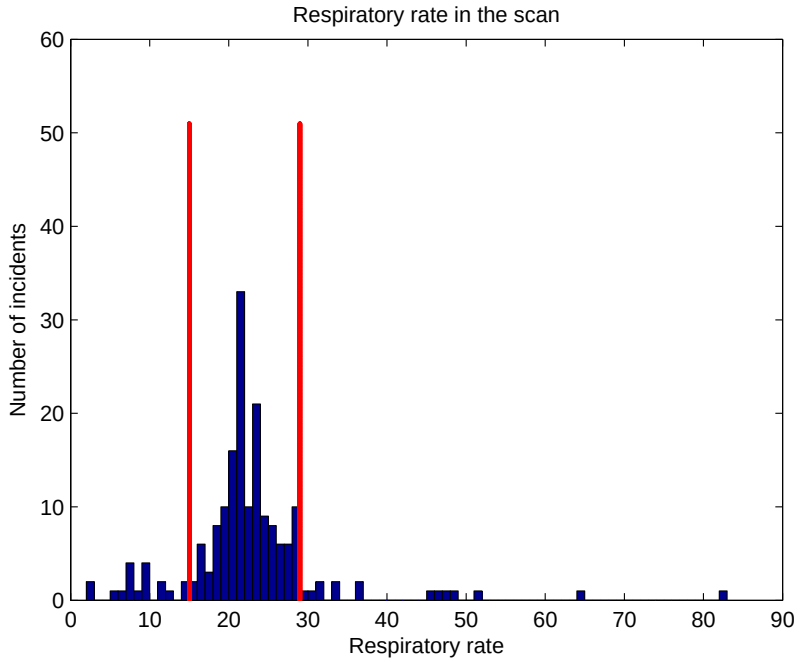

Figure C.1: Respiratory rate for patient number 6

On the above plot it is noticed that the patient is having multiple irregular breath-cycles which are found to be non-consistent. The patient are having multiple breath-cycles lasting more than 6 seconds, and some breath-cycles lasting 30 seconds. These breath-cycles are breath-cycles which are not registered by the belt. One is risking that some of the bins contains data from more than a quarter of a breath cycle when using the all the measured breath-cycles. This will introduce a blurring in the given frame(s), which will reduce effect of the breath-gating. This error is, however, known not to corrupt the data to be worse than the non-gated set-up. The frames affected by the restricted breathing pattern is analysed on the next pages.

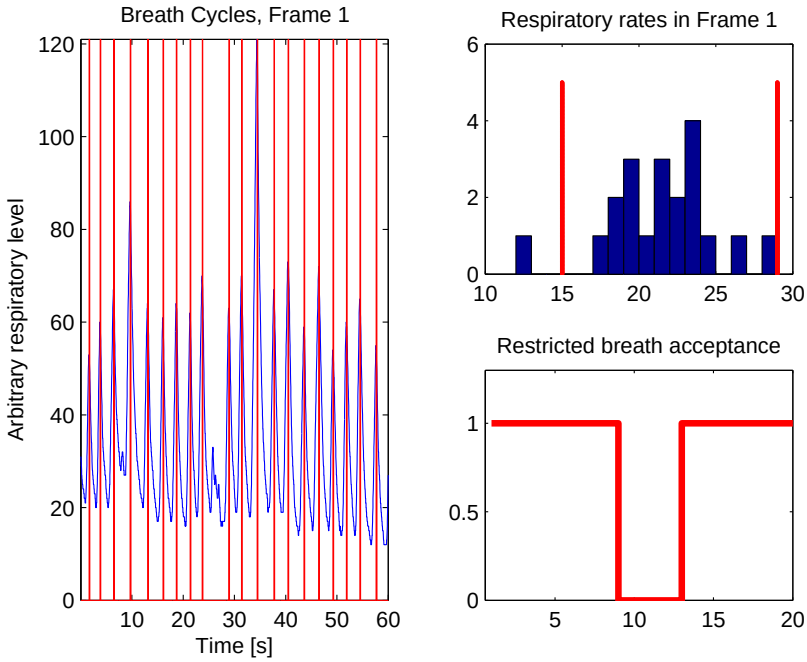

Figure C.2: Respiratory rate for the first frame

For this frame it is seen that the patient is having a quick breath with a too low amplitude to be measured by the wave-generator. If this respiration had been measured, it would have been ruining the overall estimate of the breath-gating as this superficial breathing do not move the heart. It can be seen seen that the missing breath cycle is occurring at an early point, which gives that the majority of the bolus is measured. From this it is possible to conclude that this error will not have a major impact on the estimated activities. Frame number two will be analysed on the next page.

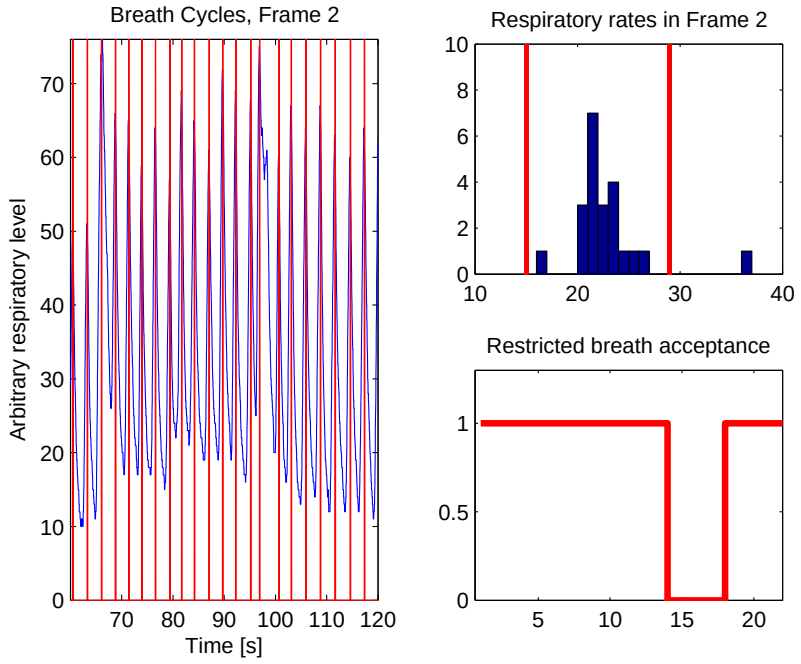

Figure C.3: Respiratory rate for the second frame

In the leftmost plot above, it can be seen that this frame contains a non-acceptable respiration. The non-accepted breath cycle is measured as a hyperventilating breathing sequence, which gives a too low temporal separation between two consecutive breath cycles. By removing this breath cycle, it is thought to give a more robust motion of the heart.

The third frame had multiple breath cycles, which had a rate outside the accepted window. This can be seen in the upper right plot in figure C.4. It can be seen that four breath-cycles are falling outside the accepted set-up, where one breath-cycle is happening too fast, and three has too long time in between. The third breath-cycle is seen to be rejected, which is due to a too short temporal distance between the breathing patterns. From this it is seen that the frame is missing data for some of the breathing patterns happening within a short time. This is thought to improve the measured activity in the heart, as this ensures a somewhat homogeneous motion of the heart. The next measurement of a non-accepted breathing pattern is happening within the 3 consecutive breath-cycles for the first rejected non-accepted respiration, thus it is not affecting the following respirations. The second breath-cycle that has too long temporal difference is occurring at 13 breath cycles, where the wave generator seems to have

missed the respiration. From this it is estimated that the restriction on the breath-cycles would have had a great benefit, if it was possible to reconstruct the images only discarding the breathing-cycle having the error.

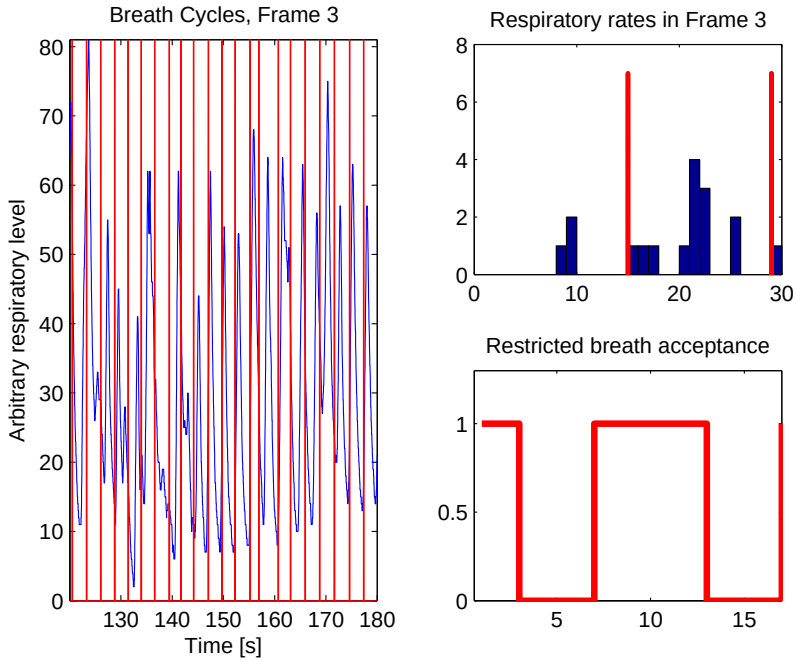

Figure C.4: Respiratory rate for the third frame

In the above figure, in the left-most plot, it can be seen that almost all the gating cycles are off the respiratory peaks by up to one second. This may have some impact on the estimated position of the heart, as the this pattern is unique for this frame. This might give a slight motion-blur in the estimated activity for frame number three. This effect is most dominant for the OSEM-reconstructed images, which can be seen in the TAC curve in figure C.10. Frame number 4 and 5 did not have any breath-cycles outside the accepted area, hence these are not analysed.
Frame number six are analysed on the next page.

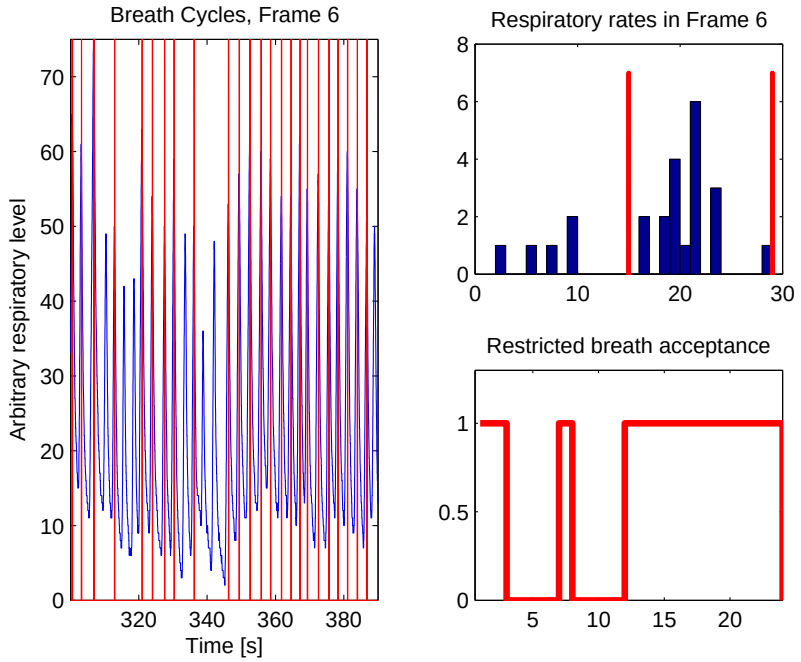

Figure C.5: Respiratory rate for the sixth frame

This frame is dominated by multiple breath-cycles which has not been measured by the wave-generator. This is seen in the third, fourth, fifth, seventh and ninth breathing cycles. Here the trigger-level are not accomplished, which gives that the data for these breathing cycles are left out from the reconstruction. The trigger level is found to be 50 on the arbitrary scale, to which the wave-generator has been calibrated. These non-accepted breath-cycles are left out due to the lack of diaphragmatic motion of the heart. The removal of the data from these breath-cycles are therefore thought to improve the breath-gated images in a hypothetical set-up, where only the non-accepted data were discarded.

On the next page is the seventh frame analysed, as this frame has some respiratory rates, which are laying outside the accepted region.

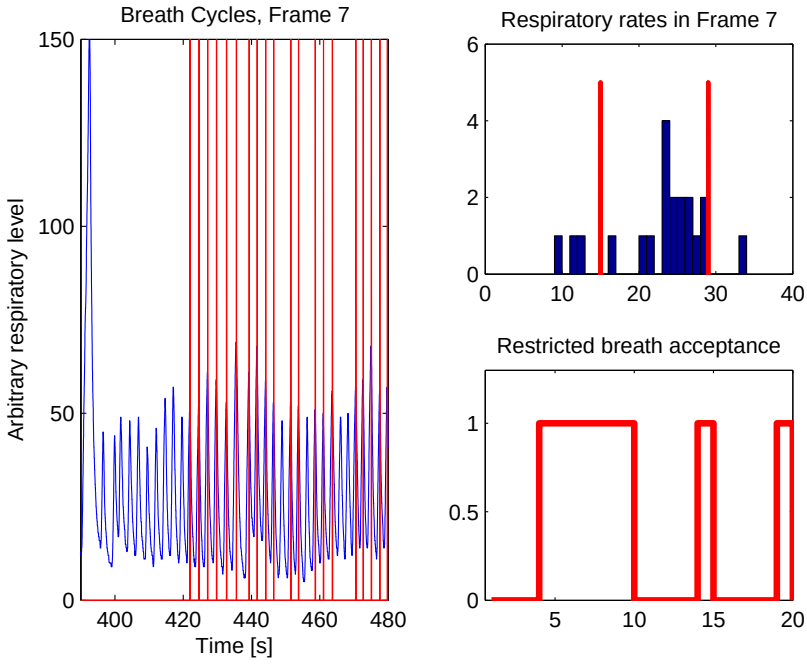

Figure C.6: Respiratory rate for the seventh frame

This frame contains several breathing cycles which are of great interest. In this frame the breath-cycles from the first twenty-three seconds are not measured by the wave-generator. The first measured breath cycle, which are shown and included in the rightmost plots are happening at 422 seconds. The first part of the frame has data left out, due to a deep respiration by the patient. This is seen as the peak of 150 arbitrary values, which is approximately a factor of 2 higher than the remaining accepted breath cycles in this frame. A such high amplitude is stressing the wave-generator, which leaves out the following breath-cycles. This is done until the breathing-pattern is stabilized again, as seen in the left-most figure. This is done to ensure that the breath-motion is somewhat homogeneous. A deep respiration has a huge translatory effect on the heart, which would have given some motion blur in the reconstruction image if this breath-cycle was included in the reconstruction.

The first three breathing cycles measured after the deep inspiration are discarded due to the listmode reconstruction algorithm. It can furthermore be seen that the the tenth and the sixteenth breath cycles are not reaching trigger level, which leaves out the consecutive breath cycles for the respective discarded cycles. From this it can be concluded that the activity measured in the seventh frame might

be highly affected by a poor SNR, hence it might be seen in the IF's and TAC's for this patient.

Below is shown the measured breath-patterns for the eight frame.

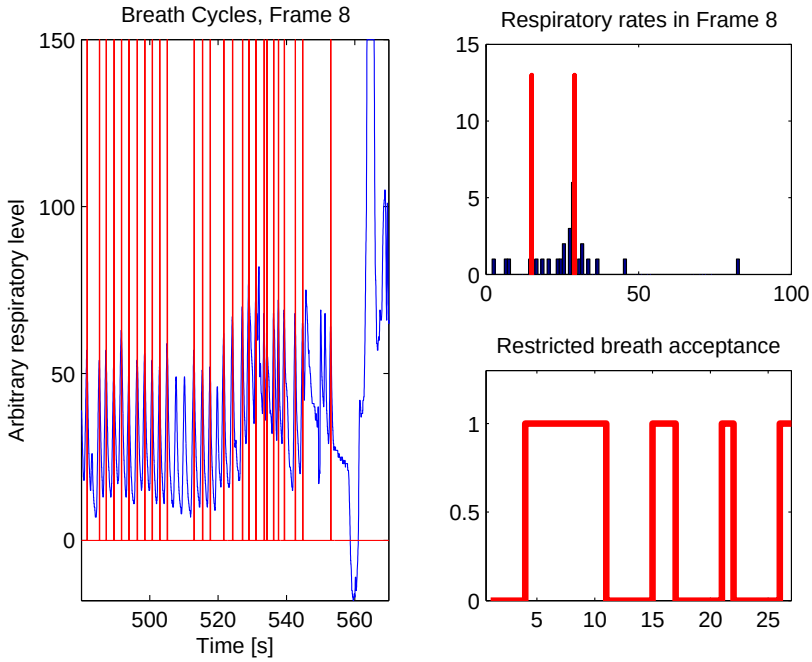

Figure C.7: Respiratory rate for the eighth frame

It can be seen that the first breath cycles measured in this frame are discarded due to a too low temporal distance between the last two breath cycles in the previous frame. This discards the information on the respiratory rate between the first two breath cycles measured in this frame. Again it is seen that two consecutive breath cycles does not reach the trigger level, hence they are discarded along the three following respiratory cycles. At the end of the frame it can be seen that the breathing pattern changes dramatically, which may be introduced by a cough. From this it can be seen that the wave-generator accepts the last measured breath-cycle at 552 seconds. This possible cough is manifesting throughout the ninth frame, shown on the next page.

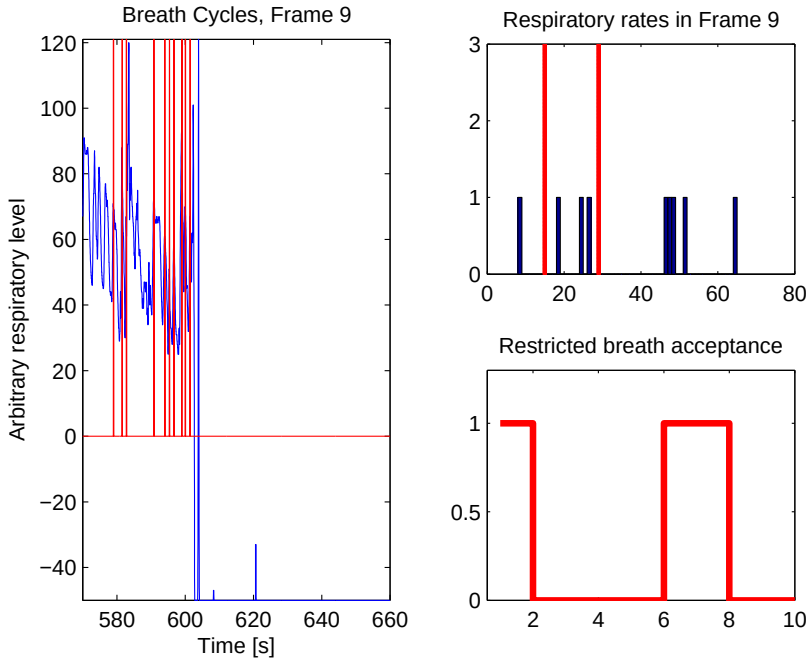

Figure C.8: Respiratory rate for the ninth frame

For this frame it can be seen that the first two breath cycles are accepted, which is thought to be an error in the data-sampling as these data would have been discarded in the correct set-up. In the beginning of this frame it can be seen that the coughing is still affecting the breath-pattern. This leaves out many of the registered breath-cycles for this frame. Furthermore are the trigger missing for the last 50 seconds. The origin for this lack of registrations are not known. A plausible answer is that the belt has shifted position during the last part of the cough. This can have mispositioned the sensory head, so that it has no contact to the skin. The poor statistics for this frame might introduce some high SNR-errors in the reconstructed images. The poor SNR is, to some extend, revealed in the analysis of the input function and the TAC. On the next page is the polar plots for the reconstruction using the restricted set-up compared against the breath-gated set-up for the analysis done using all the measured breath-cycles.

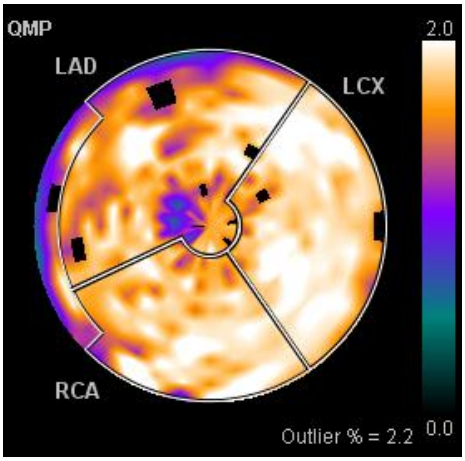

(a) Polar plot using the breath-gated data from the 2mm OSEM-reconstructed data.

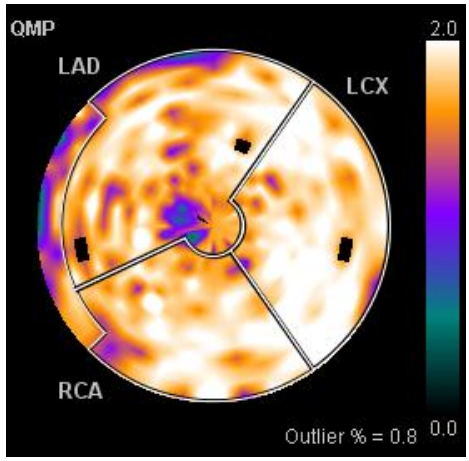

(b) Polar plot using the breath gated data from the 2mm OSEM-reconstructed data using a restricted respiratory rate.

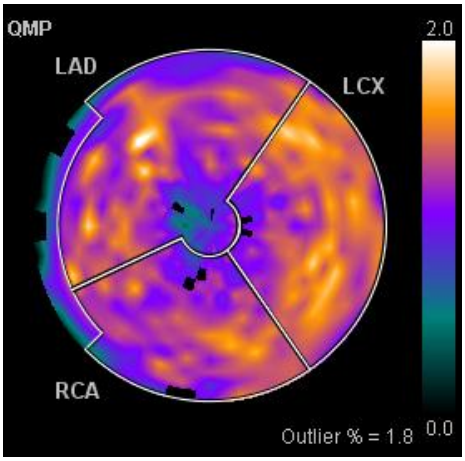

(c) Polar plot using the breath-gated data from the 2mm OSEM-TOF reconstructed data.

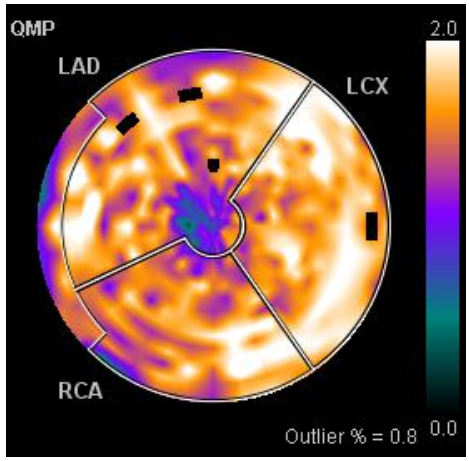

(d) Polar plot using the breath-gated data from the 2mm OSEM-TOF reconstructed data using a restricted respiratory rate.

Figure C.9: Flow analysis from Siemens Syngo comparing the breath gated data and the restricted breath-gated data

The restricted set-up is seen to have a minor impact on the estimated flow values. It is, however, seen that the OSEM-TOF reconstruction algorithms are estimating the restricted breath reconstructions to have a greater flow estimate.

The mean flows for the respective reconstructions are shown in the table below.

	Flow values in ml/g/min			
	Normal Reconstruction		TOF Reconstruction	
Region	All accepted	Restricted	All accepted	Restricted
LAD	1.60	1.64	1.14	1.43
LCX	1.87	1.88	1.37	1.71
RCA	1.79	1.79	1.23	1.54
Global	1.72	1.74	1.22	1.53

Table C.1: The estimated flow values for the restricted set-up compared to the non-restricted set-up.

In the flow values shown above, it can be seen that the breath gating are having a great effect on the OSEM-TOF reconstructed data. The effect for the OSEM-reconstructed data is, however, seen to be non-significant. The origin of the great difference in the estimated flow values are analysed in the IF's and TAC's below.

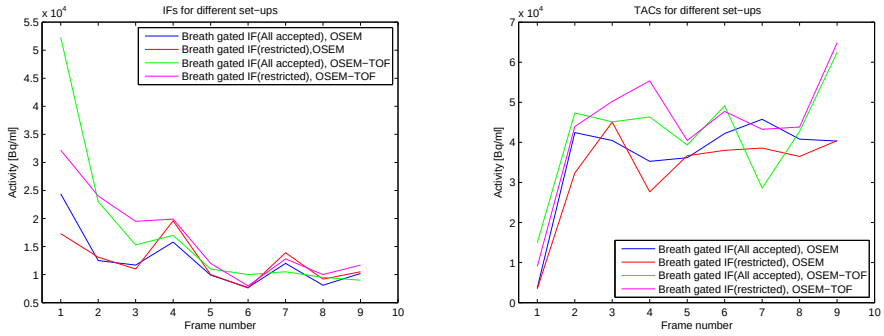

(a) Input function for the restricted set-up compared to the non-restricted set-up.

(b) Time-Activity-Curves for the restricted set-up, compared to the non-restricted set-up

Figure C.10: Input functions and Time-Activity-Curves for the restricted set-up, compared to the non-restricted set-up

In the above figure, it can be seen that the non-restricted data are having a higher activity estimate for the initial frames than the restricted data. This is due to the loss of data in the first frame, due to a non-accepted respiration. Furthermore one is able to see that the IF estimates for the fourth frame are estimated to be higher for the restricted set-up. The origin of this change is not known, as no changes has occurred in this frame. For the remaining frames are no changes that could alter the flows observed.

When analyzing the TAC's several things are noticed. The OSEM-TOF reconstruction using the restricted breath-cycles is seen to have more fluctuations in the plateau, happening from frame three and forth. Especially frame 4 is seen to deviate, this effect cannot be described as an effect of the strict gating set-up as no changes occurred in this frame.

The second change which are noticeable is that the last frame for the OSEM-TOF reconstructions are overestimating the activity in the last frame. This might be introduced by the great deviations in the breathing pattern in this frame. Besides this the activity estimates is interchanging throughout the study for the OSEM-TOF reconstructions, which gives that it is not possible to distinct the measured flows from this analysis. For the OSEM-reconstructed images using the restricted set-up is a tendency to have activity estimates below the non-restricted data observed. This is contrary to the IF's where the opposite is seen. By this one is able to extract that these flows are estimated to be higher, due to the higher uptake of the tracer available in the heart.

From these results it is concluded that the restriction on the breath-gating in general increases the flow estimates for this patient. This is happening on behalf on the loss of data in crucial frames, which might introduce a lower SNR in the reconstructed images. Due to this it is recommended that one uses all the breath cycles for the patients, even though this is known to introduce errors in the estimated flows due to erroneous breath-cycles.

Appendix D

Code

D.1 MINC code to generate the breath-corrected images

In this section the code for the co-registration is shown. Below is shown the code used for generating the breath corrected data.

```
% accessing the given frame number
cd FrameX/

% making of a new directory for the co- registrations mkdir MINC
cd MINC/
mkdir fr1
mkdir fr2
mkdir fr3
mkdir fr4
cd ..


% Converting the DICOM images into minc files, which are placed in the above
created directories.
cd Bin1/
```

```
dcm2mnc -usecoordinates *.IMA ../MINC/fr1
cd ..
cd Bin2/
dcm2mnc -usecoordinates *.IMA ../MINC/fr2
cd ..
cd Bin3/
dcm2mnc -usecoordinates *.IMA ../MINC/fr3
cd ..
cd Bin4/
dcm2mnc -usecoordinates *.IMA ../MINC/fr4
cd ..


% square root transforming the data, so the best registration is obtained.
cd MINC/fr1/Patient/
mincmath -sqrt Patient.mnc fr1sqrt.mnc
cp fr1sqrt.mnc ../../../MINC
cd ../..
cd fr2/Patient/
mincmath -sqrt Patient.mnc fr2sqrt.mnc
cp fr2sqrt.mnc ../../../MINC
cd ../..
cd fr3/Patient/
mincmath -sqrt Patient.mnc fr3sqrt.mnc
cp fr3sqrt.mnc ../../../MINC
cd ../..
cd fr4/Patient/
mincmath -sqrt Patient.mnc fr4sqrt.mnc
cp fr4sqrt.mnc ../../../MINC
cd ../../../..


% Copying the deformation fields found for the respective bins into the respec-
tive bins
cp BIN1av.xfm FrameX/MINC/
cp BIN2av.xfm FrameX/MINC/
cp BIN3av.xfm FrameX/MINC/
cp BIN4av.xfm FrameX/MINC/
cp averageFINALTOTAL.mnc FrameX/MINC/


cd FrameX/MINC/
```

```
% Transforming the original data into the reference image coordinate system
mincresample fr1sqrt.mnc -like fr1sqrt.mnc -transform
BIN1av.xfm Bin1avFull.mnc
mincresample fr2sqrt.mnc -like fr2sqrt.mnc -transform
BIN2av.xfm Bin2avFull.mnc
mincresample fr3sqrt.mnc -like fr3sqrt.mnc -transform
BIN3av.xfm Bin3avFull.mnc
mincresample fr4sqrt.mnc -like fr4sqrt.mnc -transform
BIN4av.xfm Bin4avFull.mnc


% Finding the average activity, which is estimated to be the correct activ-
ity estimate for this frame.  mincmath -add Bin1avFull.mnc Bin2avFull.mnc
Bin3avFull.mnc Bin4avFull.mnc Bin14av.mnc mincmath -div -const 4 Bin14av.mnc
averageFINAL.mnc


% Converting the data into raw format, which are used in MatLab
minctoraw -double -normalize averageFINAL.mnc > Frame9.raw


cd ../..
```

D.2 MatLab code to generate the DICOM files

DICOM

```
clear all;
close all; clc

%Reading and predefining the data.
IMAfiles=dir('*.IMA');
rawfiles=dir('*.raw');
data1=zeros(400,400,111);
data2=zeros(400,400,111,length(rawfiles));

%Loading the transformed raw files data into matlab notation
for i=1:length(rawfiles)
    fid=fopen(rawfiles(i).name);
    rawfiles(i).name
    for j=1:111
        data1(:,:,j)=fread(fid,[400,400],'double');
    end
    data1=flipdim(data1,3); data1=flipdim(data1,2);
    for k=1:111
        data1(:,:,k)=rot90(data1(:,:,k));
    end

    data2(:,:,:,i)=data1(:,:,:);
    ST=fclose(fid)

end
% Correcting for the sqrt transformation of the data.
data3=data2.^2;

% Generating the new DICOM files
for i=1:length(rawfiles);
    frnr=i

    % Finding the maximum activity, which are used to find
    % the global scaling for the patient.
    maxi=max(max(max(max(data3))));
    totalmat1=data3(:,:,:,i)./maxi;
    totalmat2=round(totalmat1*32767);

    for j=1:111
        % Loading the informations for the respective bins
        % in each frame, which are used for correction
        % of the scatter fraction.
        if i==1
            metadata=dicominfo('1.IMA');
```

```
45              metadata1=dicominfo('f1b1.IMA');
46              metadata2=dicominfo('f1b2.IMA');
47              metadata3=dicominfo('f1b3.IMA');
48              metadata4=dicominfo('f1b4.IMA');
49          elseif i==2
50              metadata=dicominfo('2.IMA');
51              metadata1=dicominfo('f2b1.IMA');
52              metadata2=dicominfo('f2b2.IMA');
53              metadata3=dicominfo('f2b3.IMA');
54              metadata4=dicominfo('f2b4.IMA');
55          elseif i==3
56              metadata=dicominfo('3.IMA');
57              metadata1=dicominfo('f3b1.IMA');
58              metadata2=dicominfo('f3b2.IMA');
59              metadata3=dicominfo('f3b3.IMA');
60              metadata4=dicominfo('f3b4.IMA');
61          elseif i==4
62              metadata=dicominfo('4.IMA');
63              metadata1=dicominfo('f4b1.IMA');
64              metadata2=dicominfo('f4b2.IMA');
65              metadata3=dicominfo('f4b3.IMA');
66              metadata4=dicominfo('f4b4.IMA');
67          elseif i==5
68              metadata=dicominfo('5.IMA');
69              metadata1=dicominfo('f5b1.IMA');
70              metadata2=dicominfo('f5b2.IMA');
71              metadata3=dicominfo('f5b3.IMA');
72              metadata4=dicominfo('f5b4.IMA');
73          elseif i==6
74              metadata=dicominfo('6.IMA');
75              metadata1=dicominfo('f6b1.IMA');
76              metadata2=dicominfo('f6b2.IMA');
77              metadata3=dicominfo('f6b3.IMA');
78              metadata4=dicominfo('f6b4.IMA');
79          elseif i==7
80              metadata=dicominfo('7.IMA');
81              metadata1=dicominfo('f7b1.IMA');
82              metadata2=dicominfo('f7b2.IMA');
83              metadata3=dicominfo('f7b3.IMA');
84              metadata4=dicominfo('f7b4.IMA');
85          elseif i==8
86              metadata=dicominfo('8.IMA');
87              metadata1=dicominfo('f8b1.IMA');
88              metadata2=dicominfo('f8b2.IMA');
89              metadata3=dicominfo('f8b3.IMA');
90              metadata4=dicominfo('f8b4.IMA');
91
```

```
92          elseif i==9
93              metadata=dicominfo('9.IMA');
94              metadata1=dicominfo('f9b1.IMA');
95              metadata2=dicominfo('f9b2.IMA');
96              metadata3=dicominfo('f9b3.IMA');
97              metadata4=dicominfo('f9b4.IMA');
98
99          end
100         % Applying the dynamic informations for the static
101         % images generated for the breath gated data.
102         metadata.RescaleSlope=maxi/32767;
103         data1=totalmat2(:,:,j);
104         metadata.RescaleIntercept=0;
105         SUP=metadata.MediaStorageSOPInstanceUID(1:51);
106         SUP1=str2num(metadata.MediaStorageSOPInstanceUID(52:
                end));
107
108         metadata.SeriesDescription= ...
                '13NH3 Breath Gated - 5t60 2mm Rest - Bell TOF';
109         metadata.ImageIndex=(i-1)*111+j;
110         metadata.NumberOfSlices=111;
111         metadata.NumberOfTimeSlices=size(data3,4);
112         Slloc=metadata.SliceLocation;
113         metadata.SliceLocation=Slloc-((j-1)*2);
114         metadata.SeriesNumber=888;
115         metadata.InstanceNumber=(i-1)*111+j;
116         if j==1
117             metadata.SOPInstanceUID=[SUP num2str(SUP1)];
118             metadata.MediaStorageSOPInstanceUID=[SUP num2str
                    (SUP1)];
119
120         else
121             SUP2=SUP1+(j-1);
122             metadata.SOPInstanceUID=[SUP num2str(SUP2)];
123             metadata.MediaStorageSOPInstanceUID=[SUP num2str
                    (SUP2)];
124         end
125         ScFr=(metadata1.ScatterFractionFactor+...
126             metadata2.ScatterFractionFactor+...
127             metadata3.ScatterFractionFactor+....
128             metadata4.ScatterFractionFactor)/4;
129         metadata.ScatterFractionFactor=ScFr;
130
131              if i>1
132                  CT1=str2num(metadata.ContentTime(1:6));
133                  CT2=metadata.ContentTime(7:end);
134                  CT1=CT1+i;
135
```

```
136                     CT11=num2str(CT1);
137                     metadata.ContentTime=[CT11 CT2];
138                 end
139                 x1=metadata.ImagePositionPatient(1);
140                 x2=metadata.ImagePositionPatient(2);
141
142                 metadata.ImagePositionPatient=[x1;x2;Slloc
                        -((j-1)*2)];
143                 data2=int16(data1);
144                 metadata.SmallestImagePixelValue=min(min(
                        data2));
145                 metadata.LargestImagePixelValue=max(max(
                        data2));
146                 dicomwrite(data2,...
147                     ['Breathgated' num2str(metadata.
                            ImageIndex) '.IMA'],...
148                     metadata,'CreateMode','copy');
149
150     end
151 end
```

Bibliography

[1] P. Hasbak, A. Kjæ r, D. Skovgaard, L. Bang, P. Grande, and L. Holmvang, "Preserved myocardial blood flow in the apical region involved in takotsubo cardiomyopathy by quantitative cardiac pet assessment," *Journal of Nuclear Cardiology*, pp. 169–171. 10.1007/s12350-011-9451-3.

[2] M. Dawood, F. Büther, M. Schäfers, K. P. S. X. Jiang, L. Stegger, and O. Schober, "Optimal number of respiratory gates in positron emission tomography: A cardiac patient study," *Medical Physics*, vol. 36, p. 1775, 2009.

[3] FDA, "Fda drug safety communication: Fda alerts healthcare professionals to stop performing heart scans with cardiogen-82 due to potential for increased radiation exposure in patients." http://www.fda.gov/Drugs/DrugSafety/ucm265278.htm, July 2011.

[4] J. ø rgen Gomme, *Isotopteknik 1 - Radioaktive isotoper og ioniserende stråling i biologi og medicin*. G.E.C Gads forlag, 1997.

[5] J. N. A. Miles N. Wernick, *Emission Tomography: The fundamentals of PET and SPECT*. Elsevier, 2005.

[6] "Positron - electron annihilation." http://geant4.cern.ch/G4UsersDocuments/UserGuides/PhysicsReferenceManual/html/node43.html, 2011.

[7] F. H. Fahey, "Data acquisition in pet imaging," *Journal of Nuclear Medicine Techol.*, vol. 30, pp. 39–49, 2002.

[8] G. B. Saha, *Basics of PET Imaging: Physics, Chemistry and Regulations*. Springer, 2004.

[9] M. E. D.-W. Joel S. Karp, Suleman Surti and G. Muehllehner, "Benefit of time-of-flight in pet: Experimental and clinical results," *Journal of Nuclear Medicine*, vol. 49, pp. 462–470, 2008.

[10] T. G. T. D. M. D. D. A. B. J.-P. V. L. W. H. J. Z. F. C. M. J. S. Timothy R. DeGrado, Michael W. Hanson and R. E. Coleman, "Estimation of myocardial blood flow for longitudinal studies with 13n-labeled ammonia and positron emission tomography," *Journal of Nuclear Cardiology*, vol. 3, pp. 494–507, 1996.

[11] PMOD Technologies, *PMOD Cardiac Modeling (PCARD)*, 3.2 ed., October 2010.

[12] K. C. R. J. K. H. S. a. D. E. K. Gary D. Hutchins, Markus Schwaiger, "Noninvasive quantification of regional blood flow in the human heart using n-13 ammonia and dynamic positron emission tomographic imaging," *Journal Am Coll Cardiol*, vol. 1, pp. 1032–1042, 1990.

[13] G. D. H. T. J. M. N. N. Otto Muzik, Rob S.B. Beanlands and M. Schwaiger, "Validation of nitrogen-13-ammonia tracer kinetic model for quantification of myocardial blood flow using pet," *Journal of Nuclear Medicine*, vol. 34, pp. 83–91, 1993.

[14] "Takotsubo cardiomyopathy." http://en.wikipedia.org /wiki/Takotsubocardiomyopathy, 1 2012.

[15] T. J. Nowak and A. G. Handford, *Pathophysiology - Concepts and Applications for Healt Care Professionals*. McGraw Hill Higher education, 2004.

[16] M. Dawood, F. Büther, N. Lang, O. Schober, and K. P. Schäfers, "Respiratory gating in positron emission tomography: A quantitative comparison of different gating schemes," *Medical Physics*, vol. 34, pp. 3067–76, 2007.

[17] R. Hudson, H.M.; Larkin, "Accelerated image reconstruction using ordered subsets of projection data," *Medical Imaging, IEEE*, vol. 13, issue 4, pp. 601–609, 1994.

[18] R. R. B. W. H. S. N. M. A. Martinez-Möller, D.Zikic and S.G.Nekolla, "Dual cardiac-respiratory gated pet: implementation and results from a feasibilty study," *Eur. J. Nuclear Medicine: Molecular Imaging*, vol. 34, pp. 1447–1454, 2007.

[19] A. M. A. P. P. R. T. P. K. Grace P. Chen, Kelley R. Branch and J. H. Caldwell, "Effect of reconstruction algorithms on myocardial blood flow measurement with 13n-ammonia pet," *Journal of Nuclear Medicine*, vol. 48, pp. 1259–1265, 2007.

[20] J. D. F. A. V. D. S. K. F. J. F. Hughes, *Computer Graphics: Principles and Practice*. Addison-Wesley, 1995.

[21] G. Klein, R. Reutter, and R. Huesman, "Four-dimensional affine registration models for respiratory-gated pet," *Nuclear Science, IEEE Transactions on*, vol. 48, pp. 756 –760, jun 2001.

[22] R. Larsen, "02505 course note in medical image analysis," tech. rep., DTU, 2008.

[23] F. S. Hillier and G. J. Lieberman, *Introduction to operations research - eight edition*. McGraw Hill Higher education, 2005.

[24] L. Collins, "Minctracc synopsis." http://www.bic.mni.mcgill.ca/ dale/helppages/mniman/minctracc.html, 1993-1995.

[25] D. C. Montgomery, *Design and Analysis of Experiments, 7th edition*. Wiley, 2009.

[26] R. A. Johnson, *Miller & Freund's Probability and Statistics for Engineers, seventh edition*. Pearson Education International, 2005.

[27] G. Carey, "Multivariate analysis of variance (manova): I. theory." Online PDF, http://ibgwww.colorado.edu/ carey/p7291dir/handouts/manova1.pdf, 1998.

[28] "Glm: Manova and mancova." http://schatz.sju.edu/multivar/manova.html.

[29] K. C. Bjarne Kjæ r Ersbø ll, *An introduction to Statistics, vol. 2*. IMM DTU, 2007.

[30] U. of Washington, "Pet introduction." http://depts.washington.edu/nucmed/IRL/pet intro/, January 1999.

[31] A. v. L. Ronald Boellaard and A. A. Lammertsma, "Experimental and clinical evaluation of iterative reconstruction (osem) in dynamic pet: Quantitative characteristics and effects on kinetic modeling," *Journal of Nuclear Medicine*, vol. 42, pp. 808–817, 2001.

[32] S. L. Inc., "The heart's structures: The champer." http://www.skillstat.com/heartscape/chambers.htm, 2005.